Aus dem Pathologischen Institut
Institut der Universität München
Direktor: Prof. Dr. med. Frederick Klauschen

Harnessing fusion transcription factors for specific gene therapy in childhood sarcoma models

Dissertation
zum Erwerb des Doktorgrades der Medizin
an der Medizinischen Fakultät der
Ludwig-Maximilians-Universität zu München

vorgelegt von
Tilman Luis Benedikt Hölting

aus
Freiburg im Breisgau

Jahr
2024

Mit Genehmigung der Medizinischen Fakultät der Universität München

Berichterstatter:	Prof. Dr. Thomas Grünewald, Ph.D.
Mitberichterstatter:	Prof. Dr. Roland Kappler Prof. Dr. Hans Roland Dürr Prof. Dr. Lars Lindner
Mitbetreuung durch den promovierten Mitarbeiter:	Dr. Maximilian Knott
Dekan:	Prof. Dr. med. Thomas Gudermann
Tag der mündlichen Prüfung:	08.02.2024

Eidesstattliche Versicherung

Tilman Luis Benedikt Hölting

Ich erkläre hiermit an Eides statt,

dass ich die vorliegende Dissertation mit dem Titel

"Harnessing fusion transcription factors for specific gene therapy in childhood sarcoma models"

selbstständig verfasst, mich außer der angegebenen keiner weiteren Hilfsmittel bedient und alle Erkenntnisse, die aus dem Schrifttum ganz oder annähernd übernommen sind, als solche kenntlich gemacht und nach ihrer Herkunft unter Bezeichnung der Fundstelle einzeln nachgewiesen habe.

Ich erkläre des Weiteren, dass die hier vorgelegte Dissertation nicht in gleicher oder in ähnlicher Form bei einer anderen Stelle zur Erlangung eines akademischen Grades eingereicht wurde.

Heidelberg, 15. Februar, 2024

Tilman Hölting

Acknowledgements

I am profoundly grateful to my thesis supervisor and principal investigator, Prof. Dr. med. Thomas Grünewald, Ph.D., whose expertise and guidance have been invaluable in enabling this research project. His dedication to mentoring and his passion for improvement of cancer care through scientific exploration have inspired me throughout this journey.

I am deeply indebted to Dr. med. Maximilian Knott, whose visionary idea laid the foundation for this research. His unwavering support, encouragement and friendship have been paramount in propelling both this work and my personal scientific development.

I would like to thank my friends, colleagues, and all those who have contributed to this research endeavor.

To my family and my partner, I express my most sincere gratitude for their continued support throughout and beyond my studies.

Contents

List of Figures

List of Tables

Zusammenfassung

Verschiedene Krebserkrankungen, wie das Ewing-Sarkom (EwS) oder das alveoläre Rhabdomyosarkom (ARMS), sind durch das Vorhandensein pathognomonischer, chimärer Fusionstranskriptionsfaktoren gekennzeichnet. Diese onkogenen Fusionsproteine sind krankheitsspezifisch und ihre epigenetischen Effekte spielen eine entscheidende Rolle für die Überlebensfähigkeit und den malignen Phänotyp der Krebszellen der jeweiligen Erkrankung. Sie stellen daher ideale Angriffspunkte für zielgerichtete Therapien dieser Krebserkrankungen dar. Da sie als Transkriptionsfaktoren kein enzymatisch aktives Zentrum besitzen, hat sich die direkte Hemmung dieser zentralen Onkogene bisher als schwierig und wenig erfolgreich erwiesen.

Ziel dieser Studie war es daher, zu untersuchen, ob die aberrante DNA-Bindungspräferenz dieser Fusions-Transkriptionsfaktoren, mit besonderem Augenmerk auf EWSR1::FLI1 (EF1) im EwS, für die Expression therapeutischer Gene ausgenutzt werden kann. Zu diesem Zweck wurde eine EWSR1::FLI1-abhängige Expressionskassette entworfen, indem ein synthetischer, minimaler Promotor, der eine begrenzte Basisaktivität mit hoher Induzierbarkeit verbindet, mit GGAA-Mikrosatelliten kombiniert wurde. Sowohl die EwS-Spezifität als auch die EF1-Abhängigkeit des so entwickelten Expressionssystems wurden in Reporterexperimenten *in vitro* bestätigt. Unter Verwendung eines auf einer Herpes Simplex Virus Thymidinkinase (HSV-TK) basierenden Prodrug-Konversions-Therapiemodells und eines lentiviralen Vektors konnte gezeigt werden, dass mittels der entwickelten Expressionskassette, spezifische Behandlungseffekte *in vitro* induziert werden können. Um die *in vivo* Anwendung lentiviraler Vektoren zu erlauben, wurde durch die Analyse von Microarray-Genexpressionsdaten GPR64 als spezifisches Antigen für die gezielte Transduktion von EwS Zellen identifiziert. Durchflusszytometrische Analysen bestätigten die Möglichkeit einer EwS-spezifischen Transduktion mit Anti-GPR64-pseudotypisierten lentiviralen Partikeln. *In vivo* Xenotransplantationsexperimente zeigten, dass die Kombination aus gezielter Transduktion und spezifischer Expression von HSV-TK mit EF1-abhängigen Promotoren therapeutische Effekte ohne erkennbare Nebenwirkungen hervorrufen konnte. Um schließlich die Anwendbarkeit des Konzepts auf andere Fusionstranskriptionsfaktoren zu demonstrieren, wurden PAX3::FOXO1-abhängige Expressionskassetten für das alveolare Rhabdomyosarkom entwickelt und deren Spezifität

mit Reporter-Assays und Modelltherapien *in vitro* getestet.

Insgesamt deuten die in dieser Studie gewonnenen Daten darauf hin, dass aberrant bindende, transaktivierende Transkriptionsfaktoren für eine tumorspezifische Genexpression, und so beispielsweise als Bestandteil zukünftiger Gentherapien oder onkolytischer Virustherapien, genutzt werden könnten.

Wesentliche Teile dieser Arbeit sind in dem folgenden Artikel veröffentlicht worden:

Tilman L. B. Hölting et al. "Neomorphic DNA-binding Enables Tumor-Specific Therapeutic Gene Expression in Fusion-Addicted Childhood Sarcoma". In: Molecular Cancer 21.1 (Oct. 13, 2022), p. 199. issn: 1476-4598. doi: 10.1186/s12943-022-01641-6.

Summary

Pathognomonic, chimeric fusion transcription factors are found in a number of aggressive cancers, including Ewing sarcoma (EwS) and alveolar rhabdomyosarcoma (ARMS). These fusion oncogenes are disease-specific and play a vital role in maintaining viability and the malignant phenotype of cancer cells. Hence, these fusion transcription factors would be ideal therapeutic targets for these diseases. However, direct inhibition of these key driver oncogenes has been difficult due to their lack of an enzymatic active site and has been, at least to date, clinically unsuccessful.

Therefore, the aim of this study was to investigate whether the neomorphic DNA binding preferences of these fusion transcription factors, with a special focus on EWSR1::FLI1 (EF1) in EwS, can be exploited for the expression of therapeutic genes. To this end, an EWSR1::FLI1-dependent expression cassette was designed by combining a core promoter, exhibiting limited basal activity and strong inducibility, with GGAA-microsatellites. Reporter assays demonstrated both the EwS-specificity and the EF1-dependency of the designed expression system. A herpes simplex virus thymidine kinase (HSV-TK) prodrug conversion therapy model using a lentiviral vector showed that the designed expression cassette allows specific treatment *in vitro*. To enable the *in vivo* use of lentiviral vectors by targeted transduction, GPR64 was identified as a specific antigen on EwS cells by *in silico* screening of microarray gene expression data. Flow cytometry analyses confirmed the possibility of EwS-specific gene delivery with anti-GPR64-pseudotyped lentiviral particles. *In vivo* xenograft experiments showed EF1-dependent promoters to be able induce therapeutic effects without observable adverse effects. Finally, to evaluate the general applicability of the concept, expression cassettes dependent on PAX3::FOXO1 in alveolar rhabdomyosarcoma were designed and their specificity was tested with reporter assays and model therapies *in vitro*.

Taken together, the data generated in this study suggest that aberrantly binding, transactivating transcription factors can be exploited for tumour-specific gene expression potentially applicable as a tool for specificity of cancer gene therapy and oncolytic virus therapy.

Essential parts of this thesis have been published in the following article:

Tilman L. B. Hölting et al. "Neomorphic DNA-binding Enables Tumor-Specific Therapeutic Gene Expression in Fusion-Addicted Childhood Sarcoma". In: Molecular Cancer 21.1 (Oct. 13, 2022), p. 199. issn: 1476-4598. doi: 10.1186/s12943-022-01641-6.

1. Introduction

1.1 Ewing sarcoma

Ewing sarcoma is a malignant neoplastic disease of bone and soft tissue [1]. First described in 1921 as "endothelioma of bone" by the American pathologist James Ewing, after whom it was later named, its usual histological morphology classifies it as an undifferentiated, small, round, blue-cell tumour [1, 2]. Since the 2013 update of the WHO classification of bone and soft tissue tumours, the entity is defined by the pathognomonic presence of balanced chromosomal translocations resulting in expressed fusions of genes from the *FET* family with members of the *ETS* gene family [3]. Thus, peripheral neuroectodermal or Askin tumours with such fusion genes, which were previously only part of the so-called 'Ewing sarcoma family', are now called Ewing sarcomas [4]. Cancers that are clinically and histomorphologically indistinguishable from Ewing sarcoma but lack a *FET:ETS* fusion gene are called 'Ewing-like sarcomas' [4].

1.1.1 Epidemiology

With a mean age at diagnosis of 13-16 years, Ewing sarcoma is most commonly diagnosed in children or young adolescents [5, 6]. In Germany between 2009 and 2018, the incidence rate of Ewing sarcoma for 10-17 year olds was between 5.4 and 6.0 per million per year, making it the second most common bone-related tumour in this age group [6]. Ewing sarcoma is slightly more frequent in males than females and ethnic factors also seem to influence the incidence as epidemiological analyses have shown it to be 9 times more common in European Americans than in African Americans [6, 7]. While it is not yet clear, to what extent this is due to environmental or genetic factors, there has been some compelling evidence that certain alleles, that are less common in African populations, are associated with higher rates of Ewing sarcoma [8, 9]. Although there is some evidence from case-control studies suggesting an increased rate of Ewing sarcoma in children of parents, particularly mothers, with a history of agricultural work, no clear environmental risk factors have been identified [10, 11, 12].

1.1.2 Genetic characteristics and pathophysiology

Central to the pathogenesis of cancer is the successive accumulation and clonal selection of genetic mutations that alter protein function and protein levels, thereby leading to the sequential acquisition of cellular characteristics that are known as the '*Hallmarks of Cancer*' [13]. Notably, in most paediatric cancers these *Hallmarks* are acquired through a lower number of somatic mutations compared to adult malignancies, as evidenced by genomic sequencing studies over the last decade [14, 15]. Ewing sarcoma is an example of this and is characterised by the presence of a single type of recurrent mutation that drives the malignant phenotype in these tumours [16]. These pathognomonic mutations are fusions between genes of the *FET* and *ETS* gene families that arise either through reciprocal translocations or, in about 40% of cases, through chromoplexy rearrangement bursts [4, 17]. The *FET* family contains three genes, *EWSR1* (*EWS RNA Binding Protein 1*), *FUS* (*FUS RNA binding protein*), and *TAF15* (*TATA-box binding protein associated factor 15*) all of which encode ubiquitously expressed RNA-binding proteins that are involved in multiple RNA processing steps and DNA repair [18, 19, 20, 21, 22]. The *ETS* family of genes, which act as 3' partners in the Ewing sarcoma fusion oncogenes, encode transcription factors involved in a variety of physiological processes [23]. Their major common feature is the highly conserved ETS domain, which confers DNA binding of ETS transcription factors to sites consisting of a central `GGA(A/T)` motif with certain flanking sequences that mediate binding affinity and specificity for different ETS transcription factors [23].

While several combinations of *FET::ETS* fusions have been identified in Ewing sarcoma, *EWSR1::FLI1*, caused by the translocation `t(11;22)(q24;q12)`, was the first to be described and is present in approximately 85% of cases [4, 24]. In the majority of the *EWSR1::FLI1*-negative tumours, *EWSR1::ERG* fusions as a product of the translocation `t(21;22)(q22;q12)` can be detected [25, 26]. An overview of the different oncogenic fusions in Ewing sarcoma and the underlying translocations and their relative frequencies is given in Table 1.1. Due to the ubiquitous activity of the promoters of the *FET* gene family, these *FET:ETS* gene fusions are expressed to produce chimeric fusion proteins consisting of the amino-terminal portion of FET fused to the carboxyl-terminal portion of ETS containing the ETS DNA-binding domain [25].

As the fusion protein present in the majority of Ewing sarcoma cases, EWSR1::FLI1 has been the most thoroughly functionally characterised [4]. By binding to DNA, altering the epigenome and altering the expression levels of many genes, it acts as an aberrant transcription factor and is the central oncogene for initiating and maintaining the malignant cellular phenotype in Ewing sarcoma [27, 28]. Gangwal et al. showed in 2008 that EWSR1::FLI1 achieves this dysregulation of the transcriptome by binding to GGAA-microsatellites with a minimum of 4 uninterrupted repeats of the motif `GGAA`, in addition to

Table 1.1: *FET:ETS* fusion oncogenes in Ewing sarcoma

FET part	ETS part	Fusion gene	Chromosomal translocation	Frequency
FUS	*FEV*	*FUS::FEV*	t(2;16)(q35;p11)	<1%
	ERG	*FUS::ERG*	t(16;21)(p11;q22)	<1%
EWSR1	*FLI1*	*EWSR1::FLI1*	t(11;22)(q24;q12)	~85%
	ERG	*EWSR1::ERG*	t(21;22)(q22;q12)	~10%
	ETV1	*EWSR1::ETV1*	t(7;22)(p22;q12)	<1%
	ETV4	*EWSR1::ETV4*	t(17;22)(q21;q12)	<1%
	FEV	*EWSR1::FEV*	t(2;22)(q33;q12)	<1%
	ETV5 (?)	*EWSR1::ETV5*	?	?
TAF15	?	?	?	?

From Grünewald & Cidre-Aranaz et al. 2018 [4].

binding to ETS-like motifs [29]. This aberrant binding preference for GGAA-microsatellites, which are conserved at specific locations in the human genome but have no known physiological binding partners, has since been confirmed in several different studies by different groups [30, 27]. Probably due to the structural similarity of the DNA binding domains of FLI1 and ERG, the second most abundant fusion protein, EWSR1:ERG, appears to have similar DNA binding preferences to EWSR1::FLI1 [26, 31]. Notably, the binding probability of EWSR1::FLI1 to GGAA-microsatellites increases with higher numbers of consecutive `GGAA` motifs up to a sweet spot of 16-25 repeats [32]. With increasing knowledge of epigenetic regulation, several studies over the last decade have shed light on the effects of EWSR1::FLI1. At GGAA-microsatellites, EWSR1::FLI1 acts as a transcription factor, inducing decondensation of chromatin and converting these microsatellites into *de novo* enhancers that interact with promoters of target genes inducing their expression (Figure 1.1) [27]. In particular, the fusion protein acts as a so called pioneer transcription factor capable of inducing *de novo* enhancers in the context of previously condensed chromatin (Figure 1.1) [33]. This effect appears to be mediated by a prion-like domain in the N-terminal, EWSR1-part of the fusion oncoprotein which allows multimerisation of EWSR1::FLI1 at GGAA-microsatellites and interacts with and recruits the BRG1/BRM-associated factor (BAF) chromatin remodelling complex, also known as the mammalian SWI/SNF complex [33]. When binding to ETS motifs, which contain a single core `GGAA`, or less commonly a `GGAT`, and occur at conserved enhancers, the EWSR1::FLI1 can also reduce the enhancer activity and hence the transcription of target genes (Figure 1.1) [27, 34]. This enhancer inactivation at some locations is experimentally demonstrated by a decrease in certain types of post-translational histone modifications that are typically associated with enhancers, such as H3K27ac, and a removal of proteins such as p300 which induce these modifications [27]. In addition to the displacement of wild-type ETS transcription factors by EWSR1::FLI1, the repressive effect may also be caused by direct recruitment of the nucleosome

remodelling deacetylase (NuRD) co-repressor complex with which the fusion transcription factor interacts [35].

As a result of these interactions with the chromatin, EWSR1::FLI1 induces a Ewing sarcoma-specific epigenetic signature leading to changes in gene expression that underlie its malignant phenotype [36]. Interestingly, this fusion oncogene only causes malignant transformation in certain cells, such as mesenchymal stem cells, whereas in others it leads to p53-dependent growth arrest and apoptosis [37, 38]. This suggests the need for genetic or epigenetic enabling factors for induction of malignancy by the fusion oncogene [16]. In addition to initiation, EWSR1::FLI1 has also been experimentally shown to be essential for maintaining tumour cell proliferation, a dependency sometimes referred to as *oncogene addiction* [39, 40].

Although other somatic mutations are less common in Ewing sarcoma, some are worth mentioning. First, certain copy number aberrations have been described to occur: gain of chromosome 1q in 18 %, chromosome 8 in 47 % and chromosome 12 in 21 % of cases, as well as loss of chromosome 16q in 17 % or deletion of the *CDKN2A* locus on chromosome 9 in 12 % [41]. Furthermore, the genes most commonly affected by other protein-coding mutations are *STAG2* in 17 % and *TP53* in 7 % of cases [41]. Notably, these two often co-occur and are associated with poor prognosis [41].

1.1.3 Clinical presentation and diagnosis

Clinical presentation

While the majority of primary tumours are bone-associated, approximately 20 - 30 % of cases are of extraskeletal origin which is more common in older patients [42, 43]. Skeletal Ewing sarcoma can arise in any bone, although the pelvis, thorax and leg are the most common sites [5]. The relative frequency of primary sites from a study population of 2635 patients with skeletal Ewing sarcoma is presented in Table 1.2.

The clinical symptoms that patients subsequently diagnosed with Ewing sarcoma typically present with are unspecific and depend on the primary location and stage of the disease [44]. The most common complaints are local tenderness or a palpable mass which occur in 70 % and 34 % of cases respectively [45]. Painful or restricted joint movement in the case of juxtaarticular tumours, or limping have also been described as possible signs at the first disease-related medical visit [45]. In about 30 % of patients, recurrent fever or other constitutional symptoms, including weight loss and night sweats, are reported at initial presentation, indicating metastasised disease [4, 45]. Indeed, around 75 % of patients present with clinically and radiologically localised disease, although it is thought that most patients have microscopic metastases at diagnosis [46, 47].

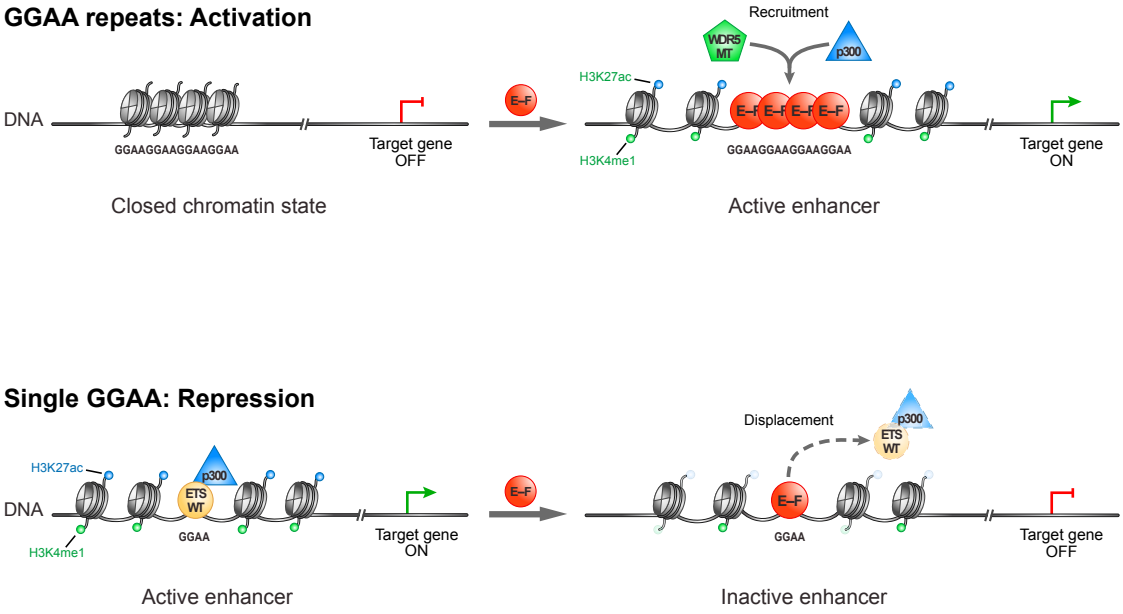

Figure 1.1: Influence of EWSR1::FLI on chromatin state and gene expression depending on the binding sequence.
The upper half shows a schematic representation of *de novo* enhancer activation upon binding of EWSR1::FLI1 to GGAA-microsatellites. Lower half shows a model for EWSR1::FLI1-induced enhancer inactivation at certain ETS motifs. Figure from Riggi et al. 2014 [27].

Table 1.2: Primary sites of osseous Ewing sarcoma.

Primary site	Frequency
Pelvis	26.9%
Head	3.6%
Spine	7.2%
Thorax	19.9%
Humerus	5.8%
Distal arm	2.5%
Femur	15.0%
Distal leg	19.1%

From Worch et al. 2018 [5].

Initial diagnostic work-up and staging

If the medical history and careful clinical examination suggest the possibility of a bone tumour, plain radiography in 2 projections is a common first step of the diagnostic work-up [44]. Typical signs of Ewing sarcoma in plain radiography include numerous lytic, 'moth-eaten', lesions of the corticalis, and signs of displaced periost called 'Onion skin' reaction and Codman's triangle [44]. Unless radiography reveals a clear cause of symptoms that does not warrant further evaluation, cross-sectional imaging, preferably magnetic resonance imaging, is necessary to assess the nature and extent of the local process [47]. To avoid missing medullary skip metastases, it is adamant to image the entire affected bone. After the initial radiological assessment, biopsy for pathological evaluation of the lesion is usually the next step [47]. Depending on the size and location of the tumour, tissue should be obtained by core needle or open biopsy so that the biopsy canal and scars can be removed during subsequent surgery [47]. Importantly, the biopsy should be performed by the surgical team that will perform the definitive resection or an interventional radiologist in consultation with that surgical team [47].

25 % of patients have macroscopic metastases at initial diagnosis [47]. These most commonly involve the lung (10 %), bone or bone marrow (10 %), or other sites [47]. Therefore, systemic staging requires contrast-enhanced computed tomography of the chest to detect pulmonary metastases [47]. For the detection of bone metastases, current European guidelines recommend whole-body MRI or whole-body FDG-PET/CT over bone scintigraphy [47]. If FDG-PET/CT is performed, bone marrow biopsy and aspiration are not required [47]. Ambiguous lesions found at staging in patients who otherwise have no evidence of systemic disease should be histologically assessed [47].

Surgical and molecular pathology

As a poorly differentiated, small, round, blue cell tumour, standard H&E (hematoxylin eosin) stains are insufficient to diagnose Ewing sarcoma and pathologists must to employ immunohistochemistry and molecular pathology to guide their diagnosis [48]. The most relevant immunohistochemical marker for Ewing sarcoma is the glycoprotein CD99 which is located at the cell surface [48]. While CD99 shows membranous staining in over 90 % of cases, its expression is not specific for Ewing sarcoma [4]. Other immunohistochemical markers expressed in Ewing sarcoma include CAV1, GLG1 and BCL11B [48, 49, 50]. The presence of typical staining patterns for these markers can guide the diagnostician to initiate molecular testing for the presence of chromosomal translocations resulting in *FET:ETS* fusions that are required for the definitive diagnosis of Ewing sarcoma [4]. This is routinely achieved by fluorescence in situ hybridisation (FISH) based detection of *EWSR1*-rearrangements or reverse transcription polymerase chain reaction (RT-PCR) [51]. It is important to note that *EWSR1*-rearrangements detectable by FISH can also occur in

other sarcomas harbouring different *EWSR1* gene rearrangements fused with non-*ETS* genes [4]. Thus, RT-PCR or next-generation sequencing (NGS) are preferred for definitive diagnosis of Ewing sarcoma [52].

1.1.4 Treatment and prognosis

During the diagnostic process, patients with Ewing sarcoma should be referred to a specialised centre experienced in the treatment of this rare disease, where therapeutic management is guided by multidisciplinary tumour boards [53, 47]. Treatment of Ewing sarcoma should be based on established protocols or carried out as part of prospective clinical trials [53, 47].

Although only 25 % of patients have visible metastases at initial diagnosis, historical data from the 20th century show that only 10 % survive more than 5 years with local treatment alone [47, 54]. In addition, relapses in patients with initially localised disease occur at sites other than the primary tumour in 68 % [55]. This suggests that even Ewing sarcoma without apparent distant metastases should be considered a systemic disease. Systemic treatment modalities are therefore an essential part of treatment protocols for Ewing sarcoma patients regardless of their metastatic status [56]. Today, standard therapy consists of up to nine cycles of neoadjuvant chemotherapy, followed by local therapy and subsequent consolidation chemotherapy, for a total duration of 10 to 12 months [47]. The chemotherapy regimens consist of vincristine, doxorubicine, etoposide and cyclophosphamide/ifosfamide [56].

For local therapy, complete surgical resection, which must include all tissues involved when the tumour was at its greatest extent, is preferred to definitive radiotherapy because of better local control rates [57]. The risk of local recurrence may be reduced by adjuvant radiotherapy, which is recommended for some patients, including those with tumour volumes greater than 200 cm^3, tumour cells reaching surgical margins, inadequate histological response to chemotherapy, or sacral involvement [47]. Definitive radiotherapy is indicated only when surgical resection is not considered feasible without unacceptable morbidity associated with surgery [47]. In particular, local treatment should also be attempted in patients with metastatic Ewing sarcoma [47, 58].

As with most solid malignancies, the main factor influencing prognosis is the presence and location of metastases [46, 59]. Without overt metastases, patients that are treated with contemporary multimodal approaches can expect an average 5-year survival rate of around 70 % [60, 59]. When the tumour has metastasised exclusively to the lung, the average survival at 5 years drops to around 50 % and in case of extrapulmonary metastasis to around 30 % [4, 59]. In addition to systemic spread, primary tumour volume and location also influence the prognosis, with large and pelvic tumours having a worse prognosis due to increased difficulty of local control [59]. An overview of survival rates for different combinations of these risk factors can be found in table 1.3 [59].

Taken together, intensive systemic treatment regimens have improved sur-

Table 1.3: Survival rates of Ewing sarcoma patients 5 years after diagnosis.

Disease extent	Location	Volume	Age	N	5-year overall survival (95% CI)
Localised	Non-pelvic	< 200 ml	< 16 years	296	88% (84–92)
			≥ 16 years	207	71% (64–78)
		≥ 200 ml		243	67% (61–73)
	Pelvic	< 200 ml		78	62% (50–74)
		≥ 200 ml		92	53% (43–63)
Pulmonary	Non-pelvic	< 200 ml		57	58% (45–71)
		≥ 200 ml		62	48% (36–60)
	Pelvic	< 200 ml		17	76% (56–96)
		≥ 200 ml		46	45% (30–60)
Extrapulmonary	Non-pelvic	< 200 ml		63	29% (17–41)
		≥ 200 ml		74	31% (20–42)
	Pelvic	< 200 ml		22	46% (25–67)
		≥ 200 ml		57	17% (07–27)

From Bosma et al. 2019 [59].

vival in patients with localised disease. However, the high intensity of systemic and local treatment strategies takes its toll in the form of long-lasting side effects, even when cure is achieved [44]. This is all the more worrying given the young age of most patients. This, combined with the still unfavourable prognosis of metastatic or recurrent Ewing sarcoma, highlights the need for new specific and effective targeted therapies for this disease. Due to its pathophysiological importance and specificity for tumour cells, EWSR1::FLI1 would be the most obvious choice for targeted therapy of Ewing sarcoma. Unfortunately, the lack of a catalytic active site and its structure make direct inhibition of its function as a transcription factor difficult [61, 44]. One way to get around this barrier is to disrupt the interaction of EWSR1::FL1 with other proteins that are essential for its function. In a promising first example, Erkizan et al in 2009 identified a small molecule that inhibits the interaction of EWSR1::FLI1 with RNA helicase A, which is essential for its oncological function, and demonstrated therapeutic potential in preclinical models [62]. Unfortunately, early clinical data for an improved variant of the compound [63] showed rather limited anti-tumour effects.

1.2 Cancer gene therapy

Neoplastic diseases are a major cause of morbidity and the second leading cause of death in developed countries [64, 65]. Important factors in cancer-related death are organ dysfunction due to local or metastatic growth combined with resistance to therapy [66, 67]. In addition, the often aggressive systemic treatment regimens can induce unwanted side effects, particularly cardiovascular

disease and infections, which contribute to cancer-related morbidity and mortality [67]. Therefore, new therapeutic approaches that are both effective and specific are urgently needed, and their identification and refinement is one of the central goals of ongoing research in oncology.

One possible therapeutic strategy that has been considered promising for the future treatment of malignancies is *cancer gene therapy*, the treatment of cancer by delivering genetic material to and expressing it in cancer cells to induce therapeutic effects [68, 69].

1.2.1 Therapeutic strategies

The classic use case for gene therapy is monogenetic diseases, where the therapeutic intent is usually to replace or repair the gene in which the diseased cells are deficient [70]. For cancer gene therapy, due to the higher genetic complexity of the underlying disease, the optimal therapeutic strategy is less obvious and different types of gene therapy approaches have been evaluated in preclinical and clinical studies [68].

First, a relatively simple way to induce anticancer effects by gene therapy is suicide gene therapy, i.e. the delivery and expression of a transgene that directly induces cell death of the cells expressing the gene [71]. The most widely studied suicide genes encode enzymes that convert prodrugs, which are relatively harmless to human cells, into toxic active metabolites. The two most prominent of these are herpes simplex virus thymidine kinase (HSV-TK), a viral enzyme that phosphorylates the nucleoside analogue ganciclovir, thereby interfering with DNA replication, and cytosine deaminase, which activates the prodrug 5-fluorocytosine to 5-fluorouracil, a compound that inhibits thymidilate synthase [71, 72]. Numerous studies have shown that these prodrug-converting systems are able to effectively induce cell death upon substrate addition in several preclinical cancer models [73, 74, 75, 76, 77]. An interesting advantage of these transgenes is that the toxic metabolites of ganciclovir and 5-fluorocytosine are able to spread to surrounding cells, allowing a so-called bystander effect, which theoretically reduces the transduction efficiency required for successful therapy [78, 79]. Unfortunately, the efficacy of these prodrug-converting systems seen in preclinical models has not yet been seen in clinical trials. For example, two phase III clinical trials of HSV-TK-based adjuvant gene therapies for glioblastoma multiforme, one using retroviruses and the other using adenoviruses as delivery systems, failed to show a benefit in overall survival, although the adenovirus-delivered therapy did show a significant benefit in time to death or re-intervention [80, 81].

Another group of genes, that could theoretically be used to combat cancer cells in gene therapy approaches are tumour suppressor genes as these prevent uncontrolled proliferation under physiological conditions [68]. Indeed, preclinical and clinical studies have demonstrated anticancer effects of therapeutic delivery and expression of *TP53*, one of the most prominent tumour suppres-

sor genes, which is often mutated in human cancers [82, 83, 84, 85]. Notably, in 2003, a human wild-type *TP53* transgene delivered by a replication-defective adenoviral vector, was approved in China for treatment of head and neck squamous cell carcinoma as the first ever gene therapy product under the name of *Gendicine*^{TM} [86]. Interestingly, *Advexin*, a similar product marketed by *Introgen Therapeutics, Inc.*, failed to gain approval by the FDA in 2008 and to this date no *TP53*-based gene therapy is in clinical use in the EU or US.

Both gene-directed prodrug-converting enzyme therapy and tumour-suppressor gene therapy conceptually rely on the direct interference of transgene-encoded proteins with malignant cell growth and survival. Another promising approach is the use of cancer gene therapy as a means of immunotherapy, using transgenes encoding secretory proteins that enhance the immune system's response to tumour cells [68]. Preclinical and clinical studies have investigated the therapeutic effects of many different such transgenes in a variety of cancers. For example, the transgene *interleukin(IL)-12*, encoding a cytokine involved in the activation of natural killer cells and T cells, delivered by a replication-incompetent adenoviral vector to a glioma mouse model induced tumour growth arrest and regression [87, 88]. In addition, Barrett et al. also confirmed increased numbers of tumour-infiltrating lymphocytes, a finding also seen in a subsequent phase I clinical trial in 31 patients with recurrent high-grade glioma [88, 89]. Apart from glioma, therapeutic effects of *IL-12* gene delivery to and expression in tumour cells have also been demonstrated in malignant melanoma, both alone and in combination with pembrolizumab [90, 91, 92]. Besides IL-12, gene delivery of many other transgenes encoding immunostimulating proteins, including *IL-15* and *CD40L*, has been investigated in *in vitro* or *in vivo* cancer models [93, 94]. Of particular note is *IFN-α2b*, the administration of which induced tumour regression in several preclinical cancer models with particular success in bladder cancer models [95, 96]. Most notably, intravesical application a replication-incompetent adenovirus delivering *IFN-α2b* has shown promising results in patients with BCG-refractory non-muscle-invasive bladder cancer in phase II and III trials, potentially leading to the FDA approval in the near future [97, 98]. This would make it the second approved cancer gene therapy encoding a cytokine after talimogene laherparepvec, also known as T-VEC, which is an oncolytic virus derived from herpes simplex virus type 1 and armed with a gene encoding human granulocyte macrophage colony-stimulating factor (GM-CSF), approved for the treatment of recurrent malignant melanoma [99, 100, 101].

1.2.2 Delivery systems

Whether to kill tumour cells directly, stimulate an immune response or achieve a combination of therapeutic effects, the effective delivery of therapeutic nucleic acids to tumour cells is essential for cancer gene therapy [102]. To achieve this, several delivery systems have been established, which can be broadly di-

vided into viral and non-viral systems [103].

Non-viral gene delivery systems include physical gene transfer, in which naked DNA enters cells through temporary physically or electrically induced membrane perturbations [104]. While most physical strategies, such as direct needle injection, gene guns and sonoporation, have been studied almost exclusively in the preclinical setting, electroporation has been successfully used to deliver genes to melanoma cells in clinical trials [92, 104]. In contrast to physical gene transfer, non-viral chemical delivery systems rely on DNA entering the cell surrounded by or bound to other molecules [104]. This includes gene delivery by liposomes of cationic lipids, such as N-[1-(2,3-dioleoyloxy)propyl]-N,N,N-trimethylammonium chloride (DOTAP):cholesterol, which allowed delivery of the transgene *TUSC2* to lung cancer cells after intravenous injection in a phase I clinical trial [105]. Alternatively, cationic polymers can be used for chemical gene transfer as they form complexes with DNA that are taken up by cells via endocytosis [106].

Because they rely on introducing their genetic material into host cells for replication, through evolution viruses have acquired properties making them suitable to serve as vectors for gene therapy [107]. Indeed, recombinant, replication-incompetent, viral vectors have become an important tool for therapeutic gene delivery [108]. The most studied types of these vectors are lentiviruses (LV), adenoviruses (Ad) and adeno-associated viruses (AAV) [107]. Unlike the nucleic acids delivered by Ad or AAV which stay episomal, the RNA payload of recombinant lentiviral vectors integrates in to the genome, allowing long term expression of transgenes at the cost of possible insertional mutagenesis [107]. While there have been clinical trials of LV-based cancer gene therapy, LV seem to be more suitable for *ex vivo* genetic modification, for example the insertion of cancer-targeted chimeric antigen receptor encoding genes into T cells [80, 108]. Recombinant AAV, which can be divided into several serotypes that differ in their capsid proteins and thus in their tissue tropism, have emerged as the leading viral vector for *in vivo* gene therapy of monogenetic genetic diseases [107, 108]. Their main advantages are their low immunogenicity and the relatively long episomal persistence of their genetic payload [107]. Although there are no published clinical data on AAV-based cancer gene therapy to date, preclinical studies have identified promising approaches that may warrant clinical trials [109].

Unlike some monogenetic diseases, where gene delivery to a fraction of cells is often sufficient to restore the function lost by the disease-causing mutation, durable remission in cancer is only possible if virtually all malignant cells are killed [110]. To achieve therapeutic effects, most cancer gene therapy approaches therefore require gene delivery to a large fraction of tumour cells [102]. While for replication incompetent vectors this implies the need to inject large amounts of gene delivery particles, another solution may be to use oncolytic viruses, which replicate preferentially in cancer cells, as vectors for nucleic acids that confer additional therapeutic effects [111]. Indeed, nu-

merous preclinical studies have investigated oncolytic viruses, including herpes simplex virus, measles virus, vaccinia virus, myxoma virus or Newcastle disease virus, which deliver genes encoding immunomodulators and have shown promising therapeutic effects in various human cancer models [111]. In particular, successive clinical trials eventually led to the FDA approval of talimogene laherparepvec, mentioned in the previous section, as the first cancer gene therapy and oncolytic virus therapy [99].

2. Aim and objectives

2.1 Research objective

Ewing sarcoma (EwS) is characterised by a single recurring driver mutation, a translocation resulting in the expression of the fusion transcription factor EWSR1::FLI1, lacking other targetable mutations. Its unfavourable prognosis and the morbidity that the highly aggressive, systemic chemotherapy regimens used in standard clinical treatment of this disease are accompanied by, require the development of both effective and specific new treatment strategies. Due to its presence in all EwS cells, the tumour cells' vital dependence on its function and its disease-specificity, i.e. its absence in non-EwS cells, EWSR1::FLI1 is an ideal therapeutic target. Unfortunately, as a transcription factor without an enzymatically active site, inhibition of EWSR1::FLI with small molecules is difficult and has been unsuccessful. Therefore, the aim of this project was to explore the possibility of using the binding of EWRSR1::FLI1 to `GGAA`-microsatellites to drive therapeutic transgenes specifically in Ewing sarcoma and to evaluate potential gene therapy approaches based on this interaction in preclinical models.

2.2 Scientific aims

1. Design of a Ewing sarcoma specific promoter consisting of `GGAA`-microsatellites and a minimal activity core promoter and evaluation of its specificity for EwS and dependence on EWSR1::FLI1.
2. Evaluation of the therapeutic applicability of EwS-specific promoters *in vitro*.
3. Establishment and evaluation of a EwS-specific targeted lentiviral transduction approach *in vitro* and *in vivo*.
4. Evaluation of therapeutic approaches based on EwS-specific gene expression and transduction *in vivo*.
5. Design of a promoter specific for PAX3::FOXO1-positive alveolar rhabdomyosarcoma and evaluation of its specificity.

3. Materials and Methods

3.1 Materials

3.1.1 Manufacturers

Table 3.1: Manufacturers

Name	Location
Abcam	Cambridge, UK
Addgene	Watertown, MA, USA
Alpha Innotech	Miami, FL, USA
American Type Culture Collection (ATCC)	Manassas, VA USA
B. Braun	Melsungen, Germany
Becton Dickinson (BD)	East Rutherford, NJ, USA
Berthold Technologies GmbH & Co. KG	Bad Wildbad, Germany
Bio-Rad Laboratories, Inc.	Hercules, CA, USA
Bio-Techne	Minneapolis, MN, USA
BioLegend	San Diego, CA, USA
Biozym	Hessisch Oldendorf, Germany
Bosch	Gerlingen, Germany
Brand	Wertheim, Germany
Camping Gaz GmbH	Hattersheim, Germany
Carl Roth GmbH + Co. KG	Karlsruhe, Germany
Carl Zeiss AG	Oberkochen,Germany
Charles River Laboratories	Wilmington, MA, USA
Cell Applications, Inc.	San Diego, CA, USA
Corning	Corning, NY, USA
Creative Biolabs	Shirley, NY, USA
Cytiva	Marlborough, MA, USA
Eppendorf SE	Hamburg, Germany
Eurofins Scientific	Luxembourg, Luxembourg
GE Healthcare	Chicago, IL, USA
Genscript Biotech	Piscataway Township, NJ, USA
German Collection of Microorganisms and Cell Cultures (DSMZ)	Brunswick, Germany
Gilson	Middleton, WI, USA
Greiner	Kremsmünster, Austria
Hartenstein	Würzburg, Germany

Table 3.1 continued from previous page

Name	Location
Heraeus	Hanau, Germany
Hettich	Tuttlingen, Germany
Integra	Zizers, Switzerland
Integrated DNA Technologies	Coralville, IA, USA
Invivogen	San Diego, CA, USA
Kern & Sohn	Balingen-Frommern, Germany
Kimberly-Clark	Irving, USA
LI-COR Biosciences	Lincoln, NE, USA
Life Technologies	Waltham, MA, USA
Lonza	Basel, Switzerland
Macherey-Nagel	Düren, Germany
Memmert	Schwabach, Germany
Merck KgaA	Darmstadt, Germany
Miele	Gütersloh, Germany
New England Bio Labs	Ipswitch, MA, USA
Peqlab	Erlangen, Germany
PerkinElmer	Waltham, MA, USA
PJK Biotech	Kleinblittersdorf, Germany
PromoCell GmbH	Heidelberg, Germany
Proteintech Europe	Manchester, UK
Roche	Basel, Switzerland
Santa Cruz Biotechnology	Dallas, TX, USA
Sartorius	Göttingen, Germany
Schott	Mainz, Germany
Selleck Chemicals	Houston, TX, USA
Siemens	Munich, Germany
Sigma-Aldrich	St. Louis, MO, USA
TAKARA BIO INC.	Kusatsu, Japan
Thermo Fisher Scientific	Waltham, MA, USA
TPP	Trasadingen, Switzerland
Vector Laboratories	Burlingame, CA, USA

3.1.2 Laboratory appliances

Table 3.2: Laboratory appliances

Device	Manufacturer	Model
Agarose gel imager	Alpha Innotech Corp.	FluorChem FC2 Imaging System
Aspiration system	Biosan	FTA-1
Aspiration system	Integra	Vacusafe
Automatic cell counter	Invitrogen	Countess II
Bacteria incubator	Heraeus	Heraeus B6030 Incubator
Bacteria incubator	Sartorius	CERTOMAT BS-1
Bunsen burner	Campingaz	Labogaz 206
Caliper gauge	A. Hartenstein	S15D

Table 3.2 continued from previous page

Device	Manufacturer	Model
Cell culture incubator	Thermo Fisher Scientific	HERAcell 240i
Centrifuge	Corning	LSE Mini
Centrifuge	Eppendorf	5415R
Centrifuge	Hettich	Rotina 320R
Centrifuge	Hettich	Universal 320
Centrifuge	Thermo Fisher Scientific	Heraeus Megafuge 40R
Centrifuge	Thermo Fisher Scientific	Heraeus Megafuge 8R
Electrophoresis gel chamber	Bio-Rad Laboratories	Sub-cell GT
Electrophoresis gel chamber	Peqlab	40-0911
Freezing container	Thermo Fisher Scientific	Mr. Frosty™
Flow cytometer	Becton Dickinson	BD FACSCanto
Ice maker	Nordcup	SPR-80
In vivo imaging system	PerkinElmer	IVIS-100
Laminar flow hood	Thermo Fisher Scientific	Maxisafe 2020
Microscope	Zeiss	Axiovert 200
Microscope	Zeiss	Axiovert 25
Microscope	Zeiss	Primovert
Microwave	Miele	8201-1
PCR thermal cycler	Bio-Rad Laboratories	T100 Thermal Cycler
PCR thermal cycler	Eppendorf	Mastercycler Pro
Pipets	Gilson	Pipetman G series
Pipette controller	Integra	Pipetboy 2
Plate reader	Berthold Technologies	Orion II microplate luminometer
Plate reader	Thermo Fisher Scientific	Varioskan Flash
Power supply unit	Bio-Rad Laboratories	PowerPac 300
Power supply unit	LifeTechnologies	PowerEase 300
qPCR thermal cycler	Bio-Rad Laboratories	CFX Connect
Repetitive Pipet	Brand	Handystep 705000
Scale	Kern und Sohn	KB1000-2
Scale	Sartorius	GE1302
Spectrophotometer	Thermo Fisher Scientific	Nanodrop 1000
Thermoshaker	Biosan	TS-100
Thermoshaker	Eppendorf	Thermomixer comfort
UV transilluminator	Thermo Fisher Scientific	Fisherbrand FT-20E/365
Vortex mixer	Corning	LSE
Western blot imaging system	LI-COR	Odyssey® XF

3.1.3 Consumables

Table 3.3: Consumables

Consumable	Manufacturer	Model
Cannulae	B. Braun	Sterican 30G, 23G, 18G
Cell culture flasks	Corning	T75, T175 flasks with filter caps (430641U, 431080)
Cell culture flasks	TPP	T25 flasks with filter caps (90026)

Table 3.3 continued from previous page

Consumable	Manufacturer	Model
Cell culture plates	Corning	96-well Clear Round Bottom (353227)
Cell culture plates	Nunclon	Delta Surface, 150 x 20mm (157150)
Cell culture plates	TPP	96-well, 24-well, 12-well and 6-well plates (92096, 92024, 92012, 92006)
Counting chamber	Carl Roth	C-Chip Neubauer improved
Laboratory film	Bemis	Parafilm
Mortar and pestle	A. Hartenstein	porcelain, rough, (PIS3, MO08)
PCR microtubes	Brooks Life Sciences	8-tube strip 0.2 ml with optically clear caps attached (045660)
PCR plate seals	Brooks Life Sciences	4ti-0560
PCR plates	Brooks Life Sciences	Framestar, 96-well, semi-skirted (4ti-0760)
Petri dishes	GBO	Petri dish, 100/20 MM, clear, with vents (664102)
Pipet tips	Biozym	10, 20, 100, 200, 1250 µl filter tips (VT0200, VT0220, VT0230, VT0240, VT0270)
Reaction tubes	A. Hartenstein	Microtubes with lid, 1,5 ml (RSF1)
Reaction tubes	A. Hartenstein	Microtubes with lid, 2 ml (RK2G)
Reaction tubes	Greiner	Tube, 15 ML, PP, 17/120 MM, conical (188261)
Reaction tubes	Greiner	Tube, 50 ML, PP, 30/115 MM, conical (227261)
Reaction tubes	Schott	DURAN Erlenmeyer flask 250ml, 500ml
Scalpels	B. Braun	CUTFIX, Typ 20 (5409808)
Serological pipets	Corning	Stripette 2ml, 5ml, 10ml, 25ml (4486, 4487, 4488, 4489)
Syringe filters	Carl Roth	Rotilabo, sterile, PVDF, 0.22 µm
Syringe filters	Carl Roth	Rotilabo, sterile, PVDF, 0.45 µm
Syringes	B. Braun	Omnifix, LuerLock 3ml, 5ml, 10ml, 50ml
Transwell plates	Corning	HTS Transwell®-96 Permeable Support with 3.0 µm Pore Polycarbonate Membrane
Vacuum filter system	Corning	250 mL, 0.22 µm, PES, Sterile (431096)
Western blotting membrane	Cytiva	Amersham™ Protran® Western blotting membrane (nitrocellulose, GE10600002)

3.1.4 Reagents, kits and solutions

Table 3.4: Chemicals, reagents and enzymes

Reagent	Manufacturer	Identifier
Acetic acid	Carl Roth	6755.1
Agarose	Carl Roth	3810.3
Albumin Fraction V, pH 5.2, Europe, 50 g	Carl Roth	2834.2
Ammonium persulfate	Sigma-Aldrich	A3678
Ampicillin sodium salt	Sigma-Aldrich	A9518
Bromophenol blue sodium salt	Carl Roth	A512.1
Dimethyl sulfoxide (DMSO)	Sigma-Aldrich	D4540
DL-Dithiothreitol solution	Sigma-Aldrich	646563

Table 3.4 continued from previous page

Reagent	Manufacturer	Identifier
DNase I recombinant	Roche	4536282001
dNTP mix 10mM	Carl Roth	L785.1
Doxycycline hyclate	Sigma-Aldrich	D9891
Dulbecco's Modified Eagle's Medium - high glucose	Sigma-Aldrich	D5796
Dulbecco's Phosphate Buffered Saline (PBS)	Sigma-Aldrich	D8537
EDTA	Carl Roth	CN06.3
Endothelial Cell Growth Medium	Cell Applications, Inc.	211-500
Ethanol	Carl Roth	K928.3
EX-CELL™ Hybridoma Medium	Sigma-Aldrich	H4281-1L
Fetal Bovine Serum	Sigma-Aldrich	S0115
Formaldehyde solution 4%	Sigma-Aldrich	1.00496
Ganciclovir	Selleck Chemicals	S1878
GeneRuler 1 kb Plus DNA-Leiter	Thermo Fisher Scientific	SM1331
Glycine	Carl Roth	0079.2
HyClone™ LS250 Lipid supplement	Cytiva	SH30555.01
Isopropanol	Carl Roth	6752.3
LB agar (Luria/Miller)	Carl Roth	X969.2
LB broth (Luria/Miller)	Carl Roth	X968.2
PEI MAX® Linear Polyethylenimine Hydrochloride (MW 40,000)	Polysciences Inc.	24765-1
Methanol	Carl Roth	4627.2
Opti-MEM® I Reduced Serum Medium	Thermo Fisher Scientific	31985-062
Phusion™ High-Fidelity DNA Polymerase	Thermo Fisher Scientific	F-530L
Polyethylene glycol 8000	Carl Roth	263.2
Powdered milk	Carl Roth	T145.3
Puromycin	Invivogen	ant-pr-1
Resazurin sodium salt	Sigma-Aldrich	R7017
RNAse free water	Carl Roth	T143.5
ROTIPHORESE®Gel 30 (37.5:1), 1 l	Carl Roth	3029.1
RPMI-1640 Medium	Sigma-Aldrich	R8758
Sodium chloride	Carl Roth	9265.1
Sodium dodecyl sulfate	Sigma-Aldrich	436143
Sucrose	Carl Roth	4621.2
Sulphuric acid 1M	Carl Roth	X873.1
T4 DNA Ligase	New England Biolabs	M0202L
TEMED	Carl Roth	2367.1
TRIS	Carl Roth	2449.2
TRIS hydrochloride	Carl Roth	9090.3
Triton™ X-100	Sigma-Aldrich	T8787
Trypan Blue Solution	Sigma-Aldrich	T8154
Trypsin-EDTA Solution 10X	Sigma-Aldrich	59418C
UltraCULTURE™ Serum-free Medium	Lonza	BP12-725F

Table 3.5: Restriction enzymes

Name	Manufacturer	Catalogue no.
AgeI-HF	New England Biolabs	R3552

Table 3.5 continued from previous page

Name	Manufacturer	Catalogue no.
AsiSI	New England Biolabs	R0630
AvrII	New England Biolabs	R0174
BamHI-HF	New England Biolabs	R3136
BlpI	New England Biolabs	R0585
Bsu36I	New England Biolabs	R0524
ClaI	New England Biolabs	R0197
EcoRI-HF	New England Biolabs	R3101
EcoRV-HF	New England Biolabs	R3195
FastDigest KflI	Thermo Fisher Scientific	FD2164
HindIII	New England Biolabs	R0104
KpnI-HF	New England Biolabs	R3142
NheI-HF	New England Biolabs	R3131
NsiI-HF	New England Biolabs	R3127
PacI	New England Biolabs	R0547
SalI	New England Biolabs	R0138
SpeI-HF	New England Biolabs	R3133

Table 3.6: Commercial kits and assays

Kit / Assay	Manufacturer	Identifier
APC Annexin V Apoptosis Detection Kit with PI	Biolegend	640932
Beetle-Juice Luciferase assay Firefly	PJK GmbH	102511
High-Capacity cDNA Reverse Transcription Kit	Thermo Fisher Scientific	4368814
Lipofectamine® LTX Reagent with PLUS™ Reagent	Thermo Fisher Scientific	15338100
NucleoBond Xtra Midi kit	Macherey-Nagel	740410
NucleoSpin Gel and PCR Clean-up	Macherey-Nagel	740609
NucleoSpin Plasmid	Macherey-Nagel	740588
NucleoSpin RNA	Macherey-Nagel	740955
NucleoSpin Tissue	Macherey-Nagel	740952
Renilla-Juice Luciferase assay	PJK GmbH	102531
SYBR SELECT Master Mix	Thermo Fisher Scientific	4472919
XenoLight™ D-Luciferin - K+ Salt Bioluminescent Substrate	PerkinElmer	122799

Table 3.7: Buffers and solutions

Solution	Concentration	Composition
APS	10%	1g ammonium persulfate to 10ml with H_2O.
Blotting buffer	1×	100ml R/B buffer, 200ml methanol, 700ml H_2O.

Table 3.7 continued from previous page

Solution	Concentration	Composition
Laemmli samples buffer	4×	10mL TRIS (1M, pH 6.8), 4g SDS, 20ml glycerol, 0.05g bromophenol blue to 50ml with H_2O.
Lentivirus Concentrator Solution	4×	40% w/v PEG8000, 1.337 M NaCl, 2.7 mM KCl, 8 mM Na2HPO4 und 2 mM KH2PO4 in H2O
Triton X lysis buffer	1×	438.3mg NaCl, 2.5ml TRIS (1M, pH 8.0), 5ml Triton X-100 to 50ml with H_2O.
Running / Blotting (R/B) buffer	10×	30.3g TRIS, 142.6g Glycine, 10g SDS to 1L with H_2O, adjust pH to 8.3.
Running buffer	1×	100ml R/B buffer, 900ml H_2O.
PEI mix	1 g/L	0.5 g linear Polyethylenimine Hydrochloride (MW 40,000) (PEI MAX®) to 500 ml H_2O. Adjust pH to 7.0 and sterilise by filtration.
SDS	10%	1g SDS, to 10ml with H_2O.
TAE	10×	48.5g TRIS, 2.9g EDTA, 11.4mL acetic acid. To 1000ml with H_2O.
TAE	1×	100ml 10x TAE, 900ml H_2O.
TBS	10×	24g TRIS, 88g NaCl, to 1L with H_2O, adjust pH to 7.6.
TBS	1×	100ml 10x TBS, 900ml H_2O.
TBS-T	1×	100ml 10x TBS, 1ml Tween 20, 899ml H_2O.
TRIS	1.0 M	60.57g to 500ml with H_2O.
TRIS Hcl	0.5 M	39.4g to 500ml with H_2O.
TRIS Hcl	1.5 M	118.2g to 500ml with H_2O.

Table 3.8: Composition of running gel for western blot

Component	Volume
30% (w/v) Acrylamid/Bisacrylamid	6 ml
1.5M Tris HCL (pH= 8.8)	3.75 ml
10% (w/v) SDS	150 µl
diH2O	5.03 ml
10% (w/v) APS	75 µl
TEMED (added last)	7.5 µl

Table 3.9: Composition of stacking gel for western blot

Component	Volume
30% (w/v) Acrylamid/Bisacrylamid	1.98 ml
0.5M Tris HCL (pH= 6.8)	3.78 ml
10% (w/v) SDS	150 µl
diH2O	9 ml
10% (w/v) APS	75 µl
TEMED (added last)	15 µl

3.1.5 Nucleic acids

Table 3.10: qPCR primers

Name	Sequence (5'-3')
RPLP0_FW	GAAACTCTGCATTCTCGCTTC
RPLP0_RW	GGTGTAATCCGTCTCCACAG
Actb_FW	GACTCATCGTACTCCTGCTTGCT
Actb_RV	GAGAGCTCACCATTCACCATCTT
EWSR1::FLI1_FW	GCCAAGCTCCAAGTCAATATAGC
EWSR1::FLI1_RV	GAGGCCAGAATTCATGTTATTGC
qPCR_HSVTK_FW	GCAGAAAATGCCCACGCTAC
qPCR_HSVTK_RV	CCAGTAAGTCATCGGCTCGG
qPCR_WPRE_FW	CCTTTCCGGGACTTTGCGTTT
qPCR_WPRE_RV	GCAGAATCCAGGTGGCAACA

Table 3.11: PCR and sequencing primers and oligos for cloning

Name	Sequence (5'-3')
3'-LTR_FW	TAGATCATAATCAGCCATACCAC
3'-LTR_OE_FW	CTGTACAAGTAATAGATCATAATCAGCCATACCAC
3'-LTR_RV	AAAGCCTAGGCCTCCAA
3'LTR_AvrII_RV	GTACGTCCCCTAGGCCTCC
3'LTR_NsiI_FW	TAATATGCATCATAATCAGCCATACCACATTTGT
AgeI_alc_FW	ATTAACCGGTCCTGCAGGATGGAGAATG
AgeI_XbaI_Insert_FW	CCGGTACGGGGAAAATTAATTAACATCCACTATGATCGATT
AgeI_XbaI_Insert_RV	CTAGAATCGATCATAGTGGATGTTAATTAATTTTCCCCGTA
BamHI_luc_FW	ATTAGGATCCGCCACCATGGAAGACGCC
CRISPR_Screen_FW	CGGATCTCGACGGTATCGGT
EGFRT_SalI_RV	GATTGTCGACTCACATGAAGAGGCCGATCC
FW_alc_cloning	AAGAGCAGTGGGAATAGGAG
GFP_ov_FW	AACCCTGGACCTATGGTGAGCAAGGGCGAGG
GFP_SalI_RV	AGCAGTCGACTTACTTGTACAGCTCGTCCATGCC
GGAA_AgeI_FW	TAATACCGGTACGGGGAAAATTAATTAAGGAA
gRNA_YBTATA_FW	TAAACAACCGCGAAAAAGTTGCGTGGTCTAGAGGGTATATAATGGGGGC CACTACTCTACTACCAGAAAGCTTGGTACCGAGCTCA
gRNA_YBTATA_RV	CTAGTGAGCTCGGTACCAAGCTTTCTGGTAGTAGAGTAGTGGCCCCCAT TATATACCCTCTAGACCACGCAACTTTTTCGCGGTTGTTTAAT
Ins1_AgeI_FW	ATTAACCGGTGGGGAGCTCACGGGGAC
Insulator_1_FW	ATTAGGGACCCTGAAAAC
Insulator_1_RV	TAATGATATCTCCGTTTTCA
Insulator_2_FW	ATTACCTAAGGAAAAGGGGC
Insulator_2_RV	TAATGCGATCGCCCTATAG
LKE_3'-LTR_FW	GGACGAGCTGTACAAGT
LKE_AsiSI_RV	GGGCTATGAACTAATGACCCCG
LKE_KflI_FW	CATTATCGTTTCAGACCCAC
LKE_Luc1_FW	ATCAAATCATTCCGGATACTGCG
LKE_Luc2_FW	ATCTTCGACGCAGGTGTCGCAG
LKE_msat_2_FW	GAAAACGGAACCGGTG

Table 3.11 continued from previous page

Name	Sequence (5'-3')
LKE_mSat_FW	AACGCTTCTCGCTGCTCTTTGAG
LKE_msat_RV	CCTCGATATGTGCATCTGTA
LKE_TK1_FW	AATGGGCATGCCTTATGCCGTG
LKE_TK2_FW	ACGCCCTGCTGCAACTTACCTC
LKE_TK3_FW	GAAAATGCCCACGCTACTGC
LKE_WPRE_FW	TACGTCCCTTCGGCCCTCAATCCAG
Luc_Fusion FW	ATTAACTAGTGCCACCATG
Luc_FW	ATGGAAGACGCCAAA
Luc_OE_RV	TCCAGCCTGCTTCAGCAGGCTGAAGTTAGTAG
Luc_ov_FW	ATTAACTAGTGCCACCATGGAAGACGCCAAA
Luc_ov_RV	CAGCAGGCTGAAGTTAGTAGCTCCGCTTCCCACGGCGATCTTTCC
Luc_RV	CACGGCGATCTTTCC
Luc_SalI_RV	TAATGTCGACCTACACGGCGATCTTTCCGC
msat_spacer_FW	TAACATCCACTATGAT
msat_spacer_RV	CGATCATAGTGGATGTTAAT
NheI_alc_FW	ATTAGCTAGCATGGAGAATGTTTGGGGTG
P2A_RV_ov	CTTGCTCACCATAGGTCCAGGGTTCTCCTCCAC
pGL4.17_insert_FW	GTACCTGAGCTCGCTAGCCTCGAGTTAATTAAGAT
pGL4.17_insert_RV	ATCTTAATTAACTCGAGGCTAGCGAGCTCAG
pGL4.17_post_insert_RV	TTTGGCATCTTCCATGGTG
pGL4.17_pre_insert_FW	GCAAAATAGGCTGTCCCC
pLenti_0_FW	CCGGTACGGGGAAAATTAATTAACATCCACTATGAT
pLenti_0_RV	CGATCATAGTGGATGTTAATTAATTTTCCCCGTACCGGTAT
pLenti_MCS_FW	CGATACCGGTAACCTTGGATGCATGGTAC
pLenti_MCS_RV	CATGCATCCAAGGTTACCGGTAT
Puro_BamHI_FW	TAATGGATCCGCCACCATGACCGAGTACAAGCCCAC
Puro_NsiI_RV	TACCATGCATTCAGGCACCGGGCTTGC
_FWPuro_Spacer	AATTCACGACCCCATGCA
Puro_Spacer_RV	TGGGGTCGTG
PuroR_NsiI_RV	CGGCATGCATTCAGGCACCGGGCTTGCG
SbfI_alc_FW	ATTACCTGCAGGATGGAGAATGTTTGGGGTGG
sbfI_Spacer_FW	TAACCTGCAGGTGCGCAGAATA
sbfI_spacer_RV	CTAGTATTCTGCGCACCTGCAGGTTAAT
SpeI_GFP_FW	ATTAACTAGTGCCACCATGGTGAGCAAGG
TK_Kozak_ATG_SpeI_FW	ATTAATACTAGTGCCACCATGGCTTCGTACCCCGGCCATC
TK_SalI_RV	TAATGCGATCGCTCCGTTTTCAGTCGACTCAGTTAGCCTCCCCC
TK-SR39_Fusion RV	TAATGCGATCGCTCC
TK-SR39_new_FW	GCTTCGTACCCCGGC
TK-SR39_OE_FW	TTCAGCCTGCTGAAGCAGGCTGGAGACG
TK-SR39_ov_FW	AAGCAGGCTGGAGACGTGGAGGAGAACCCTGGACCTGCTTCGTACCCCT GC
TK-SR39_ov_new_FW	AAGCAGGCTGGAGACGTGGAGGAGAACCCTGGACCTGCTTCGTACCCCG GC
TK-SR39_ov_RV	TAATGCGATCGCTCCGTTTTCAGGTACCTCAGTTAGCCTCCCCC
U6_prom_FW	GAGGGCCTATTTCCCATGATTC
U6_prom_SalI_FW	ATTAGTCGACGAGGGCCTATTTCCCATGATTC
WPRE_AsiSI_NsiI_RV	TAATATGCATCTCCGTTTTCAGCGATCGC
WPRE_AsiSi_RV	TAATGCGATCGCGCGGGGAGGCG
WPRE_FW	GGAACAATCAACCTCTGG
WPRE_ov_FW	ATTAGGTACCCTTGGAACAATCAACCTCTGG

Table 3.11 continued from previous page

Name	Sequence (5'-3')
WPRE_ov_RV	TAATGCGATCGCTCCGTTTTCACCTTAGGGCGGGGAGGCG
WPRE_RV	GCGGGGAGGCG
WPRE_SalI_FW	ATTAGTCGACCTTGGAACAATCAACCTCTGG
YB_TATA_FW	CGATTCTAGAGGGTATATAATGGGGGCCAA
YB_TATA_long_EcoRV_RV	ATTAGATATCGAGCTCGGTACCAAGCTTTC
YBL_SpeI_AsiSI_EcoRV_RV	AATTCGATATCTCCGTTTTCAGCGATCGCTCCGTTTTCAACTAGTGAGC TCGGTACCAAGCTTTCTGGTAGTAGAGTAGTGGCC

Table 3.12: Synthetic DNA and gene fragments

Name	Sequence (5'-3')
ALK_SE	AAATTAATTAACCTGCAGGATGGAGAATGTTTGGGGTGGACAGAAACTC CTCCAAGAAAGACAATGAAAGACAACAAGTTAGGTCACGGTGGCTAAAG AGGAGACAATGATTTGTTGTCTGACTCTCCAGCTACGATGGGGCTGTAA CTAATGAGGTTATTCTGGTTACAAAGGAAGCATTCAGCCCCTTAATGAA AAACTCTTTGGCAACTGGTGTTAGGGAAAGAAAAAACAAACCAGCAGCT TATTATTAGTTCCACAGCAAGTTAATTAATTTTTGCCAGTCACTTTGGG TCACTTGCTGGACTGAGCATCTGTCTCACTCATCGATTCTAGAGGGTAT ATAATGGGGGCCACTACTCTACTACCAGAAAGCTTGGTACCGAGCTCAC TAGTGCCACCA
IL-15_P2A_XCL1	TACCGAGCTCACTAGTGCCACCATGGATTTTCAGGTGCAGATTTTCAGC TTCCTGCTAATCAGTGCCTCAGTCATAATGTCTAGAGCCAACTGGGTGA ATGTAATAAGTGATTTGAAAAAAATTGAAGATCTTATTCAATCTATGCA TATTGATGCTACTTTATATACGGAAAGTGATGTTCACCCCAGTTGCAAA GTAACAGCAATGAAGTGCTTTCTCTTGGAGTTACAAGTTATTTCACTTG AGTCCGGAGATGCAAGTATTCATGATACAGTAGAAAATCTGATCATCCT AGCAAACAACAGTTTGTCTTCTAATGGGAATGTAACAGAATCTGGATGC AAAGAATGTGAGGAACTGGAGGAAAAAAATATTAAAGAATTTTTGCAGA GTTTTGTACATATTGTCCAAATGTTCATCAACACTTCTGGAAGCGGAGC TACTAACTTCAGCCTGCTGAAGCAGGCTGGAGACGTGGAGGAGAACCCT GGACCTATGAGACTTCTCATCCTGGCCCTCCTTGGCATCTGCTCTCTCA CTGCATACATTGTGGAAGGTAAGTCGAGTCGTTGGATCCCCACTACAGC CGATACTCAAGCTTGACGAATTCGAGTATCCAAGGTAGTGGACTAGAGT GACGCTGCTGACCCCTTTCTTTCCCTTCTGCAGGTGTAGGGAGTGAAGT CTCAGATAAGAGGACCTGTGTGAGCCTCACTACCCAGCGACTGCCGGTT AGCAGAATCAAGACCTACACCATCACGGAAGGCTCCTTGAGAGCAGTAA TTTTTATTACCAAACGTGGCCTAAAAGTCTGTGCTGATCCACAAGCCAC ATGGGTGAGAGACGTGGTCAGGAGCATGGACAGGAAATCCAACACCAGA AATAACATGATCCAGACCAAGCCAACAGGAACCCAGCAATCGACCAATA CAGCTGTGACTCTGACTGGCTAGGTCGACCTTGGAACA

Table 3.12 continued from previous page

Name	Sequence (5'-3')
Insulator_1	ATTAGGGACCCTGAAAACGGAACCGGTGGGGAGCTCACGGGGACAGCCC CCCCCCAAAGCCCCCAGGGATGTAATTACGTCCCTCCCCCGCTAGGGGG CAGCAGCGACCGCCCGGGGCTCCGCTCCGGTCCGGCGCTCCCCCCGCAT CCCGAGCCGGCAGCGTGCGGGGACAGCCCGGGCACGGGGAAGGTGGCAC GGGATCGCTTTCCTCTGAACGCTTCTCGCTGCTCTTTGAGCCTGCAGAC ACCTGGGGGATACGGGGAAAAAGCTTTATCTAGATCCGCGGGGAGCTCA CGGGGACAGCCCCCCCCCAAAGCCCCCAGGGATGTAATTACGTCCCTCC CCCGCTAGGGGGCAGCAGCGACCGCCCGGGGCTCCGCTCCGGTCCGGCG CTCCCCCCCGCATCCCGAGCCGGCAGCGTGCGGGGACAGCCCGGGCACGG GGAAGGTGGCACGGGATCGCTTTCCTCTGAACGCTTCTCGCTGCTCTTT GAGCCTGCAGACACCTGGGGGATACGGGGAAAATTAATTAATGAAAACG GAGATATCATTA
Insulator_2	ATTACCTAAGGAAAAGGGGCATAGGGGGTCCACAGACGTCCGAGTTTCT CGTCGCTCTTCGCAAGTCTCCTTTCGCTAGGGCACGGTGGAAGGGGCAC GGGCCCGACAGGGGCGTGCGACGGCCGAGCCCTACGCCCCCCTCGCGGC CTGGCCTCGCCTCGGGGCCCGCCAGCGACGACGGGGGATCGCCCCCTCC CTGCATTAATGTAGGGACCCCCGAAACCCCCCCCCGACAGGGGCACTCG AGGGGCGCCTAGATCTATTTCGAAAAAGGGGCATAGGGGGTCCACAGAC GTCCGAGTTTCTCGTCGCTCTTCGCAAGTCTCCTTTCGCTAGGGCACGG TGGAAGGGGCACGGGCCCGACAGGGGCGTGCGACGGCCGAGCCCTACGC CCCCCTCGCGGCCTGGCCTCGCCTCGGGGCCCGCCAGCGACGACGGGGG ATCGCCCCCTCCCTGCATTAATGTAGGGACCCCCGAAACCCCCCCCCGA CAGGGGCACTCGAGGGGGGAATTAGCTTGGTACTAATACGACTCACTAT AGGGCGATCGCATTA
msat_17_YB_TATA	TTAATTAAGGAAGGAAGGAAGGAAGGAAGGAAGGAAGGAAGGAAGGAAG GAAGGAAGGAAGGAAGGAAGGAAGGAAATCGATTCTAGAGGGTATATAA TGGGGGCCACTACTCTACTACCAGAAAGCTTGGTACCGAGCTCGATATC
msat_21_YB_TATA	TTAATTAAGGAAGGAAGGAAGGAAGGAAGGAAGGAAGGAAGGAAGGAAG GAAGGAAGGAAGGAAGGAAGGAAGGAAGGAAGGAAGGAAATCGAT TCTAGAGGGTATATAATGGGGGCCACTACTCTACTACCAGAAAGCTTGG TACCGAGCTCGATATC
msat_25_YB_TATA	TTAATTAAGGAAGGAAGGAAGGAAGGAAGGAAGGAAGGAAGGAAGGAAG GAAGGAAGGAAGGAAGGAAGGAAGGAAGGAAGGAAGGAAGGAAGG AAGGAAGGAAATCGATTCTAGAGGGTATATAATGGGGGCCACTACTCTA CTACCAGAAAGCTTGGTACCGAGCTCGATATC
SYN_ALK_1	TCGATACCGGTCCTGCAGGATGGAGAATGTTTGGGGTGGACAGAAACTC CTCCAAGAAAGACAATGAAAGACAACTCAATTAGTCACGGTGGCTAAGC AGGAGACAATGATTTGTTGTCTGACTCTCCAGCTACGATGGGGCTGTAA CTAATGAGGTTATTCTGGTTACAAAGGAAGCATTCAGCCCCTTAATGAA AAACTCTTTGGCAACTGGTGTTAGGGAAAGAAAAAACAAACCAGCAGCT TATTATTAGTTCCACAGCAAGTTAATTAATTTTTGCCAG
SYN_ALK_3_insert_FW	GGATGGAGAATGTTTGGGGTGGACAGAAACTCCTCCAAGAAAGACAATG AAAGACAACTCAATTAGTCACGGTGGCTAACAACTCAATTAGTCACGGT GGCTAACAACTCAATTAGTCACGGTGGC
SYN_ALK_3_insert_RV	TTAGCCACCGTGACTAATTGAGTTGTTAGCCACCGTGACTAATTGAGTT GTTAGCCACCGTGACTAATTGAGTTGTCTTTCATTGTCTTTCTTGGAGG AGTTTCTGTCCACCCCAAACATTCTCCATCCTGCA

Table 3.12 continued from previous page

Name	Sequence (5'-3')
SYN_ALK_5_insert_FW	GGATGGAGAATGTTTGGGGTGGACAGAAACTCCTCCAAGAAAGACAATG AAAGACAACTCAATTAGTCACGGTGGCTAACAACTCAATTAGTCACGGT GGCTAACAACTCAATTAGTCACGGTGGCTAACAACTCAATTAGTCACGG TGGCTAACAACTCAATTAGTCACGGTGGC
SYN_ALK_5_insert_RV	TTAGCCACCGTGACTAATTGAGTTGTTAGCCACCGTGACTAATTGAGTT GTTAGCCACCGTGACTAATTGAGTTGTTAGCCACCGTGACTAATTGAGT TGTTAGCCACCGTGACTAATTGAGTTGTCTTTCATTGTCTTTCTTGGAG GAGTTTCTGTCCACCCCAAACATTCTCCATCCTGCA
YB_TATA_long_FW	TAACATCCACTATGATCGATTCTAGAGGGTATATAATGGGGGCCACTAC TCTACTACCAGAAAGCTTGGTACCGAGCTCA
YB_TATA_long_RV	CTAGTGAGCTCGGTACCAAGCTTTCTGGTAGTAGAGTAGTGGCCCCCAT TATATACCCTCTAGAATCGATCATAGTGGATGTTAAT

Table 3.13: Plasmids

Name	Source	Catalogue no.
2.2	Addgene	#34885
Luciferase-pcDNA3	Addgene	#18964
pCD/NL-BH*DDD	Addgene	#17531
pCEF-VSV-G	Addgene	#41792
pOTTC407 - pAAV EF1a eGFP	Addgene	#60058
EF.CMV.RFP	Addgene	#17619
pET23d:HSVTK-SR39	M.Black, Washington State University	
pGL4.17[luc2/Neo]	Promega	E6721
pLenti CMV GFP Puro (658-5)	Addgene	#17448

3.1.6 Antibodies

Table 3.14: Antibodies

Name	Manufacturer	Catalogue no.
Anti GPR64 (extracted from Murine Hybridoma Cell Line OAM6 #93)	ATCC	PTA-5704
Anti-GD2 Recombinant Antibody	Creative Biolabs	TAB-731
APC anti-human CD8 Antibody	Biolegend	344722
FAT4 Antibody	Bio-Techne	NBP1-78381
Goat anti-Mouse IgG (H+L) Cross-Adsorbed Secondary Antibody, APC	Invitrogen	A-865
Goat anti-Rabbit IgG (H+L) Cross-Adsorbed Secondary Antibody, APC	Invitrogen	A-10931
HRP-conjugated GAPDH	Proteintech	HRP-60004
Human HLA Class I Antibody	Bio-Techne	MAB7098

Table 3.14 continued from previous page

Name	Manufacturer	Catalogue no.
Luciferase (C-12) HRP	Santa Cruz Biotechnology	sc-74548 HRP
Mouse IgG2b Isotype Control	Invitrogen	#02-6300
Pacific Blue™ anti-human CD3 Antibody	Biolegend	300330
PE anti-human CD4 Antibody	Biolegend	357404
Purified anti-human CD99 Antibody	Biolegend	371302
Rabbit IgG Isotype Control	Invitrogen	#02-6102

3.1.7 Cells, bacteria and mouse model

Table 3.15: Human cell lines

Tissue of origin	Name	Source
Alveolar rhabdomyosarcoma	RH30	DSMZ
Alveolar rhabdomyosarcoma	RH4	ATCC
Cervix carcinoma	HeLa	DSMZ
Embryonal kidney	293T	DSMZ
Embryonal rhabdomyosarcoma	RD	ATCC
Endothelium	HUVEC	PromoCell GmbH
Ewing sarcoma	A-673	ATCC
Ewing sarcoma	A673/TR/shEF1	M. Orth [31]
Ewing sarcoma	A673/TR/shctrl	M. Orth [31]
Ewing sarcoma	MHH-ES-1	DSMZ
Ewing sarcoma	RD-ES	DSMZ
Ewing sarcoma	SK-N-MC	DSMZ
Ewing sarcoma	TC-106	Children's Oncology Group (COG)
Ewing sarcoma	TC-71	Children's Oncology Group (COG)
Hepatoma/hepatoblastoma	Hep-G2	DSMZ
Lung fibroblasts	MRC-5	ATCC
Osteosarcoma	U2-OS	DSMZ
Pancreatic adenocarcinoma	PA-TU-8988T	DSMZ

Table 3.16: Bacteria

Bacteria	Manufacturer	Catalogue no.
Stellar™ Competent Cells	Takara Bio Inc.	636766

Table 3.17: Mouse model

Name	Full Nomenclature	Provider
NOD SCID gamma	NOD.Cg-Prkdc^{SCID}Il2rg^{tm1Wjl}/SzJ	Charles River Laboratories

3.2 Methods

3.2.1 Molecular cloning

The plasmids used for reporter assays and lentiviral vector production were generated by repeated conventional restriction ligation cloning. This involves digesting a plasmid and the DNA to be inserted into it with the same restriction enzymes. A new circular plasmid containing the inserted DNA is then formed by ligation of the resulting linear DNA fragments with compatible ends.

Agarose gel electrophoresis

Agarose gels were created by mixing 1 g of agarose with 100 ml of 1× TAE buffer and heating the resulting mixture in a microwave oven at 1000 W for 150 s. Afterwards, the solution was allowed to cool down for 2 min, 10 µl of *SYBR Safe DNA Gel Stain* was added and the resulting mix was poured into a horizontal gel electrophoresis chamber with appropriately sized combs. After 30 min of cooling and solidification at room temperature, the resulting gel was completely submerged in 1× TAE buffer, the combs removed and 50 µl of the DNA to be seperated, mixed in a 5 to 1 ratio with DNA loading dye, were loaded into the slots. For assessing DNA fragment lengths, 12 µl of *1kb plus DNA ladder* were added to another slot. Electrophoresis was performed for around 30 min at a voltage of 100 mV. Gel sections containing the desired DNA fragments were cut out with single-use scalpels on a UV transilluminator. DNA was purified from the gel segments with the *NucleoSpin Gel and PCR Clean-up kit* following the manufacturer's protocol.

Standard cloning procedures

All cloning procedures were designed using the software provided by benchling.com. For each step, 1 µg of insert DNA and 1 µg of plasmid DNA were digested simultaneously with the same two restriction enzymes according to the manufacturer's protocol for the corresponding enzyme combination. The insert DNA was either the result of polymerase chain reaction (PCR) using primers with 5' overhangs containing sequences for the desired cleavage sites, or directly digested or pre-existing plasmids. Standard reaction components and cycling conditions for endpoint PCR are described in Table 3.18 and Table 3.19. PCR products and digested DNA fragments were separated by agarose gel electrophoresis.

For ligation, 25 ng of digested plasmid DNA was mixed with digested insert DNA at a 1 to 5 molar ratio and 1 µl of T4 ligase and 2 µl of T4 ligase reaction buffer according to the manufacturer's protocol, adjusted with DNAse-free water to give a total reaction volume of 20 µl. For sticky end ligation, the reaction mixes were incubated at room temperature for 25 min, and for blunt end ligation at 16 °C for 12 hours. The *Stellar™ Competent*

Table 3.18: Components of endpoint PCR

Component	Volume [µL]
5X Phusion™ HF Buffer	10
dNTPs (10 mM)	1
Forward primer (10 µM)	1.25
Reverse primer (10 µM)	1.25
Template	1
Phusion™ High–Fidelity DNA Polymerase	0.5
H_2O	35

Table 3.19: Cycling conditions for endpoint PCR

Step	Temperature [°C]	Duration [s]	Cycles
Initial Denaturation	98	30	1
Denaturation	98	5	35
Annealing	X	30	35
Elongation	72	30s per 1kb	35
Final extension	72	300	1

Annealing temperatures were calculated based on primer sequences using the Tm Calculator provided by www.thermofisher.com. All endpoint PCRs and colony PCRs were performed as touchdown PCR starting with annealing temperatures 5 °C higher than calculated and decreasing by 0.5 °C per cycle for the first 10 cycles followed by 25 cycles with the calculated annealing temperature [112].

Cells were then transformed according to the manufacturer's protocol. After thawing the competent cells on ice, 50 µl of competent cells were mixed with 3 µl of ligation mix in a fresh 1.5ml reaction tube. After incubation on ice for 30 min, a heat shock of 45 s at 42 °C was carried out, followed by a further incubation on ice for 5 min. Then 450µl of SOC medium pre-warmed to 37ºC was gently added to the bacteria and the resulting mixture was incubated at 37ºC for 1 hour. 100 µl of the bacteria-containing medium was then spread on an LB agar plate prepared with an ampicillin concentration of 100 µg/mL.

After overnight incubation at 37 °C, 8 to 16 single colonies were picked with sterile 10 µl pipette tips and inoculated into 20 µl of LB medium supplemented with ampicillin at a concentration of 100 µg/mL. From each of the resulting 20 µl containing single colonies, 1 µl was used as template for PCR, which was performed as described in tables 3.18 and 3.19. The products of this colony PCR were separated by agarose gel electrophoresis. The presence of DNA of the expected colony PCR product length was used to indicate colonies containing correctly ligated plasmids, which were then incubated overnight in 5 ml LB medium containing 100 µg/ml ampicillin.

The next day, 500 µl of turbid cultures were mixed with 500 µl of sterile 50% glycerol to make glycerol stocks for long-term storage of transformed bacteria. Plasmids were purified from the remaining 4.5 µl of bacterial cultures using the Macherey-Nagel NucleoSpin Plasmid Kit according to the manufacturer's instructions. Plasmid concentrations were measured using a Nanodrop 1000 spectrophotometer. To confirm the sequence integrity of the resulting plasmid clones, Sanger sequencing was performed using Eurofins Genomic's SupremeRun Tube service with primers resulting in reads spanning at least the entire insert and cut sites.

Cloning of luciferase reporter plasmids

To assess the promoter activity of constructs consisting of GGAA repeats and the minimal promoter YB_TATA [113], synthetic DNA segments containing 17, 21 or 25 GGAA repeats linked to the YB_TATA promoter by a ClaI cut site (msat_17_YB_TATA, msat_21_YB_TATA and msat_25_YB_TATA) were prepared by Genscript and inserted into pGL4. 17 reporter plasmid containing a *firefly luciferase* (Fluc) transgene. First, a multiple cloning site containing a PacI restriction site (created by aligning the oligos pGL4.17_insert_FW and pGL4.17_insert_RV) was inserted into pGL4.17 after double digestion with KpnI-HF and EcoRV-HF, resulting in the plasmid pGL4-17+i. Using PacI and EcoRV-HF, the synthetic GGAA-msat YB_TATA combinations were inserted directly upstream of the luciferase, resulting in plasmids pGL4.17_17_YBL, pGL4.17_21_YBL and pGL4.17_25_YBL (Figure 3.1).

To evaluate putative PAX3::FOXO1-dependent promoter constructs, reporter plasmids were generated in a similar manner. First, a DNA segment (chr2:29,657,671-29,657,976, hg38 [114]) previously identified as a strong

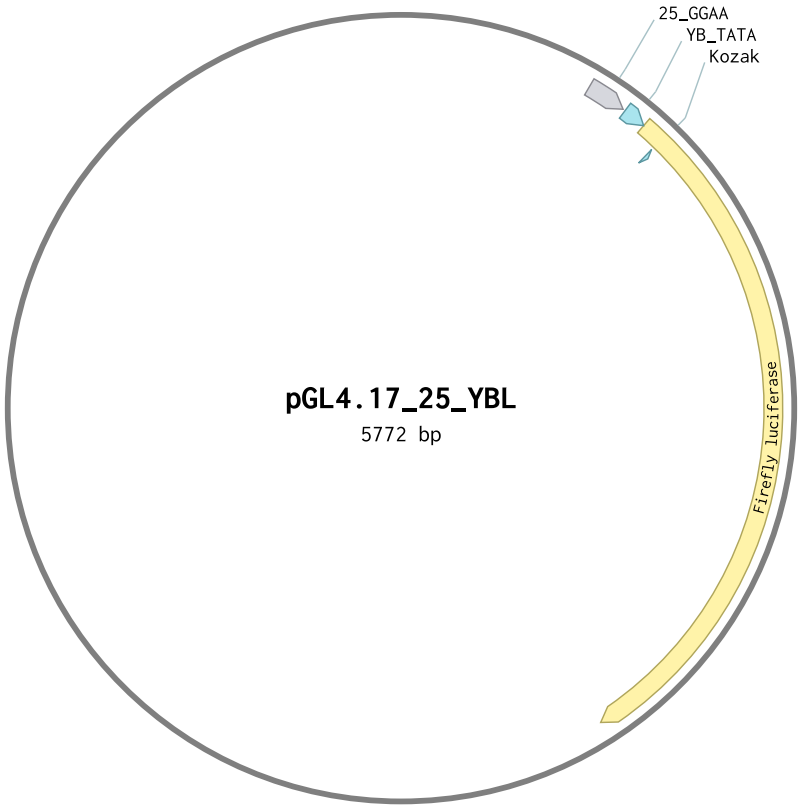

Figure 3.1: Plasmid map of pGL4.17_25_YBL.
Created using benchling.com.

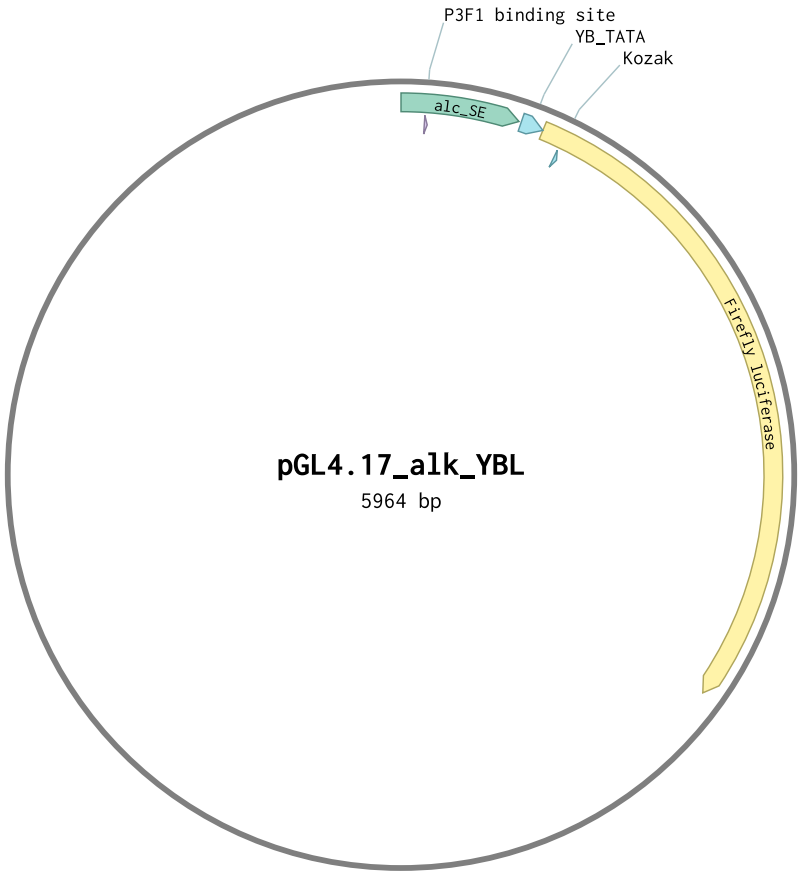

Figure 3.2: Plasmid map of pGL4.17_alk_YBL.
Created using benchling.com.

PAX3::FOXO1 binding site was synthesised using Genscript and joined at the 3' end to YB_TATA via a ClaI cut site. This combination of genomic sequence and a minimal activity promoter, termed ALK-SE, was then amplified by PCR using primers NheI_alc_FW and YB_TATA_long_EcoRV_RV, and the product cloned into pGL4.17+i using restriction enzymes NheI-HF and EcoRV-HF, resulting in plasmid pGL4.17_alk_YBL (Fig. 3.2).

Similarly, a modified version of ALE-SE containing an optimised PAX3::FOXO1 binding site (`TCAATTAGTCACGGT` vs genomic `GTCACGGT`) was created by replacing the 5' portion of ALK-SE in pGL4.17_alk_YBL with SYN_ALK_1, resulting in plasmid pGL4.17_synalk_1_YBL. This was achieved by digestion of pGL4.17_alk_YBL with PacI and EcoRV-HF, ligation of the resulting 120bp 3' fragment of ALK-SE to PacI-restricted SYN-ALK1 and PCR amplification of the correctly ligated fragment with NheI_alc_FW and YB_TATA_long_EcoRV_RV. Similarly, plasmids identical to pGL4.17_synalk_1_YBL but containing 3 or 5 of the optimised PAX3::FOXO1 binding sites instead of one were generated: pGL4.17_synalk_1_YBL was digested with BlpI and EcoRV-HF to obtain the 3' fragment of SYN_ALK_1 combined with YB_TATA and ligated to the

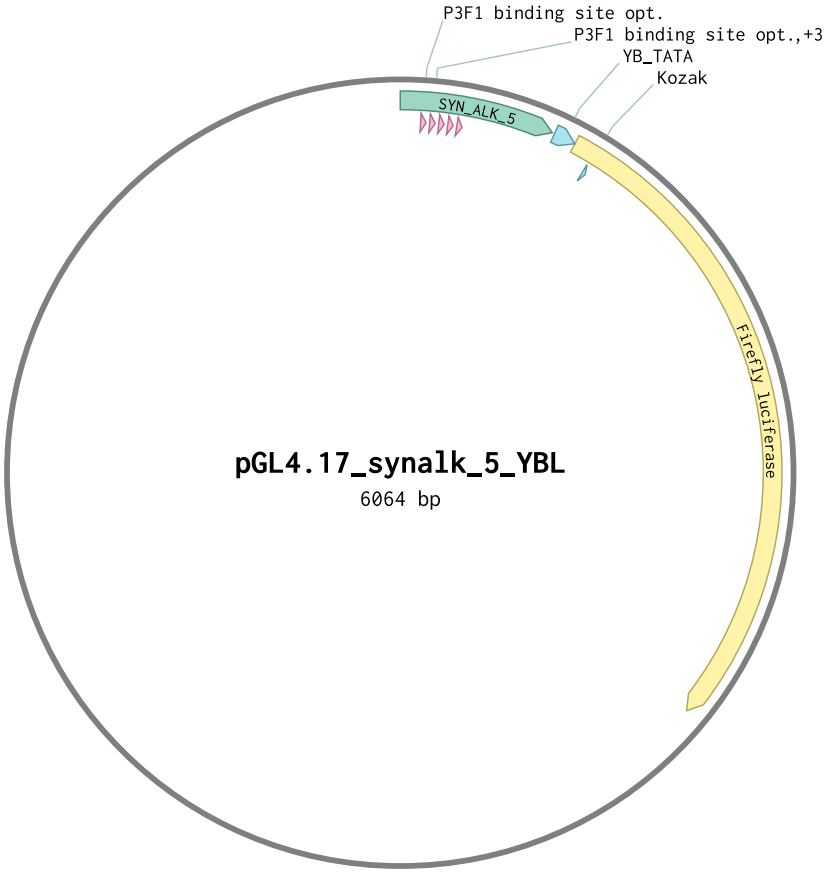

Figure 3.3: Plasmid map of pGL4.17_syn_alk_5_YBL.
Created using benchling.com.

annealed oligos SYN_ALK_3_insert_FW and RV or SYN_ALK_5_insert_FW and RV at the BlpI site. After amplification with NheI_alc_FW and YB_TATA_long_EcoRV_RV, the resulting DNA fragments were cloned into the pGL plasmid using NheI-HF and EcoRV-HF, resulting in the plasmids pGL4.17_synalk_3_YBL and pGL4.17_synalk_5_YBL (Figure 3.3).

Cloning of lentiviral plasmids

To evaluate the therapeutic applications of the 25_GGAA_YBL expression cassette, lentiviral plasmids carrying therapeutic transgenes were generated using a stepwise approach. The plasmid EF.CMV.RFP was used for the sequential assembly of an insert to be inserted into the p156RRL-sinPPT backbone of the pLenti CMV GFP Puro (658-5) construct. First, insulator_1 was inserted into EF.CMV.RFP using KflI and EcoRV. Then 25_GGAA_YBL was added after PCR amplification from pGL4.17_25_YBL using the primer YBL_SpeI_AsiSI_EcoRV_RV, which adds additional restriction sites for downstream insertion. The next insert was a herpes simplex virus-1 thymidine kinase linked to the 3' end of a firefly luciferase by a self-

cleaving P2A peptide linker by overlap extension PCR [115]. The HSV-TK mutant SR39, which induces ganciclovir-mediated cytotoxic effects at lower product concentrations than wild-type HSV-TK, was amplified from plasmid pET23d:HSV-TK-SR39, kindly provided by M. Black, Washington State University. Black, Washington State University, using TK_TK-SR39_ov_FW and TK-SR39_ov_RV primers and firefly luciferase from Luciferase pcDNA3 using Luc_ov_FW and Luc_ov_RV [116]. The luciferase and HSV-TK were extended for overlap extension using Luc_OE_RV and TK-SR39_OE_FW and the previously used forward and reverse primers, respectively. The overlap extension PCR was performed and the resulting FLuc_HSV-TK was inserted into the assembly plasmid downstream of 25_GGAA_YBL using SpeI-HF and AsiSI. Next, WPRE was amplified from pLenti CMV GFP Puro (658-5) using WPRE_SalI_FW and WPRE_ov_RV and inserted downstream of FLuc_P2A_HSV-TK using SalI-HF and Bsu36I. Then Insulator_2 was inserted using Bsu36I and AsiSI. Finally, to add a puromycin resistance gene, PuroR was amplified from pLenti CMV GFP Puro (658-5) using Puro_BamHI_FW and Puro_NsiI_RV, ligated to the 3'-LTR amplified from EF.CMV.RFP using 3'LTR_NsiI_FW and 3'-LTR_RV, and inserted into the assembly plasmid using BamHI and AvrII. A multiple cloning site based on the annealed pLenti_MCS_FW and pLenti_MCS_RV was added to pLenti CMV GFP Puro (658-5), leaving the vector backbone to which the sequentially generated insert from the assembly vector was added using AgeI and NsiI, resulting in plasmid pLenti_25_YBL_LT_Puro (Figure 3.4). An identical plasmid lacking the GGAA-microsatellite upstream of YBL was generated by insertion of the annealed oligos msat_spacer_FW and msat_spacer_RV using PacI and ClaI restriction, allowing the generation of the control plasmid pLenti_0_YBL_LT_Puro. For other plasmids, the insulators were removed to allow higher viral titres for *in vivo* experiments. This was achieved by PCR amplification of the insert from the GGAA-microsatellite to WPRE using primers GGAA_AgeI_FW and WPRE_AsiSI_RV and insertion into the backbone of AgeI and AsiSI digested pLenti_25_YBL_LT_Puro, resulting in the vector pLenti_25_YBL_LT_Puro_woIns. By amplifying WPRE with WPRE_SalI_FW and WPRE_AsiSI_NsiI_RV pLenti_25_YBL_LT_Puro_woIns and inserting it into the same backbone after NsiI and SalI restriction, the plasmid pLenti_25_YBL_LT, lacking both insulators and the puromycin resistance cassette, was generated for in vivo experiments (Fig. 3.5). As a control plasmid for in vivo experiments, pLenti_CMV_LG_Puro, a plasmid identical to pLenti CMV GFP Puro (658-5) but containing Fluc_P2A_GFP instead of regular GFP, was created. This was done by amplifying Fluc_P2A from pLenti_25_YBL_LT_Puro using primers BamHI_luc_FW and P2A_RV_ov and GFP from pLenti CMV GFP Puro (658-5) using primers GFP_ov_FW and GFP_SalI_RV. Overlap extension PCR using primers BamHI_luc_FW and GFP_SalI_RV together with the two previous PCR products yielded Luc_P2A_GFP, which replaced the

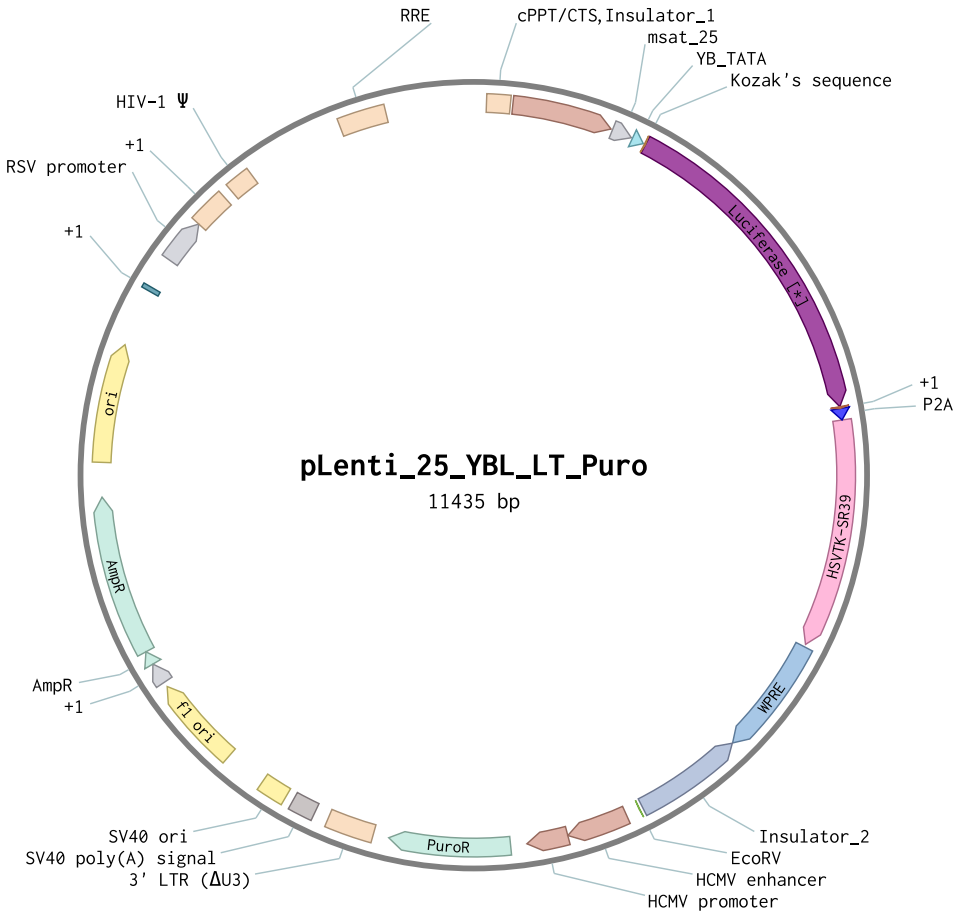

Figure 3.4: Plasmid map of pLenti_25_YBL_LT_Puro.
Created using benchling.com.

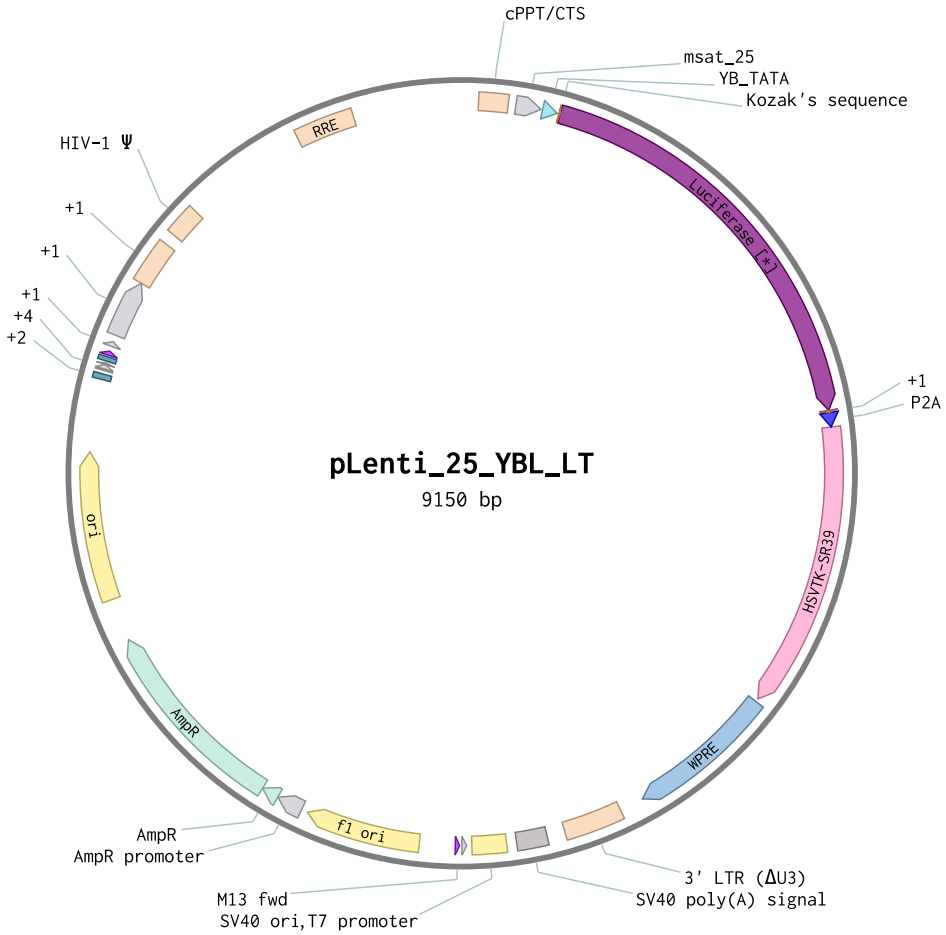

Figure 3.5: Plasmid map of pLenti_25_YBL_LT.
Created using benchling.com.

transgene GFP in pLenti CMV GFP Puro (658-5) after BamHI and SalI digestion. The plasmid pLenti_CMV_LG (Fig. 3.6) was generated deletion of the PuroR and its PGK promoter from pLenti_CMV_LG_Puro by insertion of the annealed DNA oligos Puro_Spacer_FW and Puro_Spacer_RV after a double digest with EcoRI-HF and NsiI-HF.

3.2.2 Cell culture

Cell lines

The human wild-type cell lines used in this study and their origins are listed in Table 3.15. A673/TR/shEF1 and A673/TR/shctrl, generated and provided by M. Orth, are A-673-derived cell lines that allow doxycycline-induced expression of a small hairpin RNA (shRNA) against EWSR1::FLI1 (shEF1) or a non-targeting control shRNA [31].

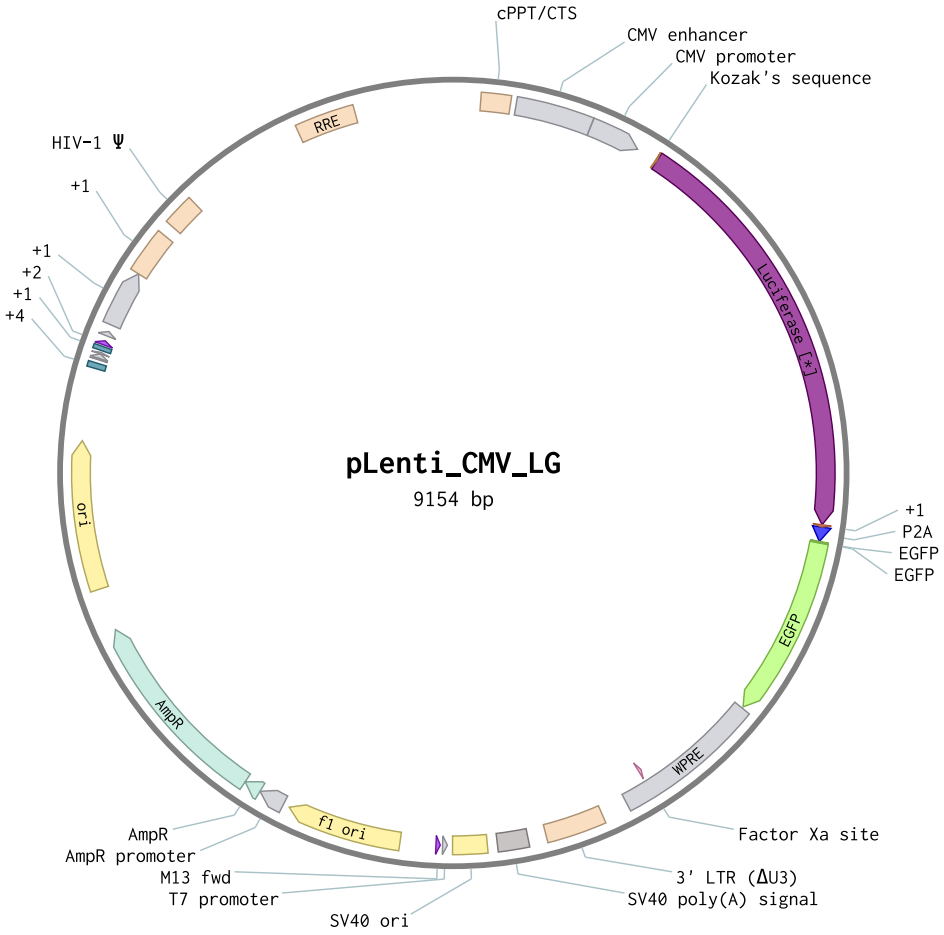

Figure 3.6: Plasmid map of pLenti_CMV_LG.
Created using benchling.com.

General culture conditions

Cell culture handling was performed under a class II laminar flow hood using aseptic technique. All cell lines used in this work were maintained in a humidified atmosphere containing 5% CO2 at 37°C. With the exception of 293T and HUVEC, all cell lines were grown in RPMI-1640 medium containing stable L-glutamine and sodium bicarbonate supplemented with 10% tetracycline-free fetal bovine serum (FCS) from Sigma-Aldrich. For 293T cells, DMEM medium containing 4500 mg/mL glucose, L-glutamine and sodium bicarbonate supplemented with 10% FCS from Sigma-Aldrich was used. HUVEC were cultured in endothelial cell growth medium. To ensure the purity, cell lines were regularly tested for mycoplasma contamination using a previously published nested PCR protocol [117]. With the exception of HUVEC, the identities of the cell lines were authenticated by comparing their STR profiles with those annotated using the human STR profile search engine provided by DMSZCellDive (https://celldive.dsmz.de/str) and CLASTR [118, 119].

Subculturing and storage

Adherent cell lines were grown at densities of $3.0 \cdot 10^4$ to $1.2 \cdot 10^5$ cells per cm^2 with 0.16 ml of medium per cm^2 of dish surface. Non-adherent Jurkat were cultured at densities of 0.5 to $1.5 \cdot 10^6$ cells per ml. For subculturing adherent cells, the covering medium was aspirated followed by gentle washing with 0.08 ml of PBS per cm^2. Detachment was achieved by adding 1-2 ml of trypsin-EDTA solution (1×) and incubation at 37 °C for 3-5 min, after which the reaction was stopped with FCS-containing cell culture medium. The detached cells were then transferred to a 15 ml reaction tube and centrifuged at 400 g for 4 min. After careful aspiration of the supernatant, the cell pellet was resuspended in fresh medium for further culture.

For short to medium term storage, cells were frozen at −80 °C. For this purpose, the pelleted cells were resuspended in a freezing solution consisting of 70 % RPMI-1640, 20 % FCS and 10 % DMSO. The resuspended cells were divided into 1ml aliquots in screw cap freezing tubes and immediately stored in a Mr.Frosty™ freezing container at −80 °C, allowing a gradual temperature decrease of approximately 1 °C per minute. For long-term storage, the frozen cells were transferred to the vapour phase of a liquid nitrogen tank.

3.2.3 Dual luciferase reporter gene assays

Reporter gene assays allow the analysis of the ability of DNA sequences to influence the expression of a downstream gene by using an easily measurable reporter gene as a surrogate. In this study, a dual luciferase reporter system was applied, combining firefly luciferase expressing pGL.4.17 for evaluation of promoters in question with a *Renilla* luciferase containing plasmid, pRL-CMV as an internal transfection and loading control.

Transient transfection

All cells except Jukat were transfected using polyethyleneimine (PEI)-mediated transfection. For this, $5 \cdot 10^4$ cells were seeded per well of a 24-well plate in 0.5 ml culture medium 24 hours before transfection. On the day of transfection, a DNA mix was prepared for each well to be transfected by mixing 210 ng pGL4.17 and 2.1 ng pRL in OPTI-MEM to a final volume of 25 µl. A PEI mix containing 0.85 µl of PEI solution [1 g / l] was added to OPTI-MEM to a final volume of 25 µl per well. After 10 min incubation at room temperature, each DNA mixture was mixed with an equal volume of PEI mixture by pipetting up and down without forming bubbles, followed by incubation at room temperature for 5 min. 50 µl of the resulting mixture were added to each well. After 12 hours of incubation, the supernatants of each well were replaced with 500 µl of fresh culture medium. After 36 hours, the supernatants were aspirated and the transfected cells were lysed by adding 100 µl of lysis buffer (1×) from the Beetle/Renilla Luciferase Assay Kits and stored at −80 °C until analysis.

In addition to the double transfection of pGL4.17 and pRL plasmids described above, for HeLa and RH30 triple transfections with an additional plasmid expressing the cDNA of EWSR1::FLI1 (pCDH-CMV-E/F1-puro) or a defective mutant (pCDH-CMV-E/F1_R2L2-puro [120]) were performed in an identical manner but with DNA mixtures containing 105 ng of pGL4.17, 105ng of pCDH-CMV-E/F1 or pCDH-CMV-E/F1_R2L2-puro, and 1.05 ng of pRL.

For A673/TR/shEF1 and A673/TR/shCtrl, cells were seeded in 4 wells for each plasmid and replicate. Half of the wells were supplemented with doxycycline 1 µg/ml to achieve shRNA-mediated knockdown of EF1. Of the resulting two wells per condition, one was harvested with PJK Lysis Juice for luciferase assays. RNA was extracted from the other well for RT-qPCR based confirmation of EF1 knockdown (KD).

Due to low transfection efficiency with PEI, Jurkat cells were transfected with Lipofectamine™ LTX according to the protocol recommended by the manufacturer for this cell line: $1 \cdot 10^5$ cells were plated into wells of a 24-well plate in 0.5ml of complete medium on the day of transfection. For the pGL4.17 derived plasmid, 500 ng of said pGL4.17 plasmid and 5 ng of pRL were mixed with OPTI-MEM to a total volume of 100 µl. 0.5 µl of PLUS™ reagent was added to each mix and the resulting solution was incubated for 10 min at room temperature. Next, 2 µl Lipofectamine™ LTX was added and the resulting mixtures dispersed by repeated pipetting. After a further incubation of 25 min at room temperature, 100 µl of transfection mix was added to each cell well. After 48 hours, the cells were harvested, centrifuged at 400g for 4 min, the supernatants discarded and the pellets lysed with 100 µl of lysis buffer as described above.

Luciferase assay

Dual luciferase assays were performed using the Beetle-Juice Luciferase Assay Firefly and Renilla-Juice Luciferase Assay kits from PJK GmbH and an Orion II microplate luminometer with 2 reagent injectors. Technical replicates of 5 µl of each cell lysate were added to wells of a white, opaque 96-well plate. Firefly and *Renilla* luciferase mediated luminescence was measured for each well 3 seconds after 50 µl of Beetle and Renilla juice was added to the well using reagent injectors.

Average luminescence values of technical replicates were calculated for data analysis. Background luminescence values for firefly and *Renilla* luciferase were obtained from wells containing lysis juice only and were subtracted from the sample values. For each well, the background corrected luminescence values obtained after the addition of beetle juice (corresponding to firefly activity) were divided by the luminescence values obtained after the addition of Renilla juice (corresponding to *Renilla* activity) as an internal control. These relative luminescence values were then normalised to that of pGL.4.17_0_YBL for each cell.

3.2.4 Analysis of RNA abundance by quantitative PCR (qPCR)

RNA extraction

RNA from up to $2 \cdot 10^6$ cells per sample was extracted using the NucleoSpin RNA mini kit according to the manufacturer's protocol. The purity and concentration of RNA were assessed using a Nanodrop 1000 spectrophotometer. To reduce the likelihood of RNA degradation, all steps involving cell lysates or eluted RNA were performed on ice and samples were centrifuged at 4 °C. After elution in RNAse-free water, samples were immediately stored at −80 °C or further processed.

Reverse transcription

To enable quantification of RNA molecules by qPCR, an initial reverse transcription to cDNA is required. This was performed using the High-Capacity cDNA Reverse Transcription Kit. A master mix consisting of 2 µl 10×RT Buffer, 2 µl 10×RT Random Primers, 0.7 µl dNTP mix (100 mM) and 0.7 µl MultiScribe™ Reverse Transcriptase per sample. 5.4 µl of this master mix was mixed with 14.6 µl of extracted RNA in a PCR microtube and briefly centrifuged. The microtubes were then placed in a Mastercycler® pro thermocycler and reverse transcription was conducted using the protocol described in Table 3.20.

Table 3.20: Thermocycler settings for reverse transcription.

Step	Temperature [°C]	Duration [min]
1	25	10
2	37	120
3	85	5
4	4	∞

Table 3.21: Cycling conditions for qPCR

Cycles	Description	Temperature [°C]	Duration [s]
1	Polymerase heat activation an initial denaturation	95	120
40	Denaturation	95	10
	Annealing, Elongation, Signal measurement	60	30
1	Final denaturation	95	2
	Cooling	60	60
60	Melting curve (Measurement, increase temperature by 0.5 °C and repeat)	65 - 95	5

qPCR

The abundance of specific cDNA molecules, as a surrogate for their expression, was measured by qPCR using the SYBR® Select Master Mix and a CFX Connect real-time PCR detection system. Primer mixes were prepared by mixing forward and reverse primers at a stock concentration of 100 µM with RNAase-free water in a 1:1:8 ratio. Primer sequences for *EWSR1::FLI1* and *RPLP0*, the latter used as housekeeping gene, were generated by M. Orth [31]. Suitable primer sequences for HSV-TK were obtained using the Primer-BLAST tool and their efficiency was validated by qPCR on serially diluted template [121].

For qPCR, 6.75 µl of sample cDNA diluted 1:9 with RNAse-free water was added to 4 wells per sample, corresponding to two technical replicates per two primer pairs. Master mixes for the gene of interest and the housekeeping control gene were prepared with 7.5 µl SYBR® and 0.75 µl primer mix containing forward and reverse primers at 10 µM per well. 8.25 µl of master mix was added to each well, giving a total reaction volume of 15 µl. PCR plates were then sealed, centrifuged at 400 g for 1 min, inserted into the CFX Connect and qPCR was performed using the cycling protocol described in table 3.21.

Data were analysed using the $2^{-\Delta\Delta CT}$ method [122].

3.2.5 Lentivirus production, titration and generation of transduced cell lines

Lentivirus production was performed as previously reported using PEI-based transfection of 293T cells and second generation lentiviral plasmids [123].

Production of VSV-G-pseudotyped lentivirus

Viral particles with the common envelope protein Vesicular Stomatitis Virus G (VSV-G), which allows non-specific transduction of a variety of different cells using the LDL receptor, were prepared with DMEM containing 10 % FCS [124]. For in vitro use, $5.3 \cdot 10^5$ 293T cells were seeded in 2 ml medium per well of a 6-well plate 24 hours before transfection. On the day of transfection, the medium was replaced by 2 ml serum-containing DMEM. For each well, 1020 ng lentiviral transfer plasmid, 680 ng pCD/NL-BH*DDD and 340 ng pCEF-VSV-G were mixed with Opti-MEM for a total volume of 100 µl plasmid mix. In addition, 15.12 µl of PEI was mixed with Opti-MEM for a total volume of 100 µl per well. Both plasmid and PEI mixtures were vortexed and incubated at room temperature for 5 min, after which 100 µl of PEI mixture was added to 100 µl of plasmid mixture and mixed by repeated pipetting. After a further incubation of 2 min, 200 µl of the resulting plasmid-PEI mixture was added per well. After 16 hours, the medium was replaced with 2 ml of fresh DMEM containing 10 % FCS.

Media containing lentiviral particles were harvested after 48 hours and centrifuged at 1000g for 4 min to reduce cellular debris. To remove residual cells, the supernatants were then passed through 0.45 µm PDVF syringe filters and the resulting virus-containing medium was frozen at −80 °C for further use.

For *in vivo* use, virus production was scaled up to 150 mm round dishes using ten times the number of cells, media and reagents.

Production of 2.2-pseudotyped lentivirus

To allow transduction based on a specific antigen-antibody interaction, lentiviral particles enveloped by a modified Sindbis envelope protein (2.2) containing the Fc-binding domain of protein A were used [125]. Lentivirus pseudotyped with 2.2 was produced as described above for the common VSV-G envelope protein with minor modifications. Instead of 340 ng of pCEF-VSV-G, 680 ng of 2.2 plasmid per well was used for transfection, and 17.64 µl of PEI was used to accommodate the higher total amount of DNA. In addition, 2.2-enveloped viral particles were produced under serum-free conditions to prevent bovine immunoglobulins from interfering with specific antibody coating in downstream processes. Therefore, on the day of transfection of 293T cells, FCS-containing DMEM was replaced with UltraCULTURE serum-free medium, which was

changed to UltraCulture supplemented with 0.4% HyClone LS250 Lipid Supplement.

Lentivirus concentration by PEG precipitation

To increase the concentration of lentiviral particles for *in vivo* experiments, a polyethylene glycol 8000-based precipitation was performed. To this end, 37.5 ml of filtered virus-containing supernatant was mixed with 12.5 ml lentivirus concentrator solution (4×) in 50 ml screw-capped reaction tubes for 24 hours at 4 °C. The incubated mixtures were then centrifuged at 2000 g for 60 min at 4 °C to produce pellets of precipitated virus particles, which were resuspended in PBS to a final volume of 0.5 ml.

Titration of lentivirus batches

The concentrations of transducing particles of different lentivirus batches were assessed by a qPCR-based titration approach previously described by Kuroda et al. [123]. Briefly, 293T cells were transduced with different volumes of lentiviral preparations. For each well, integrated viral DNA and 293T genomic DNA were quantified by qPCR on extracted DNA using primers amplifying segments of the viral WPRE or the human gene RPLP0, respectively. Using standard Ct values derived from qPCR on dilutions of WPRE-containing plasmid DNA and wild-type 293T genomic DNA on the same plate, integrated viral genomes per 293T genome could be estimated.

First, $5 \cdot 10^4$ 293T cells were plated in 1 ml DMEM containing 1% FCS per well of a 12-well plate. After 24 hours, the medium was carefully replaced with 0.5 ml DMEM containing 1% FCS and cells from two wells were counted to determine the number of cells per well on the day of transduction.

Aliquots of the lentivirus batches to be measured were thawed and cells transduced by adding 5 µl and 25 µl of unconcentrated supernatant to two wells. For concentrated virus stocks, similar volumes were added after 200x dilution with PBS. Lentiviruses produced with the modified envelope protein 2.2, which only allows transduction mediated by an antibody-antigen interaction, were mixed with human HLA class I antibody at a concentration of 5 µg/ml and incubated at 37 °C for 2 min prior to transduction. 24 hours after transduction, the medium was replaced with DMEM containing 10 U/ml DNAseI to digest any remaining plasmid DNA. After incubation for 15 min at 37 °C, the medium was replaced with DMEM supplemented with 10 % FCS and cultured for a further 48 hours, after which genomic DNA was harvested using the Nucleospin Tissue Kit according to the manufacturer's protocol.

For quantification of 293T genome copies, a standard dilution was created with 10, 2, 0.4, 0.08 and 0.016 ng of human genomic DNA per µl of RNAse-free water. For integrated virus DNA, the WPRE containing plasmid pLenti CMV GFP Puro (658-5) was used to create a standard diltution ranging from $0.2 \cdot 10^7$ to $0.2 \cdot 10^2$ copies per µl. For qPCR, 5 µl of sample DNA were added to

Table 3.22: Cycling conditions for genomic qPCR for lentiviral titration

Cycles	Description	Temperature [°C]	Duration [s]
1	Polymerase heat activation an initial denaturation	95	600
40	Denaturation	95	10
	Annealing, Elongation, Signal measurement	60	30
1	Final denaturation	95	2
	Cooling	4	∞

four wells of a 96-well qPCR plates per primer pair and an equal volume of standard DNA was added to two wells allowing technical replicates for each reaction. Master mixes were prepared as described in chapter 3.2.4 with an additional 1.75 µl RNAse-free water per well. For a total volume of 15 µl, 10 µl of master mix was added per well and qPCR performed using the cycling conditions described in table 3.22.

Data analysis was performed using R and functions from the stats package. For each standard dilution, a linear model of log2 of genomic or plasmid copy numbers (assuming 1 ng genomic DNA corresponding to 333 genomic copies) versus Ct values was fitted using the *lm* function. Means of technical replicates for sample Ct values were used to calculate the number of virus and genome copies per DNA sample using the *predict* function. Transducing particles per µl were calculated using the formula U/ml= $(C \cdot N \cdot 1000)/V$, where C is the number of virus copies per genome, N is the number of cells transduced per well and V is the volume of virus preparation added per well for transduction.

Generation of transduced cell lines

For each cell line to be transduced, $5 \cdot 10^4$ cells were seeded in two wells of a 6-well plate. Equal volumes of lentivirus-containing supernatant prepared as described above, corresponding to an MOI of 2, were added to one well per cell line. After 72 hours, viral particles were removed by replacing the medium and puromycin was added, allowing selection of cells that had obtained and expressed *PuroR* as a result of successful transduction.

3.2.6 Western blot

Western blot allows antibody-mediated detection of specific proteins in a mixture after separation by size. For this purpose, protein lysates were obtained by plating $3 \cdot 10^5$ cells in 2 ml of medium per well of a 6-well plate. Cells were washed with PBS after 48 hours, lysed with 100 µl of Triton X Lysis Buffer

supplemented with cOmplete, Mini Protease Inhibitor Cocktail and the lysates stored at −80 °C until further processing.

Western blots were performed as previously described [126]. Briefly, proteins were separated by sodium dodecyl sulfate-polyacrylamide gel electrophoresis using a running gel containing 12.5 % acrylamide/bisacrylamide and blotted onto a nitrocellulose membrane. Membranes were blocked with TBS containing 5 % milk powder and washed with TBS-T. Detection of specific bands for firefly luciferase or GAPDH was performed using an HRP-conjugated monoclonal anti-luciferase antibody (sc-74548 HRP, Santa-Cruz) diluted 1:2000 in 1× TBS containing 5 % milk and an HRP-conjugated monoclonal murine anti-GAPDH antibody (HRP-60004, Proteintech) diluted 1:50000.).

3.2.7 Resazurin reduction cell viability assay

To assess the cytotoxic effects of putative anticancer agents in vitro, assays that measure the viability of cultured cells are useful. One such method is to measure the rate of conversion of resazurin to resofurin, which is dependent on the reducing agent NADH produced by viable, metabolically active cells. Resofurin, unlike resazurin, emits a fluorescent signal at a wavelength of 584 nm when excited at 579 nm [127].

For resazurin reduction assays, $5{-}10 \cdot 10^3$ transduced Ewing sarcoma (EwS) and non-EwS cells were plated in 90 µl of medium per well of a 96-well plate. After 24 hours, ganciclovir dissolved in medium containing 0.05% DMSO was added at final concentrations of 0.01 µM to 50 µM and a final volume of 100 µl per well. Following 3 days of ganciclovir treatment, 25 µl of resazurin solution (0.1 g/l) was added per well. Resazurin fluorescence was measured after 1 to 6 hours using a Varioskan Flash plate reader.

Where indicated, wild-type cells were used and transduced by the addition of 1000 TU of lentiviral particles 24 hours after seeding. Cells were treated with GCV to a final concentration of 20 µM or a DMSO control 24 hours later.

Data were analysed in R using the packages *stats* and *drc* [128]. Fluorescence units (FU) from wells containing only medium and resazurin solution were subtracted from the sample values as a background control. For each cell and biological replicate, the median FU of 6 technical replicates per treatment condition was normalised to the median FU of wells treated with 0.05% DMSO only.

3.2.8 APC Annexin V / PI apoptosis assays

APC-labelled annexin V and propidium iodide (PI) staining were used to analyse apoptosis induction after *in vitro* treatment. Annexin V binds to phosphatidylserine, a phospholipid normally present in the inner layer of the cell membrane, and translocates to the outer layer, making it available for extracel-

lular detection of apoptosis. As a non-membrane permeable DNA-intercalating dye, PI is useful for detecting apoptotic cells whose membrane integrity is compromised, such as necrotic and late apoptotic cells.

For these assays, $5 \cdot 10^4$ cells were plated in 0.5 µl of medium per well of a 24-well plate. GCV was added 24 hours after initial seeding to a final concentration of 0.4 µM. Cells were harvested, washed with PBS and stained with APC and PI according to the manufacturer's protocol after 72 hours. Cells were analysed by flow cytometry using a BD FACSCanto II. An example of the gating strategy is shown in Fig. 3.7.

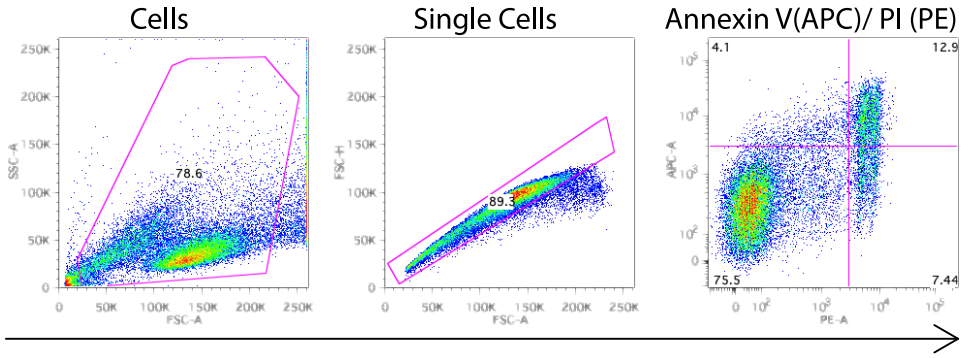

Figure 3.7: Representative gating strategy for Annexin V / PI staining.

3.2.9 Analysis of gene expression microarray data

To find genes encoding membrane proteins that are overexpressed in Ewing sarcoma compared to normal tissues, a previously published dataset of publicly available gene expression microarray data (Affymetrix HG-U133Plus2.0) comprising 50 samples from Ewing sarcoma and 928 from normal tissues was obtained from GEO [49]. Study accession codes are listed in Table 3.23. Data were analysed using R and the packages *affy* (version 1.76.0) and *limma* (version 3.54.1) from the Bioconductor repository [129, 130]. First, the CEL files were read and Robust Multiarray Average (RMA) normalisation and calculation of expression measures were performed using the function *just.RMA*. [131]. The functions *lmFit*, *constrasts.fit* and *treat* from the *limma* package were used to identify differentially expressed genes in EwS compared to each of the other tissues in the data set with a minimum log2 fold change of 1. *Limma*'s *decideTests* function, using the Benjamini-Hochberg adjustment for multiple testing and a false discovery rate of 0.05, allowed the extraction of 36 genes that were significantly overexpressed in EwS compared to any other tissue. Using information from uniprot.com, these genes were manually filtered for the membrane-associated location of their products. Three genes encoding surface proteins with commercially available antibodies targeting extracellular domains were selected for experimental evaluation.

Table 3.23: Study accession codes of microarray data

Tissue	Accession codes	N
EWING_SARCOMA	GSE34620	50
NORMAL_ADRENAL	GSE10927, GSE19750, GSE43346, GSE7307	19
NORMAL_BCELLS	GSE31048	15
NORMAL_BLADDER	E-MTAB-1940, GSE30522, GSE43346, GSE61352	10
NORMAL_BONE_MARROW	GSE11504	25
NORMAL_BRAIN_ACCUMBENS	GSE7307	14
NORMAL_BRAIN_AMYGDALA	GSE7307	8
NORMAL_BRAIN_CAUDATE	GSE7307	4
NORMAL_BRAIN_CORPUS_CALLOSUM	GSE7307	9
NORMAL_BRAIN_CORTEX	GSE7307	35
NORMAL_BRAIN_HIPPOCAMPUS	GSE7307	8
NORMAL_BRAIN_HYPOTHALAMUS	GSE7307	8
NORMAL_BRAIN_MIDBRAIN	GSE7307	7
NORMAL_BRAIN_NODOSE_NUCLEUS	GSE7307	8
NORMAL_BRAIN_PALLIDUM	GSE7307	6
NORMAL_BRAIN_PITUARY_GLAND	GSE7307	6
NORMAL_BRAIN_PUTAMEN	GSE7307	13
NORMAL_BRAIN_SUBSTANTIA_NIGRA	GSE7307	16
NORMAL_BRAIN_SUBTHALAMIC_NUCLEUS	GSE7307	9
NORMAL_BRAIN_THALAMUS	GSE7307	9
NORMAL_BRAIN_TRIGEMINAL_GANGLIA	GSE7307	8
NORMAL_BRAIN_VENTRAL_TEGMENTAL_AREA	GSE7307	7
NORMAL_BRAIN_VESTIBULAR_NUCLEI_SUPERIOR	GSE7307	7
NORMAL_BREAST	GSE26457	25
NORMAL_BRONCHUS	GSE14461, GSE7307	6
NORMAL_CEREBELLUM	GSE7307	11
NORMAL_CERVIX	GSE27678, GSE7307	7
NORMAL_COLON_MUCOSA	GSE8671	25
NORMAL_ESOPHAGUS	GSE43346, GSE63626, GSE63941, GSE7307	14
NORMAL_FAT	GSE41168	25
NORMAL_GALLBLADDER	GSE43346, GSE63626	4
NORMAL_GINGIVA	GSE16134	25
NORMAL_HAIR_FOLLICLE_STEM_CELLS	GSE44765	18
NORMAL_HEART	GSE18676, GSE43346, GSE7307	10
NORMAL_HEMATOPOIETIC_STEM_CELLS	GSE19429	9
NORMAL_KIDNEY	GSE11151, GSE18676, GSE43346, GSE7307	14
NORMAL_LIVER	GSE40231	22
NORMAL_LUNG	GSE40791	25
NORMAL_LYMPH_NODE	GSE43346, GSE7307	5
NORMAL_MACROPHAGES	GSE2125, GSE43346	30
NORMAL_MONOCYTES	GSE7158	25
NORMAL_NEVUS	GSE53223	12
NORMAL_OCULAR_ENDOTHELIUM	GSE20986	8
NORMAL_ORAL_MUCOSA	GSE30784	25
NORMAL_OVARY	GSE18520, GSE43346, GSE7307	13
NORMAL_PANCREAS	GSE18676, GSE22780, GSE43346, GSE7307	4
NORMAL_PENIS	GSE7307	6
NORMAL_PHARYNGEAL_MUCOSA	GSE7307	4
NORMAL_PROSTATE	GSE43346, GSE7307	14
NORMAL_RETINA	GSE12621, GSE28133	20
NORMAL_SALIVARY_GLAND	GSE18676, GSE40611, GSE7307	11
NORMAL_SKELETAL_MUSCLE	GSE40231	14
NORMAL_SKIN	GSE13355	25
NORMAL_SMALL_INTESTINE	GSE18676, GSE43346, GSE63626, GSE7307	20
NORMAL_SPINAL_CORD	GSE7307	9
NORMAL_SPLEEN	GSE18676, GSE25550, GSE43346, GSE7307	13
NORMAL_STOMACH	GSE18676, GSE43346, GSE7307	14
NORMAL_SYNOVIAL_MEMBRANE	GSE7307	6
NORMAL_T_CELLS	GSE14926, GSE6338	25
NORMAL_TESTES	GSE25518, GSE43346, GSE7307	10
NORMAL_THYMUS	GSE18676, GSE43346, GSE46170, GSE7307	10
NORMAL_THYROID	GSE33630	25
NORMAL_TONGUE	GSE7307	10
NORMAL_TONSIL	GSE43346, GSE7307	4
NORMAL_TRACHEA	GSE18676, GSE43346, GSE7307	6
NORMAL_URETHRA	GSE7307	5
NORMAL_UTERUS_ENDOMETRIUM	GSE7307	23
NORMAL_UTERUS_MYOMETRIUM	GSE7307	22
NORMAL_VAGINA	GSE7307	4
NORMAL_VEIN	GSE43346, GSE7307	7
NORMAL_VESSELS_ARTERY	GSE43346, GSE7307	8

N is the number of samples used in this study.

3.2.10 Detection of surface proteins by indirect flow cytometry

To validate the expression of surface proteins on EwS cells, $2 \cdot 10^5$ EwS or control cells were plated in 1 ml of medium per well of a 12-well plate. After 24 hours, cells were detached with trypsin and FCS-containing medium, counted and washed three times with PBS. The cells were then stained with 0.25 µg of primary antibody against the indicated antigens per $1 \cdot 10^6$ cells in 100 µL PBS and incubated for 30 min at room temperature. After three washes with PBS, the appropriate secondary antibody was added at a concentration of 0.375 µg per $1 \cdot 10^6$ cells in 100µL PBS. Following 30 min of incubation in the dark under a light shield at room temperature, cells were washed three times, co-stained with PI and analysed using a BD FACSCanto II cytometer. An example of the gating strategy is shown in Figure 3.8. Table 3.14 shows the antibodies used for staining (3B2/TA8, NBP1-78381, PTA-5704, TAB-731, #02-6300, #02-6102, A-10931, A-865). PTA-5704 was extracted from supernatant of the hybridoma cell line OAM6 #93 using the Mouse TCS Antibody Purification Kit from abcam according to the manufacturer's standard protocol.

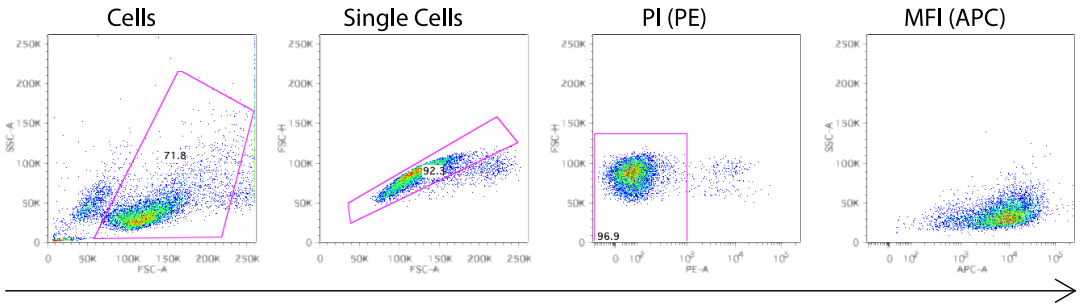

Figure 3.8: Representative gating strategy for indirect flow cytometry.

3.2.11 Evaluation of antibodies for targeted transduction *in vitro*

Antibodies were compared for their ability to mediate transduction of EwS and non-EwS cells by lentiviral particles produced with the envelope protein 2.2 and a CMV promoter-driven GFP transgene. To this end, $5 \cdot 10^4$ cells were plated in 400 µl of FCS-containing medium per well of a 24-well-plate. After 24 hours, 100 µl of lentivirus-containing supernatant was mixed with 0.5 µg of different monoclonal antibodies or isotype control and added per well. The supernatants were replaced with fresh medium after 24 hours. After a further 24 hours, cells were harvested with trypsinisation and FCS-containing medium, washed with PBS and analysed on a BS FACSCanto II. The gating strategy is shown in Fig. 3.9.

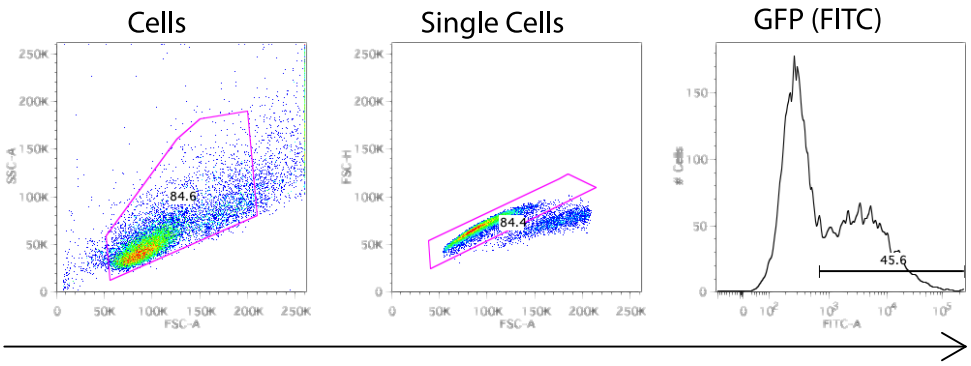

Figure 3.9: Representative gating strategy for detection of GFP expressing cells.

3.2.12 *In vivo* experiments

All animal experiments were applied for and approved by the government of Upper Bavaria. They were conducted in accordance with ARRIVE guidelines, the recommendations of the European Community (86/609/EEC), and the UKCCCR (guidelines for the welfare and use of animals in cancer research). NOD.Cg-Prkdc^{SCID}Il2rg^{tm1Wjl}/SzJ (NSG) mice were used for all experiments. These mice that lack mature T cells, B cells, natural killer cells, multiple cytokine signaling pathways and a functional hemolytic complement system [132]. NSG mice were obtained from Charles River Laboratories and maintained in individually ventilated cages under specific pathogen-free conditions. They were provided with food and water ad libitum and monitored daily for signs of infection or distress unless specified otherwise. The light cycle was set to 14 hours of light and 10 hours of dark during which the mouse rooms were not entered. The temperature and humidity were controlled at 18-23 °C and 40-60%, respectively. The diet consisted of a standard mouse chow with 4-11% fat content.

Evaluation of promoter activity and specificity by *in vivo* bioimaging

To qualitatively assess promoter activity in non-EwS tissues, $2 \cdot 10^7$ transducing units (TU) of lentivirus produced with the VSV-G envelope protein and either pLenti_25_LT or pLenti_CMV_LG as transfer plasmid were diluted to 200 µl in PBS and injected into the peritoneal cavity of NSG mice. 7 days after virus injection, mice were sedated with ketamine/xylazine (50 mg and 10 mg per kg body weight, respectively) and 3 mg of XenoLight D-luciferin were injected intraperitoneally per mouse. Luminescence was measured on an IVIS-100 bioimaging system using Living Image® software (version 2.5, Perkin Elmer) with an exposure time of 120s. Following bioimaging, mice were sacrificed by cervical dislocation and organs were obtained by dissection. Genomic DNA was extracted from heart, intestine, kidney, liver, lung

and spleen separately for each mouse. To estimate the number of integrated virus copies per mouse DNA, genomic qPCR was performed as described in section 3.2.5. Instead of human (293T) DNA, murine genomic DNA extracted from liver tissue of an NSG mouse was used for the genomic standard dilution. Primers Actb_new_FW and Actb_new_RV, which amplify a 149 bp segment of murine *ACTB* across an intron-exon boundary, were used for qPCR-based quantification of murine genomes.

HSV-TK suicide gene therapy in pre-transduced Ewing sarcoma xenografts

In the absence of a faithful mouse model for Ewing sarcoma (EwS), xenografts of human EwS cell lines are commonly used as *in vivo* models of this disease [4]. For experiments with subcutaneous Ewing xenografts, A-673 or RD-ES expressing a HSV-TK under a 25 GGAA + YB_TATA promoter were mixed with Cultrex Basement Membrane Extract Type 3 in a 1:1 ratio and $2 \cdot 10^6$ cells in 100 µl were injected subcutaneously into the flanks of 6 to 8 week old NSG mice. Once tumours were palpable at the injection site, mice were randomised to receive valganciclovir (VGCV) dissolved in drinking water with 5 % w/v sucrose at concentrations of 1 mg/ml, 0.5 mg/ml or 0.1 ml/ml ad libitum or a vehicle control. Mice were examined daily for clinically apparent adverse effects. Tumour size and mouse weight were determined every 2 days, the former using a caliper and the formula $V = (a \cdot b^2)/2$, where a is the longest and b is the smallest diameter. All mice were sacrificed by cervical dislocation when the majority of the tumour volume in the control group had reached 1500 mm^3.

Antibody-mediated transduction of subcutaneous EwS xenografts

Xenografts of either A-673 or RD-ES were established by subcutaneous injection into NSG mice as described above. Lentiviral particles produced with one of the transfer plasmids pLenti_25_YBL_LT or pLenti_CMV_LT, either coated with VSV-G or 2.2, were injected into the tumours when they reached a mean diameter of 5 mm. For each mouse, $0.5 \cdot 10^6$ viral particles were diluted in PBS to give a total injection volume of 100 µl. Virus enveloped with Fc-binding 2.2 protein was incubated and injected with 15 µg/ml monoclonal antibody as indicated. In vivo bioimaging was performed to analyse luminescence activity as described above.

HSV-TK suicide gene therapy in wild-type subcutaneous wild-type EwS xenografts

A-673 were subcutaneously xenografted into the flanks of NSG mice as described above. Once tumours were palpable, mice were randomised to receive either intratumoral injections of $1 \cdot 10^{7}$ TU of lentivirus produced with

pLenti_25_YBL_LT and 2.2 in 100 µl PBS containing 15 µg/ml GPR64 antibody or a vehicle control of 100 µl PBS. Half of the mice in each group were randomised to receive oral VGCV ad libitum by supplementation of their drinking water with 0.5 mg/ml VGCV and 5 % w/v sucrose. Drinking water for the other half contained only 5 % sucrose. Mice were examined daily for clinically apparent adverse effects. Mouse weights and tumour sizes were measured every two days as described above. Virus or vehicle was injected twice a week. All mice were sacrificed by cervical dislocation when the majority of the tumour volume in the control group had reached 1,500 m^2.

HSV-TK suicide gene therapy of a peritoneal metastasis model

A-673 expressing firefly luciferase under the control of a CMV promoter were generated by lentiviral transduction using the lentiviral vector plasmid pLenti_CMV_LG_Puro to create an EwS cell line that would allow quantification of a disseminated tumour mass. Transduced cells were selected by adding puromycin at the lowest concentration to kill all cells in the non-transduced control wells.

To generate intraperitoneal EwS models, $2 \cdot 10^6$ cells of luciferase-expressing A-673 cells were injected into the peritoneal cavity of NSG mice in 100 µl PBS on day 0. On days 3 to 5, mice were treated by intraperitoneal injection of $2 \cdot 10^7$ TU of lentivirus produced with the transfer plasmid pLenti_25_YBL_TK and the envelope plasmid 2.2 in 200 µl PBS or a PBS-only control. On day 6, bioluminescence was measured after intraperitoneal injection of 3 mg D-luciferin as a surrogate for intraperitoneal tumour mass as described above. After imaging, the mice were returned to their cages and treatment with oral VGCV ad libitum was initiated by supplementing their drinking water with 0.5 mg/ml VGCV and 5 % w/v sucrose and continued until the end of the experiment. A further three-day cycle of intraperitoneal virus or PBS injections was administered on days 13 to 15. Follow-up bioimaging was performed on days 12 and 19. Imaging at every time point was performed on an IVIS-100 bioimaging system using Living Image® software (version 2.5, Perkin Elmer) with an exposure time of 2s.

4. Results

4.1 Synthetic GGAA-microsatellite-based promoter designs allow EF1-dependent gene expression

In Ewing sarcoma, GGAA-microsatellites (GGAA-msats), which are normally condensed chromatin, are converted to *de novo* enhancers by EWSR1::FLI1 [29, 30, 133, 27]. This fusion transcription factor is disease-specific and its effect on GGAA-msats is unique [33]. It was therefore hypothesised that its transactivating activity when bound to GGAA-msats could be harnessed by combining these repetitive sequences with core promoters [113]. This should produce gene expression systems that show only the basal transcription rate of the core promoter and induced expression in EwS cells containing EF1.

To test this hypothesis, synthetic GGAA-msat sequences of either 17, 21 or 25 repeats in length were cloned directly upstream of the previously published core promoter YB_TATA [113]. The resulting constructs and YB_TATA alone as a baseline control were inserted into a firefly luciferase (Fluc) reporter plasmid (pGL4.17). In Dual-Luciferase Reporter assays using a CMV-driven *Renilla* luciferase plasmid (pRL-CMV) as an internal control, the promoter activities of the different msat-containing expression cassettes relative to the YB_TATA only control were assessed in a panel of 6 EwS cell lines (A-673, MHH-ES-1, RD-ES, SK-N-MC, TC-106 (expressing EWSR1::ERG), and TC-71) and 7 non-EwS cell lines comprising different non-EwS cancer entities and tissues (HeLa, Hep-G2, Jurkat, MRC5, PA-TU-8988T, RH30, U2-OS). In line with the hypothesis, promoter activities in EwS cell lines A-673, MHH-ES-1, RD-ES, SK-N-MC, TC-106 and TC-71 were up to 100 times higher than in non-EwS control cells (Fig. 4.1).

To characterise whether this difference in reporter induction between EwS and non-EwS cell lines is directly dependent on the presence of EF1, reporter assays were performed using the same plasmids in A673/TR/shEF1 and A673/TR/shctrl. These are derivatives of the EwS cell line A-673 carrying doxycycline (Dox)-inducible shRNAs against the EF1 fusion oncogene or a non-targeting control shRNA. Indeed, shRNA-mediated knockdown (KD) of EF1 resulted in reduced promoter activity (Figure 4.2). The KD of EF1 was

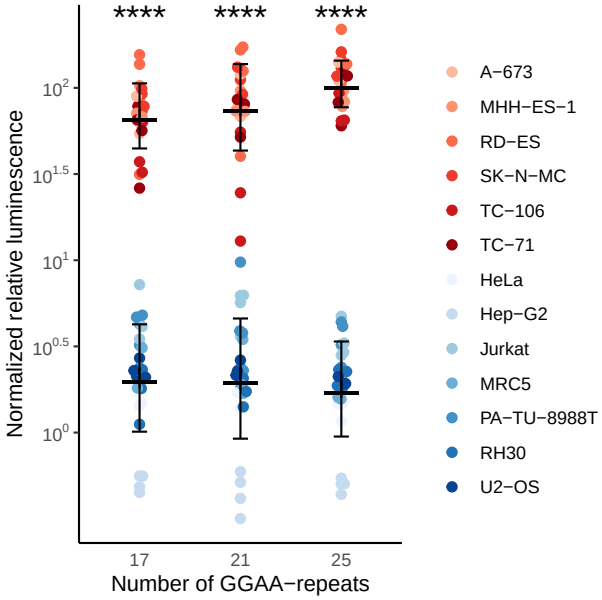

Figure 4.1: GGAA-msats combined with YB_TATA have higher promoter activity in EwS than in non-EwS cell lines.

Luciferase reporter assays of EwS and non-EwS cell lines co-transfected with a reporter plasmid containing the indicated number of GGAA-repeats upstream of the minimal promoter YB-TATA and a constitutively expressed *Renilla*-encoding plasmid. Dots indicate Firefly to *Renilla* luminescence ratios normalised to a YB_TATA-only reporter plasmid from 4 independent experiments. Horizontal bars indicate mean and whiskers standard deviation per group. Figure adapted from Hölting et al. [134].

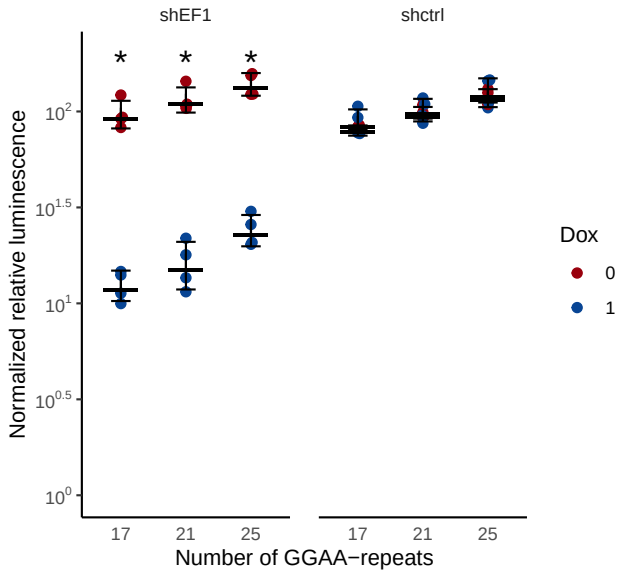

Figure 4.2: KD of EF1 decreases reporter expression by GGAA-msat containing expression cassettes.

Luciferase reporter assays of A673/TR/shEF1 and A673/TR/shCtrl with the plasmids as in Fig. 4.1 with 1 µg / ml Dox (1) or without Dox (0). Dots indicate Firefly to *Renilla* luminescence ratios normalised to a YB_TATA-only reporter plasmid from 4 independent experiments. Horizontal bars indicate mean and whiskers standard deviation per group. Figure adapted from Hölting et al. [134].

confirmed by qPCR using ribosomal protein lateral stalk subunit P0 (*RPLP0*) as a housekeeping gene (Figure 4.3).

Conversely, it was evaluated whether the fusion oncogene alone was able to increase the promoter activity in non-EwS cells. To this end, reporter assays were performed using the same luciferase plasmids in HeLa and RH30 ectopically expressing either EF1 or a DNA-binding defective mutant of the fusion transcription factor (EF1_R2L2)[120]. In line with our hypothesis, GGAA-msat containing expression cassettes showed increased activity in the presence of EF1 compared to the defective control. Taken together, these data suggest that a 25 GGAA repeat element in combination with the core promoter YB_TATA produces an EWSR1::FLI1 or EWSR1::ERG dependent expression cassette specific for EwS cells.

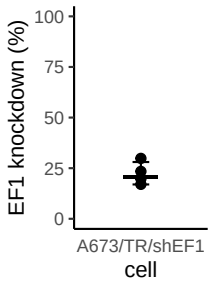

Figure 4.3: Quantification of EF1-KD in A673/TR/shEF1 after Dox treatment by qPCR.

RNA abundance of *EWSR1::FLI1* was determined by breaktpoint-region spanning qPCR using *RPLP0* as control. Dots indicate EWSR1::FLI1 RNA abundance relative to non-Dox condition analysed by the $2^{-\Delta\Delta Ct}$ method. Figure adapted from Hölting et al. [134].

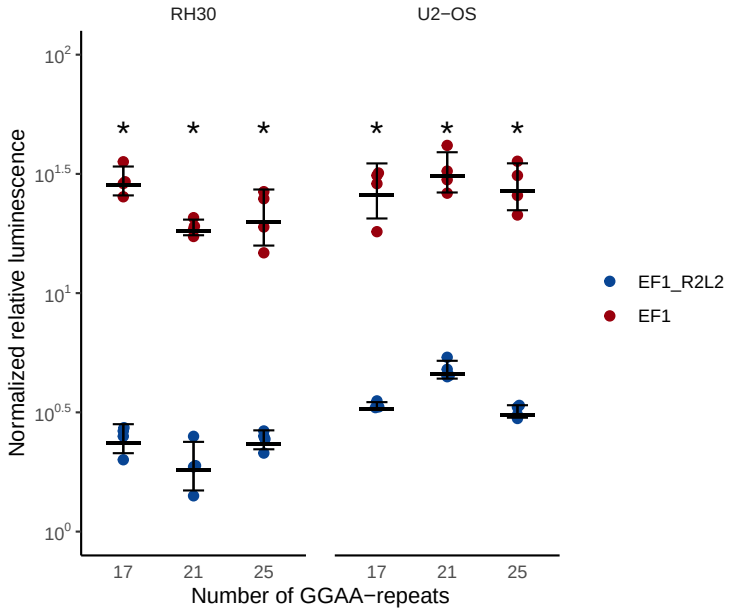

Figure 4.4: Ectopic expression of EF1 increases reporter expression by GGAA-msats containing expression cassettes.

Luciferase reporter assays of HeLa and RH30 with the plasmids as in Fig. 4.1 co-transfected with EF1 or defective EF1_R2L2 expressing plasmids. Dots indicate Firefly to *Renilla* luminescence ratios normalised to a YB_TATA-only reporter plasmid from 4 independent experiments. Horizontal bars indicate mean and whiskers standard deviation per group. Figure adapted from Hölting et al. [134].

4.2 A synthetic GGAA-microsatellite-based promoter enables EwS-specific therapeutic effects

This expression cassette should allow the expression of therapeutic transgenes, such as suicide genes, in an EwS-specific manner, minimising the effects on non-EwS cells. To test this hypothesis, cancer gene therapy using lentiviral particles carrying a herpes simplex virus thymidine kinase (HSV-TK) suicide gene was chosen as a model therapy. Therefore, a second-generation lentiviral transfer plasmid called pLenti_25_LT_Puro was created containing a regulatory element consisting of 25 GGAA repeats and the YB_TATA core promoter upstream of the previously published *HSV-TK SR39* gene, coupled to a *Firefly luciferase* (Fluc) by a P2A linker peptide. HSV-TK SR39, generated by mutagenesis of wild-type *HSV-TK*, metabolizes the antiviral drug ganciclovir (GCV) to a cytotoxic compound and has been shown to induce higher sensitivity to GCV and increased tumour killing than the wild-type gene [116]. To allow selection of transduced cells, a second expression cassette containing a CMV promoter *PuroR*, which induces resistance to the otherwise cytotoxic compound puromycin, was added downstream of the first cassette.

A panel of 6 EwS cell lines (A-673, MHH-ES-1, RD-ES, SK-N-MC, TC-106 and TC-71) and 8 non-EwS control cell lines (HeLa, Hep-G2, HUVEC, Jurkat, MRC5, PA-TU-8988T, RH30, U2-OS) were transduced with this plasmid or a variant lacking the 25 GGAA repeats (pLenti_0_LT_Puro). Cell lines that were successfully transduced were selected with puromycin. To confirm the EwS specificity of GGAA-msat mediated gene expression when delivered by integrating lentivirus, cells were subjected to qPCR analysis for HSV-TK expression. Consistent with observations in episomal reporter assays, a significant increase in HSV-TK abundance was detected in EwS cell lines transduced with pLenti_25_LT_Puro compared to the msat-deficient variant, whereas levels in non-EwS were similar for both vectors (Fig. 4.5). Similarly, immunoblotting using GAPDH as a loading control confirmed higher protein levels of Fluc, expressed equimolar to HSV-TK in transduced cells, which could only be detected in EwS cells (Fig. 4.6). Since only a limited number of cell lines can be modelled with cell lines and these *in vitro* models can not adequately reflect the complexity of tissues and organs, the activity of the GGAA-msat promoter was assessed *in vivo*. For this purpose, a lentiviral transfer plasmid called pLenti_25_LT, identical to pLenti_25_LT_Puro but without the Puromycin resistance inducing second expression cassette was generated. To compare activity of the GGAA-msat promoter to a CMV promoter, $1 \cdot 10^7$ TU of lentiviral particles produced with the envelope protein VSV-G and either pLenti_25_LT or pLenti_CMV_LG, expression a Fluc P2A-coupled to a GFP, as a control were injected intraperitoneally into the abdominal cavity of mice. Bioluminescence measurements after the application of D-luciferin

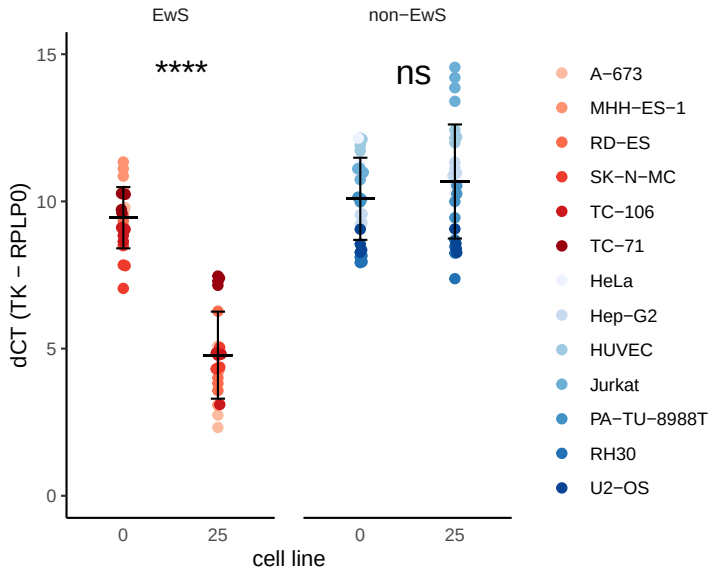

Figure 4.5: *HSV-TK* mRNA abundance in EwS and non-EwS cell lines transduced with pLenti_25_LT_Puro or pLenti_0_LT_Puro.

RNA abundance of *HSV-TK* in was determined by qPCR using *RPLP0* as housekeeping control. Dots indicate -ΔCt values of *HSV-TK* to *RPLP0*. Horizontal bars indicate mean and whiskers standard deviation per group. Figure adapted from Hölting et al. [134].

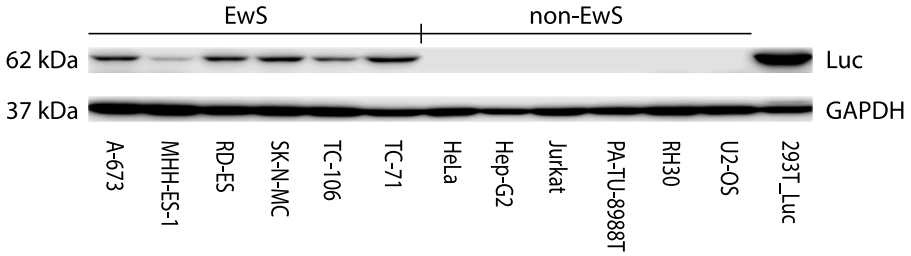

Figure 4.6: Detection of Fluc by immunoblotting in EwS and non-EwS cell lines transduced with pLenti_25_LT_Puro.

Detection of Firefly luciferase and GAPDH in protein lysates from EwS and non-EwS cell lines transduced with pLenti_25_LT_Puro by western blot. Figure adapted from Hölting et al. [134].

revealed detection of luciferase signals only in the CMV-group and no luminescence in the msat group (Fig. 4.7). To exclude unequal transduction rates as the cause for differences in luminescence intensities, numbers of integrated viral genomes in genomic DNA extracted from organ samples of each imaged mice were quantified. Therefore, copies of the virus-specific *Woodchuck Hepatitis Virus (WHV) Posttranscriptional Regulatory Element (WPRE)*, as a surrogate for integrated lentivirus copies, and the murine *Actin Beta (Actb)*, as a surrogate for murine genome copies, were measured by qPCR on genomic DNA from different organs. Similar numbers of integration events, determined as *WPRE* copies per genome (inferred by the number of *Actb* copies) were found for both groups (Fig. 4.7).

To assess whether the observed differences in GGAA-msat promoter activity in EwS and control cells can induce specific treatment effects, EwS and non-EwS cell lines transduced with pLenti_25_LT_Puro as shown in Fig. 4.5 were assessed for their sensitivity to ganciclovir (GCV). After treatment with GCV concentrations ranging from 0.01 µM to 50 µM for 72 hours, cell viability was assessed in resazurin assays, which showed approximately 100-fold lower ED_{50} (effective dose) values for transduced EwS compared to non-EwS control cell lines (Fig. 4.8). To correct for transgene-independent differences in GCV sensitivity between EwS and control cell lines, similar assays were performed for pLenti_0_LT_Puro transduced cells. Fig. 4.9 shows the combined results for both plasmids and shows that 25 GGAA repeats upstream of the core promoter YB_TATA induce toxicity only in EwS cells. As GCV induces apoptosis in cells expressing HSV-TK, flow cytometry was used to confirm the suspected test rates of apoptosis in transduced EwS and non-EwS cell lines after GCV exposure. To this end, transduced cells as in Fig. 4.8 were treated GCV with a concentration of GCV equal to the mean ED50 for EwS cell calculated from Fig. 4.8 (0.4 µM) or DMSO control for 72 hours. Flow cytometry staining of Annexin V and PI revealed significant induction of apoptosis (Annexin V+) only in treated EwS cells 4.10.

Taken together the results of these experiments indicated that a GGAA-msat promoters allow EwS-specific expression of a suicide gene delivered by lentivirus leading to selective therapeutic effects *in vitro*.

4.3 The orphan receptor GPR64 allows targeted gene delivery to EwS cells

Following the successful design and characterisation of a highly EwS-specific expression cassette *in vitro*, it was necessary to evaluate its specificity and ability to induce tumour-specific treatment effects in a more complex *in vivo* model. Lentiviral vectors used in laboratories around the world are most commonly produced and pseudotyped with the VSV-G surface protein derived from vesicular stomatitis virus [124]. This envelope protein allows effective transduction

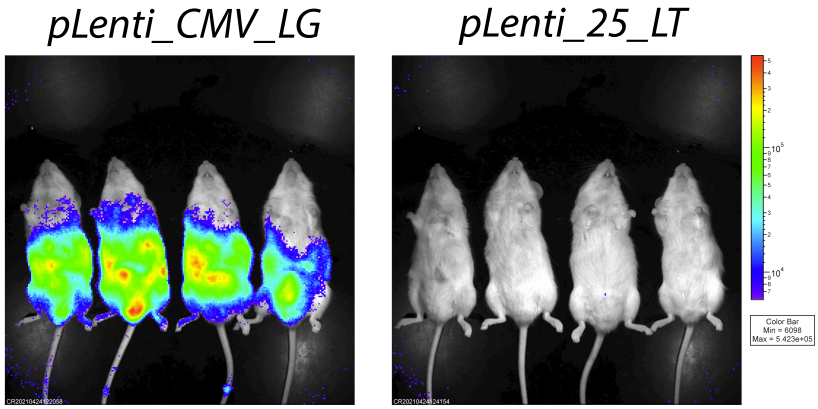

Bioluminescence measurements using a 2 min exposure time in NSG mice 14 days after intraperitoneal injection of $1 \cdot 10^{10}$ TU of lentiviral particles produced with VSV-G and transfer vectors pLenti_25_LT or pLenti_CMV_LG. Figure adapted from Hölting et al. [134].

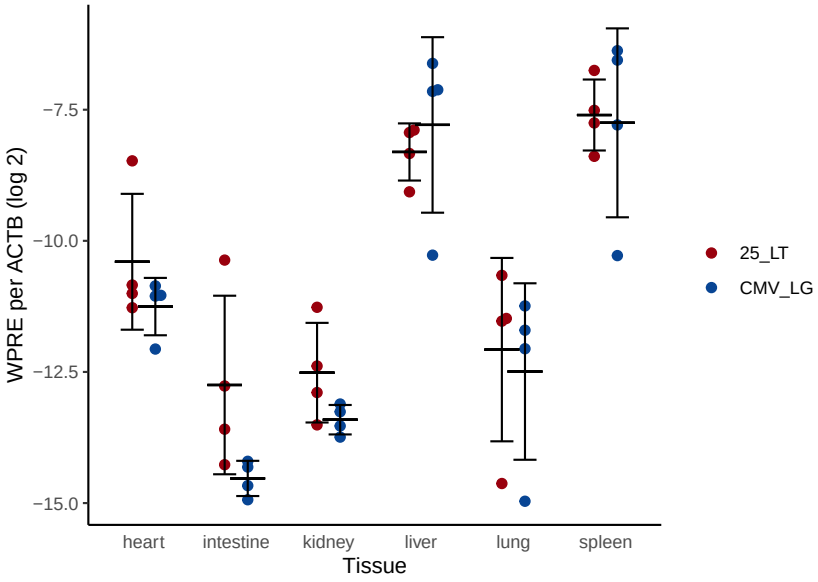

Quantification of *WPRE* and murine *Actb* on DNA extracted from organs of mice by qPCR. Dots indicate dCT(*Actb* - *WPRE*) for 4 individual mice per group. Figure adapted from Hölting et al. [134].

Figure 4.7: Low background activity of GGAA-msat promoters in murine tissues.

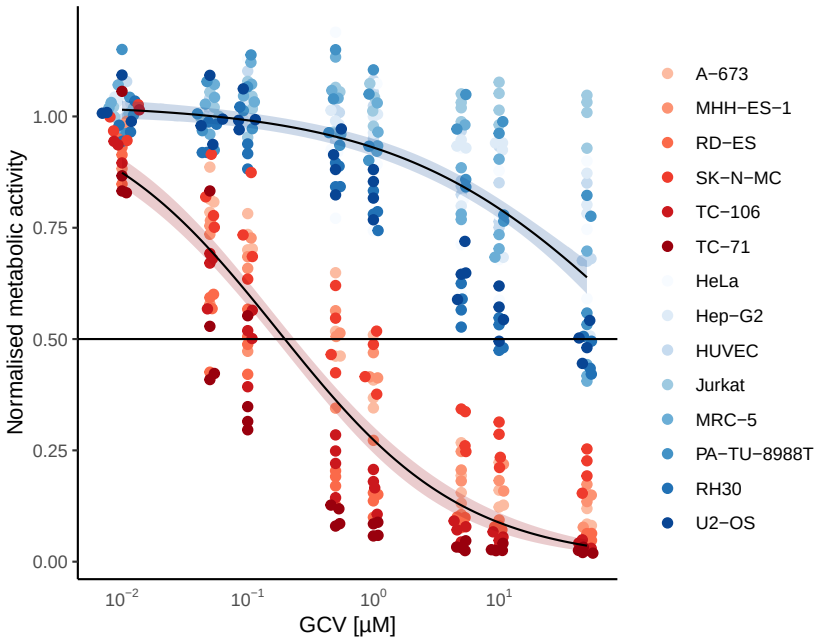

Figure 4.8: Increased GCV sensitivity of EwS compared to non-EwS cell lines transduced with pLenti_25_LT_Puro.
Resazurin-based cell viability assay of pLenti_25_LT_Puro-transduced and selected EwS and non-EwS cell lines 72 h after GCV addition. Dots represent 4 biologically independent experiments with relative fluorescence units normalised to vehicle control. Lines show dose-response curves with 95% confidence intervals based on a three-parameter log-logistic regression model calculated for EwS and non-EwS cells, respectively. Figure adapted from Hölting et al. [134].

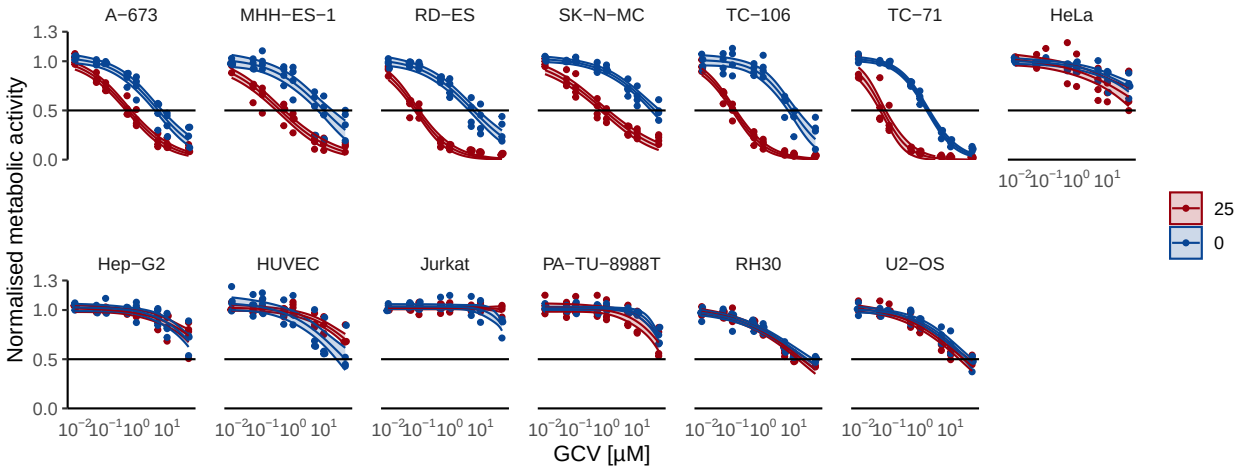

Figure 4.9: Increased GCV sensitivity of EwS compared to non-EwS cell lines transduced with pLenti_25_LT_Puro.
Resazurin-based cell viability assay of pLenti_25_LT_Puro (from Fig. 4.8)- or pLenti_0_LT_Puro-transduced and selected EwS and non-EwS cell lines 72 h after GCV addition. Dots indicate relative fluorescence units normalised to vehicle control for 4 biologically independent experiments. Lines show dose-response curves with 95% confidence interval based on a three-parameter log-logistic regression model calculated for EwS or non-EwS cells respectively. Figure adapted from Hölting et al. [134].

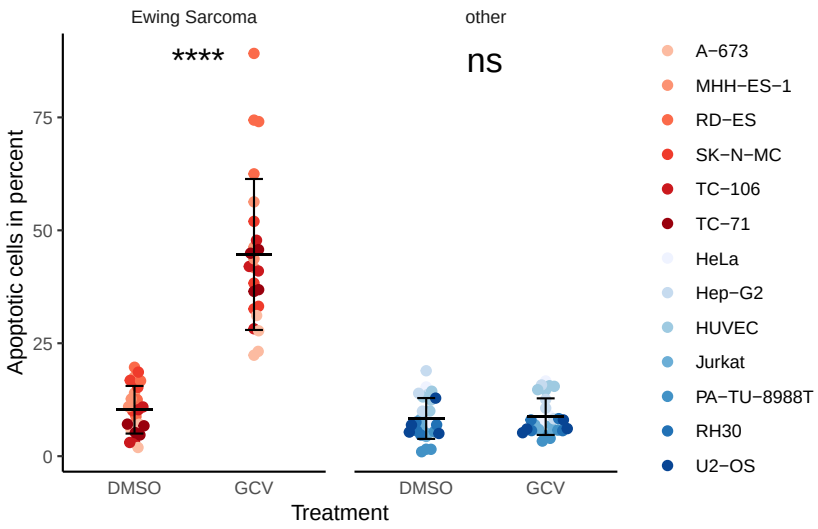

Figure 4.10: Specific induction of apoptosis after GCV exposure in EwS cell lines transduced with pLenti_25_LT_Puro.

Flow cytometry analysis of Annexin V and PI stained EwS and non-EwS transduced with pLenti_25_LT_Puro after 72 h of treatment with 0.4 µM GCV. Dots indicate the percentage of Annexin V positive cells for 4 independent experiments. Horizontal bars indicate mean and whiskers standard deviation per group.

of a wide variety of cells by binding to the almost ubiquitously expressed human and murine LDL receptor [124]. To limit integration-associated toxicity by transduction of normal tissues and loss of lentivirus particles to non-target cells, tropism can be limited by using more specific envelope proteins that induce lentivirus binding by other means. For this study, the previously published envelope protein 2.2, which is based on a modified and optimised Sindbis virus glycoprotein containing the Fc-binding domain of protein A, was used to allow antibody-mediated transduction of target cells [125]. It has been shown that 2.2 allows transduction only after pseudotyping/mixing with IgG directed against antigens on target cells with greatly reduced non-specific infectivity [125, 135]. Several cancer models have been successfully transduced *in vivo* using this envelope protein with antibodies directed against antigens expressed on the surface of the respective cancer cell [125, 135, 136].

In principle, CD99 would be a highly expressed surface protein in EwS. However, its ubiquitous expression in normal tissues makes it an unsuitable target for such an approach [49]. To identify EwS-specific candidate surface proteins that are highly expressed in EwS but minimally expressed in normal tissues, a previously described set of gene expression microarray data from 50 EwS and 928 normal tissues (comprising 70 tissue types) was analysed for differentially expressed genes between EwS and each other tissue [49]. Using a false discovery rate of 0.05, 36 genes were identified that were significantly overexpressed in EwS compared to any other normal tissue (Table 4.1). Three of these genes were selected for further investigation as putative targets due to them being surface proteins with commercially available monoclonal antibodies against their extracellular domains: *ADGRG2* encoding the orphan receptor GPR64, *CNMD* encoding LECT1, and *FAT4* (Fig. 4.11).

To assess the expression and surface-presence of these proteins on 6 Ewing sarcoma cell lines, indirect flow cytometry was performed using such monoclonal antibodies. In addition, the presence of GD2, a membrane-bound disialoganglioside that has been identified as a therapeutic target in neuroblastoma and potentially Ewing sarcoma, was assessed in a similar manner [137, 138]. Of the antigen-antibody interactions that were evaluated, the staining of GPR64 resulted in the highest fluorescence intensities on the EwS cell lines, with the exception of the positive control CD99 (Fig. 4.12). Therefore, GPR64 was chosen for further investigation of its suitability for targeted transduction. For this purpose, lentiviral particles were produced using the envelope plasmid 2.2 and a transfer plasmid expressing a GFP reporter under a CMV promoter. These vectors were then combined with either a GPR64 antibody, a CD99 antibody or an isotype control to transduce EwS (A-673, RD-ES, TC-71) and non-EwS (HeLa, Jurkat, U2-OS) cell lines. Flow cytometric analysis of cells transduced with anti-GPR64-coated virus revealed specific GFP-expression in EwS cells and no expression of the reporter gene in either group transduced using isotype control antibody (Fig. 4.13). Use of anti-CD99-coated virus resulted in relevant transduction levels in both EwS and control cells demon-

Table 4.1: Genes differentially expressed between primary EwS and normal tissues.

Gene	logFC	AveExpr	adj.P.Val
PAX7	5.553933837	4.57532765	1.0735E-223
JAKMIP2	4.699414952	4.698844466	1.5469E-109
PCDH8	6.862870038	4.02322166	2.61328E-92
RBM11	6.137905562	3.940960885	2.87962E-92
HS3ST4	4.541931316	5.147430249	2.1564E-84
DKK2	6.474379865	4.299751886	2.54387E-74
LIPI	5.376713499	3.352684915	4.09906E-72
CCDC171	4.015652728	3.518686501	9.72933E-70
NR0B1	4.685013995	4.674193876	6.50988E-52
HOTAIR	4.419379729	3.395172254	4.92757E-50
CNMD	3.766061211	4.936652595	1.56698E-44
LOXHD1	3.688915185	4.747858337	4.06151E-43
CLEC11A	3.602501923	6.24170085	9.72426E-43
PGLYRP2	3.678884968	4.67243184	1.26442E-41
GLCE	4.35002272	5.664340125	4.7021E-40
SIAH3	3.649937118	3.51814478	1.98533E-39
SOX11	4.713850292	4.142252711	2.41487E-38
SUGT1-DT	3.550338662	4.450249772	1.04388E-36
POU4F2	4.50518287	3.70279176	1.20413E-36
ZDHHC21	2.90991701	4.920131587	1.54168E-31
ADGRG2 (*GPR64*)	5.09717847	5.024568785	1.67703E-31
CD99P1	3.29116497	6.286130494	6.72967E-29
ARTN	2.529775794	5.183816282	2.38207E-26
SLC17A8	3.452175525	3.099155228	9.64092E-26
KDSR	3.403876343	6.572682535	1.05411E-24
CYP26B1	3.185744959	5.654069244	4.96153E-24
BDP1	2.926879327	6.050506121	1.43056E-22
TDRD3	2.532684943	6.299690174	1.11072E-21
CHD3	2.412442909	7.48058909	3.6174E-21
FCGRT	2.711723756	8.656366124	6.86924E-21
LOC101929759	2.369781929	4.203776162	9.2238E-21
LPAR4	2.226213342	3.584723207	2.02259E-20
FAT4	3.217402043	6.060423731	2.235E-19
QRFPR	2.699212426	3.638798436	3.93943E-16
ADRB3	2.150934213	5.106971627	1.39935E-13
GLG1	1.877690617	8.99222347	2.32414E-09

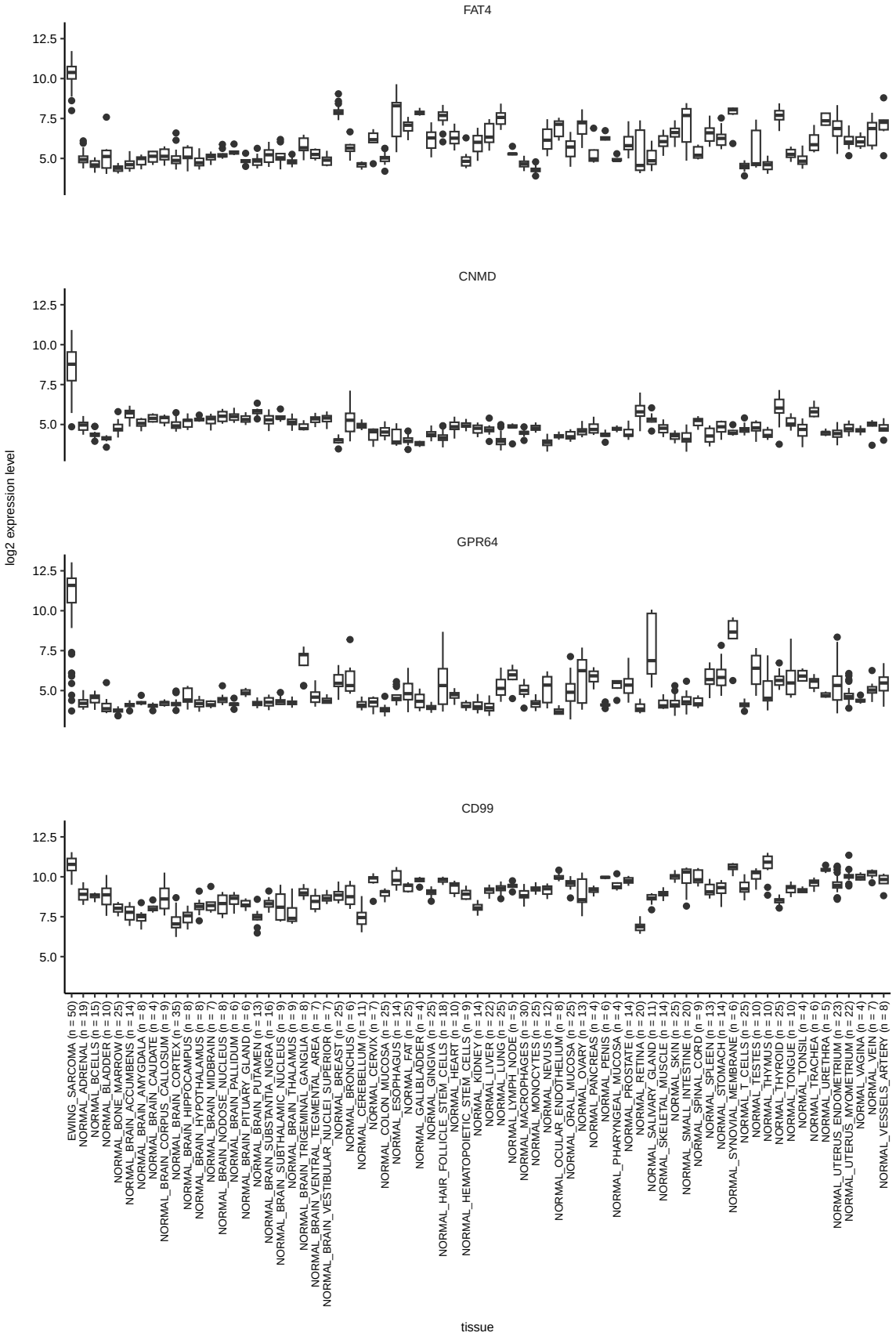

Figure 4.11: Expression levels of *FAT4*, *CNMD*, *GPR64* (*ADGRG2*) and *CD99* in Ewing sarcoma and normal tissues.
Microarray gene expression data of 50 Ewing sarcoma samples and 928 samples of 70 different normal tissue types. Figure adapted from Hölting et al. [134].

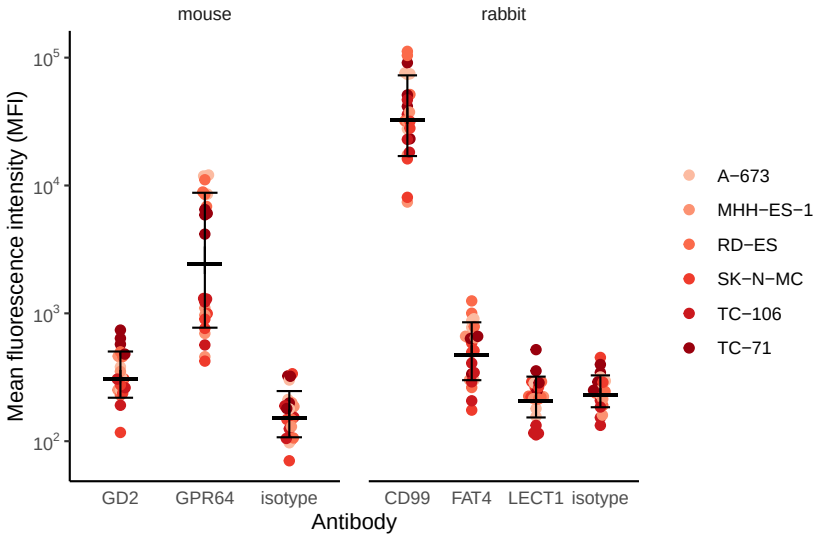

Figure 4.12: Flow cytometry of EwS cell lines stained for different potential surface targets.

Detection of surface presence of GD2, GPR64, CD99, FAT4 and LECT1 by antibody staining and flow cytometry. Isotype controls for both antibody host species were included separately. Dots indicate mean fluorescent intensity (MFI) for 4 independent experiments. Mean and standard deviation per group are depicted as horizontal bars and whiskers. Figure adapted from Hölting et al. [134].

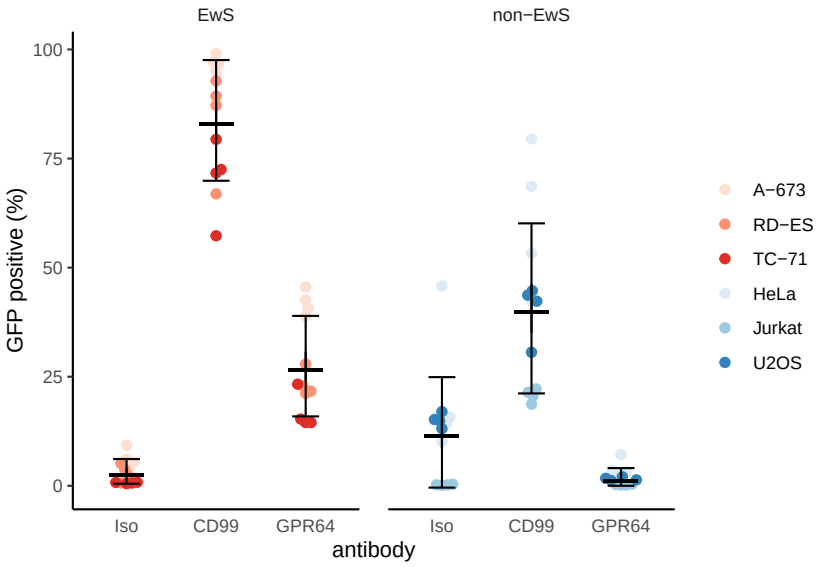

Figure 4.13: Flow cytometry of EwS and non-EwS cell lines after transduction with antibody-targeted, GFP-encoding lentiviruses.
Dots indicate the percentage of GFP-positive cells determined by flow cytometry from 4 biologically independent experiments. Horizontal bars and whiskers represent the mean and standard deviation per group. Figure adapted from Hölting et al. [134].

strating the lack of specificity of this antigen for EwS (Fig. 4.13).

Having demonstrated anti-GPR64-mediated transduction of EwS cells to be feasible *in vitro*, it was next to be assessed in a more complex *in vivo* model. To this end, 2.2-pseudotyped and antibody-coated lentiviral particles carrying the Firefly luciferase transgene under regulatory control of the 25_GGAA_YBL (pLenti_25_LT) or a CMV promoter (pLenti_CMV_LG) were injected into subcutaneous RD-ES xenografts. Bioimaging at 14 days showed that intratumoral injection of anti-CD99 and anti-GPR64 coated viral particles resulted in detectable bioluminescence signals, a surrogate for transduced RD-ES cells, comparable to VSV-G pseudotyped lentiviral particles used as a positive control (Fig. 4.14). However, 2.2 enveloped lentivirus without antibody coating did not result in effective transduction of tumour cells, as evidenced by the absence of detectable luminescence (Fig. 4.14 (top)). Experiments with A-673 xenografts confirmed the feasibility of anti-GPR64 mediated transduction of EwS *in vivo* and the antibody-dependency of 2.2 enveloped lentivirus (Fig.4.14 (bottom)).

Overall, these experiments suggested antibody-mediated lentiviral transduction of EwS cells to be possible both *in vitro* and *in vivo*.

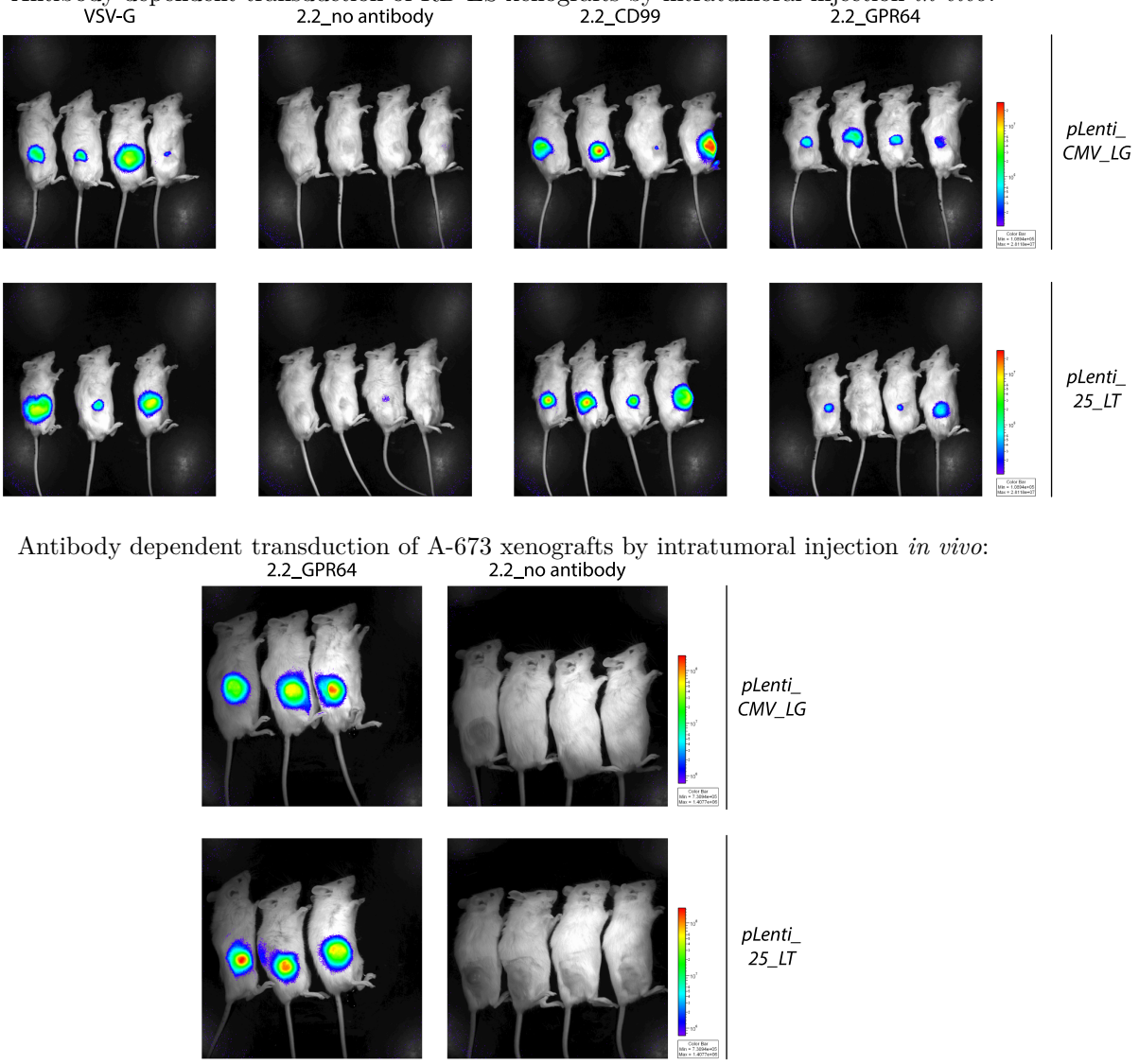

Figure 4.14: Antibody dependent transduction of RD-ES and A-673 xenografts by intratumoral injection *in vivo*.

Bioluminescence measurements using a 20 s exposure time in NSG mice 14 days after intratumoral injection of $0.5 \cdot 10^6$ TU of lentiviral particles enveloped with either VSV-G, or 2.2 and coated with the indicated antibodies or no antibody. Viral particles were produced with the transfer plasmids pLenti_25_LT or pLenti_CMV_LG as indicated. Figures adapted from Hölting et al. [134].

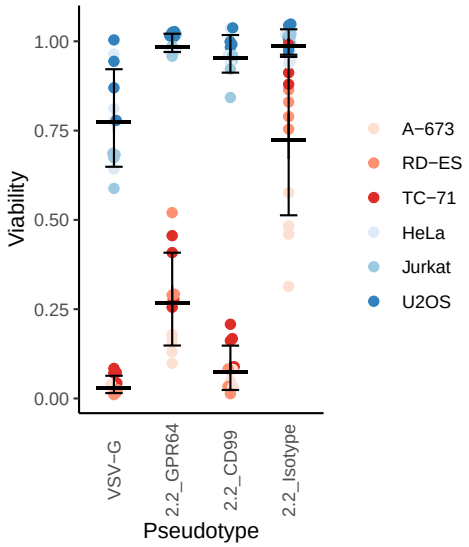

Figure 4.15: Combining targeted transduction with a EwS-specific gene expression increases therapeutic specificity *in vitro*.
Resazurin-based cell viability assay of EwS and non-EwS cell lines treated with GCV (20 M) or DMSO vehicle control 24 h after GPR64-targeted transduction with pLenti_25_LT. Readout was performed 72 h after GCV addition. CD99-targeting lentiviruses, non-targeting lentiviruses (isotype) and VSV-G pseudotyped lentiviruses were included as controls. Dots indicate the percentage of GFP-positive cells determined by flow cytometry from 4 biologically independent experiments. Horizontal bars and whiskers represent the mean and standard deviation per group. Figure adapted from Hölting et al. [134].

4.4 Targeted tumour therapy combining EwS-specific delivery and transcription

Following the development of a EwS-specific expression cassette and the evaluation of a EwS-targeted delivery system, the question arose as to whether the specific treatment effects achieved with the former could be improved by combination with the latter. To evaluate this *in vitro*, a panel of 3 of each of the EwS and control cell lines was treated with lentivirus produced with the transfer plasmid pLenti_25_LT and enveloped with either VSV-G or 2.2, coated with anti-GPR64, anti-CD99 or isotype control antibodies. Following viral treatment, cells were exposed to 20 µM of GCV and viability assayed at 72 hours using a resazurin-based readout. These assays showed that non-EwS cells treated with anti-GPR64 coated viral particles were significantly less affected by GCV than the VSV-G virus treated cells (Fig. 4.15). Indeed, while still inducing a significant reduction in viability in EwS cells, no relevant effect of GCV on viability of control cells was detected when compared to similarly transduced but vehicle treated control cells (Fig. 4.15).

Having gained this *in vitro* evidence of therapeutic effects of such a double-targeted suicide gene therapy approach for EwS, its effectiveness was to be assessed in an *in vivo* model. As a first step, the capability of the orally available ganciclovir pro-drug valganciclovir (VGCV) to induce tumour regression in the hypothetical case of 100 % transduced tumours was assessed. For this purpose, EwS cell lines A-673 and RD-ES, transduced and selected for transduction with pLenti_25_LT_Puro as described in section 4.2, were subcutaneously xenografted into the flanks of immunocompromised NSG mice. Addition of VGCV to the drinking water after tumours had grown to approximately 5mm in diameter induced complete regression of the transduced xenografts, while tumours in contol mice reached the size exclusion cut off of 1500 m^3 within around 3−4 weeks 4.16.

With these data hinting at the therapeutic effectiveness of this expression cassette in the ideal case of complete tumour transduction, a more realistic treatment setting was investigated next. To this end, subcutaneous xenografts of the wild-type EwS cell line A-673 were established in the flanks of NSG mice. After reaching an average of 5 mm in diameter, GPR64-directed treatment (pLenti_25_LT) or mock (pLenti_CMV_LG) virus was injected into the subcutaneous tumours and mice treated with oral VGCV ad libitum or sucrose control. Indeed, mice injected with treatment virus and receiving oral VGCV showed reduction in tumour growth compared with mice receiving treatment virus without the prodrug, or mock virus (Fig. 4.17).

Having demonstrated the therapeutic efficacy of this GGAA-msat-based suicide gene therapy in wild-type cells, the next step was to evaluate its applicability in a more systemic treatment setting that more closely resembles the actual clinical problem of metastatic EwS. To this end, A-673 EwS cells expressing a firefly luciferase reporter under the control of a CMV promoter were injected into the peritoneal cavity of NSG mice. These animals were then treated with repeated intraperitoneal injections of GPR64-directed 2.2 pseudotyped lentivirus produced with the thymidine kinase-bearing transfer plasmid pLenti_25_TK or a PBS control and oral VGCV. Bioluminescence measurements over the course of treatment showed a significant reduction in tumour growth, as indicated by reduced luminescence intensities in the treatment group, with no clinically apparent adverse effects of treatment (Fig. 4.18).

Collectively, these data suggested that GGAA-mast based expression of therapeutic genes delivered by anti-GPR64 targeted lentivirus allows specific induction of anti-tumour effects in EwS models *in vivo*.

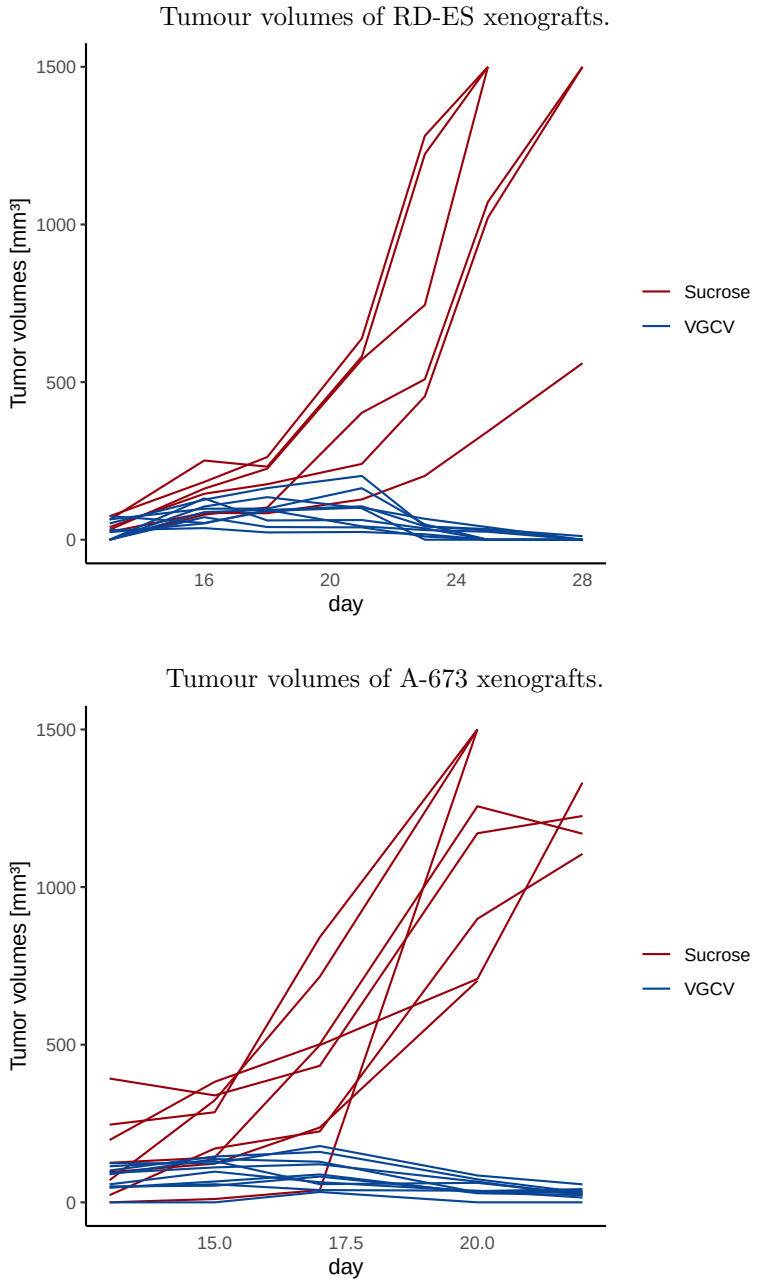

Figure 4.16: A-673 and RD-ES xenografts transduced with pLenti_25_LT_Puro are eradicated by VGCV treatment.
Tumour volumes of subcutaneous xenografts of the indicated cell EwS-cell lines pre-transduced with pLenti_25_LT_Puro. Once the tumours had reached a mean diameter of 5 mm, Valganciclovir (0.5 mg/ml in drinking water supplemented with 5% sucrose) or sucrose (5% in drinking water) was administered orally ad libitum. Figure adapted from Hölting et al. [134].

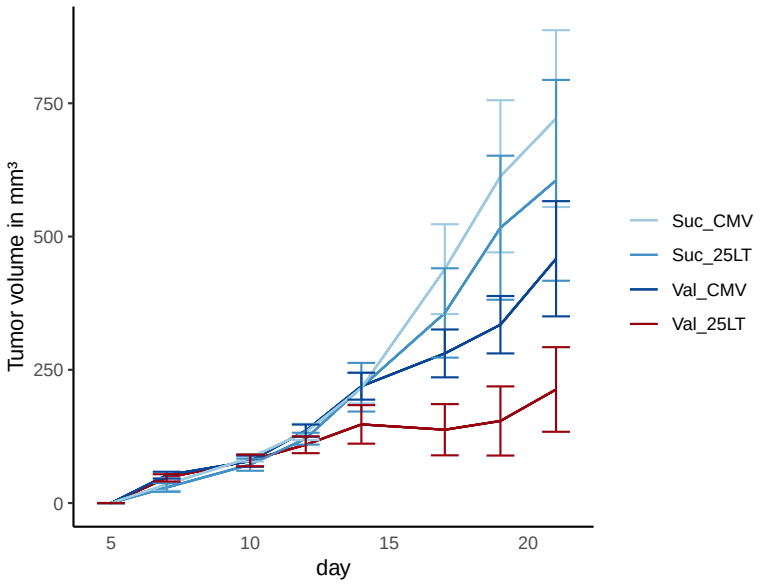

Figure 4.17: GGAA-msat based suicide gene expression confers anti-tumour effects in intratumoral injection treatment models.
Tumour volumes of A-673 subcutaneous xenografts treated with GPR64-targeting pLenti_25_LT or pLenti_CMV_LG (sham) lentiviruses. When tumours reached a mean diameter of 5 mm, valganciclovir (VGCV, 0.5 mg/ml in drinking water supplemented with 5% sucrose) or sucrose (5% in drinking water) was administered orally ad libitum. Starting on day 7, lentiviruses were injected intratumourally twice a week. Data are presented as mean tumour volume and SEM of 6-7 mice per treatment condition. Figure adapted from Hölting et al. [134].

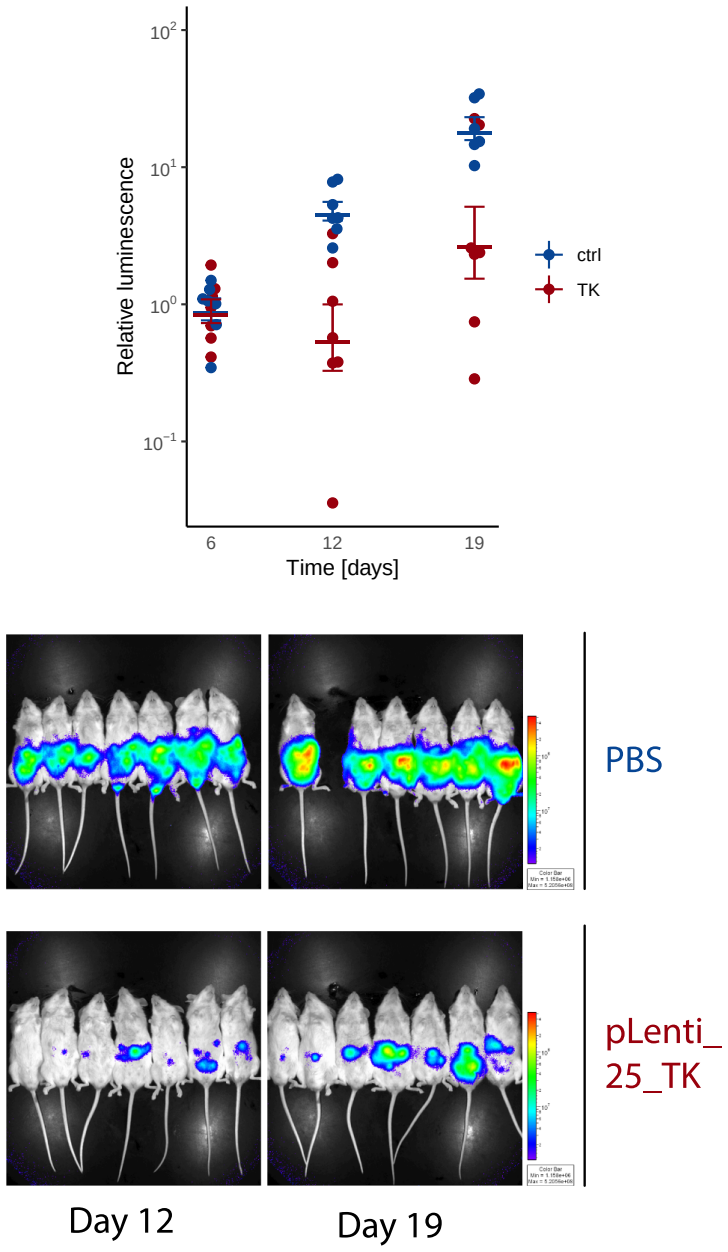

Figure 4.18: GGAA-msat based suicide gene expression confers anti-tumour effects in intraperitoneal injection treatment models.
Relative bioluminescence (right) and bioluminescence images (left) of NSG mice after intraperitoneal tumour inoculation with firefly luciferase-expressing A-673. 3 days after tumour injection, mice were randomised to receive repeated intraperitoneal injections of either GPR64-directed 2.2. pseudotyped lentivirus (pLenti_25_TK) or PBS. In both groups, VGCV was administered orally 3 days after the first viral injection. The representative bioluminescence images show both groups 12 and 19 days after tumour inoculation. The dots indicate the bioluminescence signal relative to the mean measured at the start of VGCV (day 6) for 6-7 mice per group. Horizontal bars indicate mean and whiskers SEM per group. Figure adapted from Hölting et al. [134].

4.5 PAX3::FOXO1-occupied super-enhancer sequences allow specific transgene expression in alveolar rhabdomyosarcoma

The experiments described above suggest that the aberrant DNA binding preferences of the EWSR1::FLI1 fusion oncogene in EwS can be exploited to drive EwS-specific gene therapy. This approach should be conceptually possible for other cancers driven by fusion transcription factors if (1) their DNA binding diverges from the binding motifs of their constituents and (2) they are able to induce a direct transactivating effect. Another suitable candidate entity is alveolar rhabdomyosarcoma (ARMS) harbouring the fusion transcription factor PAX3::FOXO1 (P3F1) as the dominant oncogene in 50 % of cases [139]. Similarly to EWSR1::FLI1, P3F1 is expressed into a chimeric transcription factor that binds to certain DNA motifs and has been found to establish pathogenic super-enhancers (SE) and to induce the expression of target genes [114]. For example, Gryder and colleagues described a PAX3::FOXO1 binding site in the third intron of the *ALK* gene, coinciding with a super-enhancer (SE) in fusion positive ARMS cell lines and tumours but not in fusion negative controls [114].

To assess whether this aberrant P3F1-dependent enhancer could be used to express delivered genes specifically in cell line models of alveolar rhabdomyosarcoma, a DNA segment of approximately 300 bp containing a known P3F1 binding site was synthesised from the human reference genome (chr2:29,657,671-29,657,976 in hg38) and cloned upstream of the minimal promoter YB_TATA into a luciferase reporter plasmid. The ability of the resulting construct, called ALK-SE, to induce reporter expression was assessed in luciferase assays after transfection of 2 fusion-positive ARMS cell lines (Rh30 and Rh4) and 4 control cell lines, including the fusion-negative embryonal rhabdomyosarcoma cell line RD. As expected, promoter activities were significantly higher in fusion-positive ARMS cell lines Rh4 and Rh30 than control cell lines (Fig. 4.19). Gryder et al. were able to show that the transactivating activity of the ALK-SE could be abrogated by two point mutations of a single P3F1 binding motif, consisting of `GTCACGGT`, indicating the necessity of P3F1- binding for its influence on transcription [114]. To enhance the ARMS-specific transactivating activity, the putative P3F1 binding site in ALK-SE was altered to completely match the binding motif `ATTWGTCACGGT` annotated for PAX3::FOXO1 at HOMER motifs resulting in a construct called SYN_ALK_1. Cloned upstream of the YB_TATA minimal promoter this alteration improved reporter expression levels specifically in ARMS cell lines (Fig. 4.19). Notably, the addition of two or four additional `ATTWGTCACGGT` sequences as P3F1-binding sites (called SYN_ALK_3 and SYN_ALK_5), lead for further increases in promoter activity in RH4 and Rh30 compared to control cell lines (Fig. 4.19). These experiments gave first evidence of the possibility to achieve ARMS-specific gene expression by combining sequences containg P3F1-binding sites

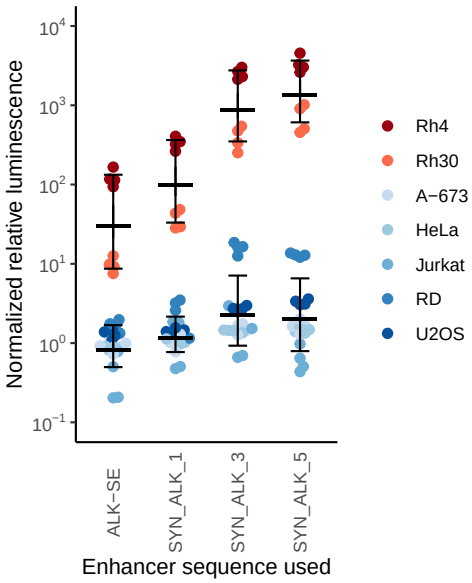

Figure 4.19: A P3F1-binding site containing DNA segment combined with YB_TATA has higher promoter activity in fusion-positive ARMS than in control cells.

Luciferase reporter assays of fusion-positive ARMS (RH4 and RH30) and control cell lines after co-transfection with a reporter plasmid containing the alk-SE or derivative DNA segments upstream of the minimal promoter YB-TATA and a constitutively expressed *Renilla* luciferase encoding plasmid. The dots indicate the ratio of Firefly to *Renilla* luminescence normalised to those obtained with a reporter plasmid without alk-SE. Horizontal bars indicate mean and whisker standard deviation per group. Figure adapted from Hölting et al. [134].

with a core promoter.

To assess whether these cassettes could be used to induce specific treatment effects in ARMS, similarly to the observations with EwS, the best performing cassette, SYN_ALK_5, was inserted into a lentiviral plasmid expressing the *HSV-TK* upstream of the core promoter YB_TATA. Fusion positive ARMS cell lines Rh30 and Rh4 and 4 control cell lines were transduced with lentivirus produced using this plasmid or a control plasmid containing the YB_TATA alone. In concordance with the previous observations in EwS, only ARMS cell lines showed increased sensitivity to GCV when transduced with the SYN_ALK_5 (Fig. 4.20).

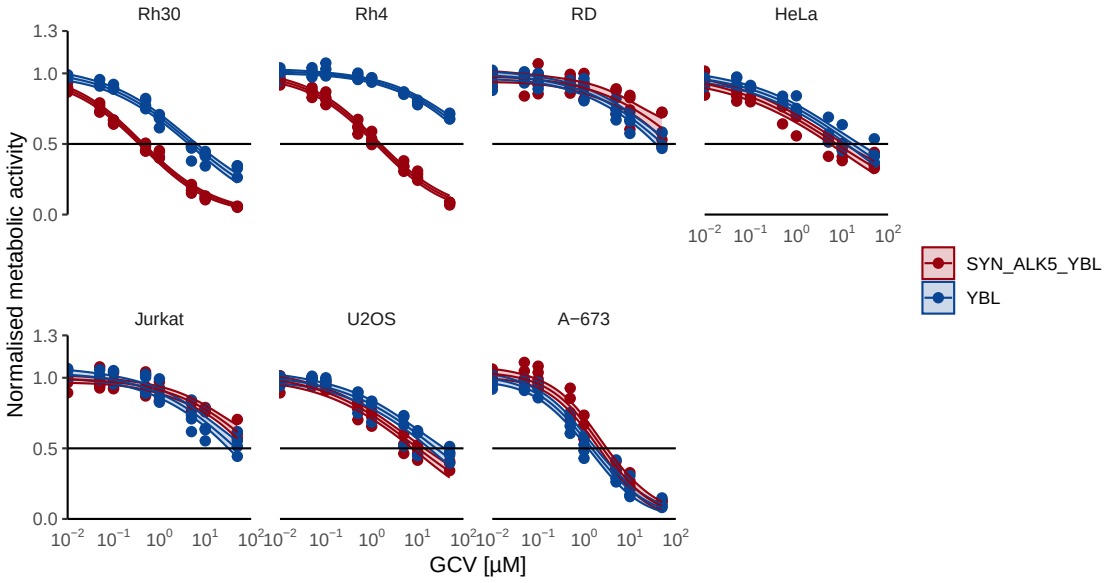

Figure 4.20: Increased GCV sensitivity of ARMS transduced with pLenti_syn_alk_5_LT_Puro compared to a control plasmid.

Resazurin-based cell viability assay of P3F1-negative control cell lines transduced as in Fig. 3c. For 4 biologically independent experiments, dots indicate relative fluorescence units normalised to vehicle control. The lines show dose-response curves with a 95% confidence interval, based on a three-parameter log-logistic regression model that was calculated for each cell line. Figure adapted from Hölting et al. [134].

5. Discussion

Outcomes for patients with paediatric sarcomas, including EwS and ARMS, have greatly improved in recent decades, particularly for localised disease, probably due to improvements in risk-stratified multimodal therapy [140, 141]. However, patients with recurrent or metastatic disease still have a poor prognosis despite the often crippling and highly toxic nature of the treatment regimens used [4, 142]. Only a small number of targeted therapies have been tested in early phase clinical trials and these have shown limited or no activity in these entities [61]. There is an unmet need for innovative treatment strategies that not only improve the prognosis of children and adolescents with these diseases, but also reduce the side effects of standard treatment.

EF1 and P3F1 would constitute ideal targets for EwS and ARMS therapy, were it not for their lack of enzymatic activity impeding the design of small molecules to inhibit their function [61]. Hence, these oncogenic transcription factors have often been considered undruggable [61]. Notably, recent evidence in EwS suggested low levels of EF1 expression or activity to promote metastasis rather than to suppress tumour progression [143, 144]. This further discourages from using direct inhibition of EF1 as a therapeutic strategy. To circumvent this conundrum, the aim of this project was to establish and investigate a way to exploit the neomorphic DNA-binding properties of chimeric fusion transcription factors for tumour-specific therapeutic gene expression, focusing on EwS.

To this end, in this thesis an expression system was rationally designed by combining the aberrant binding site of the disease-specific fusion transcription factors and a synthetic minimal activity promoter. Disease-specific expression activity of the resulting construct and its EF1-dependence were demonstrated in reporter both episomally and genomically integrated after lentiviral delivery by reporter assays, qPCR and immunoblotting. *In vitro* experiments using HSV-TK-mediated prodrug conversion suicide gene therapy as a treatment model then confirmed that the EwS-specificity of transgene expression could be translated into specific treatment effects in *in vitro* models. For *in vivo* evaluation of the ability of these constructs to induce specific treatment effects, a combination with a targeted delivery system was chosen to mitigate toxicity through non-specific integration of lentiviral vectors. Analysis of a curated microarray dataset identified GPR64 as a suitable surface target for EwS and

demonstrated its specific presence on EwS cell lines as well as its suitability for targeted transduction using flow cytometry. The combination of the novel expression cassette and the published transduction system could induce specific treatment effects *in vivo* demonstrated in experiments employing intratumoral injections in subcutaneous xenografts and peritoneal metastasis models. Finally, the generalisability of the proposed promoter design principle to other diseases characterised by transactivating aberrant transcription factors was demonstrated with fusion-positive alveolar rhabdomyosarcoma models.

The development of gene therapy and gene editing has been rapid in recent decades and may soon be part of the arsenal of cancer therapies in clinical use [145, 146]. However, compared to the recent successes of gene therapy in monogenic, inherited diseases such as haemophilia, gene therapy for cancer has lagged behind [147]. Unlike in monogenetic disorders, whose clinical correction only needs transgene delivery to a fraction of targeted cells, for cancer gene therapy almost all cancer cells need to be killed either by transduction or by indirect effects of the transgene [102]. This will require not only further improvements in delivery systems, which were not investigated in this study, but also improved safety mechanisms to limit the cytotoxic effects of the genetic payload on cancer cells, as off-target gene delivery is expected to increase when optimising for high tumour transduction rates. For this purpose, tumour-specific gene expression cassettes are a promising tool and have been generated for a variety of malignancies, with varying degrees of success [148, 149]. Previously published tumour-specific promoters have most often been based on endogenous promoter sequences of genes overexpressed by the respective cancer entities. Examples include the promoter of *human telomerase reverse transcriptase (hTERT)* or *prostate-specific antigen (PSA)* [150, 151]. While these promoters are only active in a select subset of human tissues and certain cancers, they do occur in the human genome and physiologically allow transcription in non-cancerous cells. For example, the *hTERT* promoter is active in certain stem cells and normal prostate tissue expresses *PSA*.

Unlike previous studies, this thesis does not employ endogenous promoter sequences, but combines synthetic core promoters with fusion oncogene-dependent enhancer sequences. This design exploits the aberrant DNA binding of mutant oncoproteins, which are not present in non-transformed healthy tissue, by relying on such *de novo* enhancers. Furthermore, because expression of these fusion transcription factors are essential for maintaining the malignant phenotype of their corresponding cancer cells, escape mechanisms by loss or persistent downregulation seem unlikely.

Since, apart from EWSR1::FLI1, only transcriptional repressors have been described to bind to GGAA-microsatellites, an expression system based on this neomorphic interaction should have superior specificity [152, 153, 153]. This study is the first to investigate this approach, and presents promising data supporting this claim. However, while its specificity was demonstrated in 8 different human control cell lines and murine tissues, potential off-target

activity of this expression cassette in certain human tissues can not yet be excluded definitively. But, due to its simple design, lacking genomic flanking regions of regulatory core elements (i.e. GGAA-msats), there should be fewer points of failure than in conventional promoter based approaches.

Because of its strong and well-characterised phenotype, *HSV-TK* was chosen as the transgene for the treatment experiments in this study. Despite promising results by us and others in preclinical models, suicide gene therapy in clinical use is limited because it induces toxic effects only to transduced cells, and for some transgenes such as *HSV-TK*, cells in the immediate vicinity [145]. This makes high transduction rates a necessity for achieving relevant effects, limiting the usefulness of suicide gene therapy for cancer with current non-replicating delivery systems. On the other hand, gene therapy approaches overexpressing cytokines improving the normally immunosuppressive microenvironment of EwS and ARMS might be a promising approach alone or in combination with cellular immunotherapies [154]. In these cases, specific expression of these cytokines may be necessary to prevent immune-related adverse events and the promoter design proposed in this study may therefore be a valuable tool [155].

As discussed earlier, the effective delivery of transgenes to target cells is an important bottleneck in gene therapy in general and especially in cancer gene therapy. In this study, non-replicating lentiviral vectors were used for this purpose. These HIV-derived vectors are relatively easily and inexpensively produced at small scale and have the ability to transduce cells regardless of their proliferation rate [156]. Extensive research and optimisation have made lentiviral vectors not only the most popular tool for stable gene delivery to mammalian cells in laboratories but also a frequently used vector for clinical applications [157]. While they have been used successfully in recent clinical trials for inherited haematological disorders, all of these trials involved *ex vivo* transduction and subsequent engraftment of the transduced cells [158, 159, 160]. True *in vivo* use of lentiviral vectors is hampered by the fact that they are integrating viruses that insert their genetic material into the host cell's genome potentially causing long-lasting toxicity due to insertional mutagenesis [161]. To circumvent this problem, this study employed a targeted lentiviral transduction approach using GPR64, identified with *in silico* and *in vitro* analyses, as a putative surface target on EwS cells. Exploiting this target protein, EwS-specific transduction was demonstrated, albeit using only a limited set of control cell lines, suggesting that this approach may be successful in preventing unwanted integration events in normal cells upon systemic delivery.

However, lentiviral vectors as they are used in this study are unlikely to be a suitable delivery system for cancer gene therapy in human patients, not only because of their integrating nature, but also for the difficulty of transducing sufficient numbers of tumour cells. Instead, non-integrating vectors, such as adenovirus and adeno-associated viruses are more likely to be used in clinical trials. As the activity and specificity of the promoters designed in this

study were also demonstrated in the episomal setting, they should be usable with such viral vectors as long as their genome is encoded in DNA rather than RNA [103]. These promoters could be particularly valuable for use with oncolytic viruses (OVs). Because OVs are able to replicate in tumour cells, they can potentially have greater effects than non-replicating vectors and therefore require better mechanisms to direct these effects to target cells. In these cases, specific expression cassettes, such as those designed in this study, could be used to allow replication of the viral particles only in the presence of a fusion transcription factor [162]. Alternatively, they could be used to drive the expression of immunostimulatory therapeutic genes of so-called armed OVs, an approach currently being tested in several phase I and II clinical trials with non-specific promoters in other tumour entities [162].

In conclusion, this work provides evidence that the aberrant DNA-binding preferences of some disease-specific fusion transcription factors can be exploited for tumour-specific gene expression. The model used to test the therapeutic applicability of the designed expression systems lacks clinical translatability mainly due to the limitations of the available vector system. Nevertheless, the concept demonstrated in this study could be a promising way to limit off-target effects for any future therapeutic approach that relies on gene expression in tumour cells, especially replicating oncolytic DNA viruses such as adenoviruses.

Limitations and future perspectives

While the present study has provided convincing data for a novel expression system in EwS and its potential application for specific therapy, as discussed above, several limitations should be acknowledged. These limitations may impact the translatability and robustness of the findings, and therefore warrant further investigation.

One notable limitation of this study is its reliance on cell line and xenograft experiments without the use of a syngenic mouse model. Such models play a vital role in mimicking the complex tumour microenvironment and immune interactions, which provides a more precise picture of pathophysiological disease progression. Regrettably, to the present day, no syngenic mouse model for EwS has been established. The cell line based models employed in this study do not allow a complete assessment of the proposed treatment strategy's efficiency and safety in an immunocompetent context. Patient-derived xenografts (PDX) present an alternative that could be an improvement over the cell line models used in this study as they are believed to more precisely replicate the disease of origin. Nevertheless, a syngenic mouse model is a direly needed tool for the preclinical research in EwS and its interactions with the host's immune system and their potential exploitation.

Besides the disease model used, the primary delivery system for the gene

therapy approach in this study using lentiviruses is a significant limitation. As discussed above, the integration of lentiviruses into the host genome causes concerns about potential off-target effects and insertional mutagenesis.

To overcome this challenge, this study used a targeting approach that relies on the surface protein GRP64 for specific transduction of EwS cells. As this surface antigen was not detected in all EwS cell lines tested and its pathophysiological role for EwS has not been described, one can assume that antigen escape is likely to be a problem for any anti-GPR64 directed treatment, which could potentially limit its effectiveness in the clinical setting. To avoid the issues associated with genomic integration, non-integrating viral vectors should be used to further evaluate the promoter designs of this study. As mentioned earlier, adenoviruses are promising substitutes that not only facilitate episomal gene delivery but also allow tumour-specific replication, which may increase the inducible therapeutic effects. Subsequent investigations could therefore assess the efficacy of the expression systems defined in this study in selectively delivering therapeutic payloads of oncolytic, i.e. replicating, adenoviruses.

References

[1] Olivier Delattre et al. "The Ewing Family of Tumors – A Subgroup of Small-Round-Cell Tumors Defined by Specific Chimeric Transcripts". In: *New England Journal of Medicine* 331.5 (Aug. 4, 1994), pp. 294–299. ISSN: 0028-4793. DOI: 10.1056/NEJM199408043310503. pmid: 8022439.

[2] James Ewing. "THE CLASSIC: Diffuse Endothelioma of Bone". In: *Clinical Orthopaedics and Related Research®* 450 (Sept. 2006), pp. 25–27. ISSN: 0009-921X. DOI: 10.1097/01.blo.0000229311.36007.c7.

[3] Leona A. Doyle. "Sarcoma Classification: An Update Based on the 2013 World Health Organization Classification of Tumors of Soft Tissue and Bone". In: *Cancer* 120.12 (2014), pp. 1763–1774. ISSN: 1097-0142. DOI: 10.1002/cncr.28657.

[4] Thomas G. P. Grünewald et al. "Ewing Sarcoma". In: *Nature Reviews Disease Primers* 4.1 (Dec. 2018), p. 5. ISSN: 2056-676X. DOI: 10.1038/s41572-018-0003-x.

[5] Jennifer Worch et al. "Age Dependency of Primary Tumor Sites and Metastases in Patients with Ewing Sarcoma". In: *Pediatric Blood & Cancer* 65.9 (2018), e27251. ISSN: 1545-5017. DOI: 10.1002/pbc.27251.

[6] Friederike Erdmann et al. *German Childhood Cancer Registry - Annual Report 2019 (1980-2018).* Institute of Medical Biostatistics, Epidemiology and Informatics (IMBEI) at the University Medical Center of the Johannes Gutenberg University Mainz, 2020.

[7] Muhammad U. Jawad et al. "Ewing Sarcoma Demonstrates Racial Disparities in Incidence-Related and Sex-Related Differences in Outcome". In: *Cancer* 115.15 (2009), pp. 3526–3536. ISSN: 1097-0142. DOI: 10.1002/cncr.24388.

[8] Sophie Postel-Vinay et al. "Common Variants near TARDBP and EGR2 Are Associated with Susceptibility to Ewing Sarcoma". In: *Nature Genetics* 44.3 (Mar. 2012), pp. 323–327. ISSN: 1061-4036, 1546-1718. DOI: 10.1038/ng.1085.

[9] Thomas G P Grünewald et al. “Chimeric EWSR1-FLI1 Regulates the Ewing Sarcoma Susceptibility Gene EGR2 via a GGAA Microsatellite”. In: *Nature Genetics* 47.9 (Sept. 2015), pp. 1073–1078. ISSN: 1061-4036, 1546-1718. DOI: 10.1038/ng.3363.

[10] Lisa Hum, Nancy Kreiger, and Murray M Finkelstein. “The Relationship between Parental Occupation and Bone Cancer Risk in Offspring”. In: *International Journal of Epidemiology* 27.5 (Oct. 1, 1998), pp. 766–771. ISSN: 0300-5771. DOI: 10.1093/ije/27.5.766.

[11] Jonathan D. Buckley et al. “Epidemiology of Osteosarcoma and Ewing’s Sarcoma in Childhood”. In: *Cancer* 83.7 (1998), pp. 1440–1448. ISSN: 1097-0142. DOI: 10.1002/(SICI)1097-0142(19981001)83:7<1440::AID-CNCR23>3.0.CO;2-3.

[12] Patricia Casarolli Valery et al. “Farm Exposures, Parental Occupation, and Risk of Ewing’s Sarcoma in Australia: A National Case–Control Study”. In: *Cancer Causes & Control* 13.3 (Apr. 1, 2002), pp. 263–270. ISSN: 1573-7225. DOI: 10.1023/A:1015036109130.

[13] Douglas Hanahan. “Hallmarks of Cancer: New Dimensions”. In: *Cancer Discovery* 12.1 (Jan. 12, 2022), pp. 31–46. ISSN: 2159-8274. DOI: 10.1158/2159-8290.CD-21-1059.

[14] E. Alejandro Sweet-Cordero and Jaclyn A. Biegel. “The Genomic Landscape of Pediatric Cancers: Implications for Diagnosis and Treatment”. In: *Science* 363.6432 (Mar. 15, 2019), pp. 1170–1175. DOI: 10.1126/science.aaw3535.

[15] Michael S. Lawrence et al. “Mutational Heterogeneity in Cancer and the Search for New Cancer-Associated Genes”. In: *Nature* 499.7457 (7457 July 2013), pp. 214–218. ISSN: 1476-4687. DOI: 10.1038/nature12213.

[16] Brian D. Crompton et al. “The Genomic Landscape of Pediatric Ewing Sarcoma”. In: *Cancer Discovery* 4.11 (Nov. 2014), pp. 1326–1341. ISSN: 2159-8274, 2159-8290. DOI: 10.1158/2159-8290.CD-13-1037.

[17] Nathaniel D. Anderson et al. “Rearrangement Bursts Generate Canonical Gene Fusions in Bone and Soft Tissue Tumors”. In: *Science* 361.6405 (Aug. 31, 2018), eaam8419. DOI: 10.1126/science.aam8419.

[18] Jessica I. Hoell et al. “RNA Targets of Wild-Type and Mutant FET Family Proteins”. In: *Nature Structural & Molecular Biology* 18.12 (12 Dec. 2011), pp. 1428–1431. ISSN: 1545-9985. DOI: 10.1038/nsmb.2163.

[19] Shinsuke Ishigaki et al. “Position-Dependent FUS-RNA Interactions Regulate Alternative Splicing Events and Transcriptions”. In: *Scientific Reports* 2.1 (1 July 24, 2012), p. 529. ISSN: 2045-2322. DOI: 10.1038/srep00529.

[20] Geoffrey G. Hicks et al. "Fus Deficiency in Mice Results in Defective B-lymphocyte Development and Activation, High Levels of Chromosomal Instability and Perinatal Death". In: *Nature Genetics* 24.2 (2 Feb. 2000), pp. 175–179. ISSN: 1546-1718. DOI: 10.1038/72842.

[21] Hongjie Li et al. "Ewing Sarcoma Gene EW Is Essential for Meiosis and B Lymphocyte Development". In: *The Journal of Clinical Investigation* 117.5 (May 1, 2007), pp. 1314–1323. ISSN: 0021-9738. DOI: 10.1172/JCI31222. pmid: 17415412.

[22] Xiangting Wang et al. "Induced ncRNAs Allosterically Modify RNA-binding Proteins in Cis to Inhibit Transcription". In: *Nature* 454.7200 (7200 July 2008), pp. 126–130. ISSN: 1476-4687. DOI: 10.1038/nature06992.

[23] Gina M. Sizemore et al. "The ETS Family of Oncogenic Transcription Factors in Solid Tumours". In: *Nature Reviews Cancer* 17.6 (June 2017), pp. 337–351. ISSN: 1474-175X, 1474-1768. DOI: 10.1038/nrc.2017.20.

[24] Olivier Delattre et al. "Gene Fusion With an ETS DNA · binding Domain Caused by Chromosome Translocation in Human Tumours". In: *Nature* 359 (1992).

[25] Jessica Zucman et al. "Combinatorial Generation of Variable Fusion Proteins in the Ewing Family of Tumours." In: *The EMBO Journal* 12.12 (Dec. 1993), pp. 4481–4487. ISSN: 0261-4189. pmid: 8223458.

[26] Poul H. B. Sorensen et al. "A Second Ewing's Sarcoma Translocation, t(21;22), Fuses the EWS Gene to Another ETS–Family Transcription Factor, ERG". In: *Nature Genetics* 6.2 (2 Feb. 1994), pp. 146–151. ISSN: 1546-1718. DOI: 10.1038/ng0294-146.

[27] Nicolò Riggi et al. "EWS-FLI1 Utilizes Divergent Chromatin Remodeling Mechanisms to Directly Activate or Repress Enhancer Elements in Ewing Sarcoma". In: *Cancer Cell* 26.5 (Nov. 2014), pp. 668–681. ISSN: 15356108. DOI: 10.1016/j.ccell.2014.10.004.

[28] Eleni M. Tomazou et al. "Epigenome Mapping Reveals Distinct Modes of Gene Regulation and Widespread Enhancer Reprogramming by the Oncogenic Fusion Protein EWS-FLI1". In: *Cell Reports* 10.7 (Feb. 24, 2015), pp. 1082–1095. ISSN: 2211-1247. DOI: 10.1016/j.celrep.2015.01.042.

[29] Kunal Gangwal et al. "Microsatellites as EWS/FLI Response Elements in Ewing's Sarcoma". In: *Proceedings of the National Academy of Sciences* 105.29 (July 22, 2008), pp. 10149–10154. ISSN: 0027-8424, 1091-6490. DOI: 10.1073/pnas.0801073105.

[30] Noëlle Guillon et al. "The Oncogenic EWS-FLI1 Protein Binds In Vivo GGAA Microsatellite Sequences with Potential Transcriptional Activation Function". In: *PLOS ONE* 4.3 (Mar. 23, 2009), e4932. ISSN: 1932-6203. DOI: 10.1371/journal.pone.0004932.

[31] Martin F. Orth et al. "Systematic Multi-Omics Cell Line Profiling Uncovers Principles of Ewing Sarcoma Fusion Oncogene-Mediated Gene Regulation". In: *Cell Reports* 41.10 (Dec. 6, 2022). ISSN: 2211-1247. DOI: 10.1016/j.celrep.2022.111761. pmid: 36476851.

[32] Kirsten M. Johnson et al. "Role for the EWS Domain of EWS/FLI in Binding GGAA-microsatellites Required for Ewing Sarcoma Anchorage Independent Growth". In: *Proceedings of the National Academy of Sciences* 114.37 (Sept. 12, 2017), pp. 9870–9875. DOI: 10.1073/pnas.1701872114.

[33] Gaylor Boulay et al. "Cancer-Specific Retargeting of BAF Complexes by a Prion-like Domain". In: *Cell* 171.1 (Sept. 2017), 163–178.e19. ISSN: 00928674. DOI: 10.1016/j.cell.2017.07.036.

[34] Iftekhar A Showpnil et al. "EWS/FLI Mediated Reprogramming of 3D Chromatin Promotes an Altered Transcriptional State in Ewing Sarcoma". In: *Nucleic Acids Research* 50.17 (Sept. 23, 2022), pp. 9814–9837. ISSN: 0305-1048. DOI: 10.1093/nar/gkac747.

[35] Savita Sankar et al. "Mechanism and Relevance of EWS/FLI-mediated Transcriptional Repression in Ewing Sarcoma". In: *Oncogene* 32.42 (Oct. 17, 2013), pp. 5089–5100. ISSN: 0950-9232, 1476-5594. DOI: 10.1038/onc.2012.525.

[36] Nathan C Sheffield et al. "DNA Methylation Heterogeneity Defines a Disease Spectrum in Ewing Sarcoma". In: *Nature Medicine* 23.3 (Mar. 2017), pp. 386–395. ISSN: 1078-8956, 1546-170X. DOI: 10.1038/nm.4273.

[37] Nicolò Riggi et al. "EWS-FLI-1 Expression Triggers a Ewing's Sarcoma Initiation Program in Primary Human Mesenchymal Stem Cells". In: *Cancer Research* 68.7 (Apr. 1, 2008), pp. 2176–2185. ISSN: 0008-5472. DOI: 10.1158/0008-5472.CAN-07-1761.

[38] Stephen L Lessnick, Caroline S Dacwag, and Todd R Golub. "The Ewing's Sarcoma Oncoprotein EWS/FLI Induces a P53-Dependent Growth Arrest in Primary Human Fibroblasts". In: *Cancer Cell* 1.4 (May 1, 2002), pp. 393–401. ISSN: 1535-6108. DOI: 10.1016/S1535-6108(02)00056-9.

[39] Kazuhiro Tanaka et al. *EWS-Fli1 Antisense Oligodeoxynucleotide Inhibits Proliferation of Human Ewing's Sarcoma and Primitive Neuroectodermal Tumor Cells.* Jan. 15, 1997. DOI: 10.1172/JCI119152.

[40] Siwen Hu-Lieskovan et al. "Sequence-Specific Knockdown of EWS-FLI1 by Targeted, Nonviral Delivery of Small Interfering RNA Inhibits Tumor Growth in a Murine Model of Metastatic Ewing's Sarcoma". In: *Cancer Research* 65.19 (Oct. 3, 2005), pp. 8984–8992. ISSN: 0008-5472. DOI: 10.1158/0008-5472.CAN-05-0565.

[41] Franck Tirode et al. "Genomic Landscape of Ewing Sarcoma Defines an Aggressive Subtype with Co-Association of *STAG2* and *TP53* Mutations". In: *Cancer Discovery* 4.11 (Nov. 2014), pp. 1342–1353. ISSN: 2159-8274, 2159-8290. DOI: 10.1158/2159-8290.CD-14-0622.

[42] Mark A. Applebaum et al. "Clinical Features and Outcomes in Patients with Extraskeletal Ewing Sarcoma". In: *Cancer* 117.13 (2011), pp. 3027–3032. ISSN: 1097-0142. DOI: 10.1002/cncr.25840.

[43] Andrew D. Lynch et al. "Extraskeletal versus Skeletal Ewing Sarcoma in the Adult Population: Controversies in Care". In: *Surgical Oncology* 27.3 (Sept. 1, 2018), pp. 373–379. ISSN: 0960-7404. DOI: 10.1016/j.suronc.2018.05.016.

[44] Nicolò Riggi, Mario L. Suvà, and Ivan Stamenkovic. "Ewing's Sarcoma". In: *New England Journal of Medicine* 384.2 (Jan. 14, 2021), pp. 154–164. ISSN: 0028-4793. DOI: 10.1056/NEJMra2028910. pmid: 33497548.

[45] Björn Widhe and Thorulf Widhe. "Initial Symptoms and Clinical Features in Osteosarcoma and Ewing Sarcoma". In: *The Journal of Bone and Joint Surgery. American Volume* 82.5 (May 2000), pp. 667–674. ISSN: 0021-9355. DOI: 10.2106/00004623-200005000-00007. pmid: 10819277.

[46] S.J. Cotterill et al. "Prognostic Factors in Ewing's Tumor of Bone: Analysis of 975 Patients From the European Intergroup Cooperative Ewing's Sarcoma Study Group". In: *Journal of Clinical Oncology* 18.17 (Sept. 17, 2000), pp. 3108–3114. ISSN: 0732-183X. DOI: 10.1200/JCO.2000.18.17.3108.

[47] S. J. Strauss et al. "Bone Sarcomas: ESMO–EURACAN–GENTURIS–ERN PaedCan Clinical Practice Guideline for Diagnosis, Treatment and Follow-Up". In: *Annals of Oncology* 32.12 (Dec. 1, 2021), pp. 1520–1536. ISSN: 0923-7534. DOI: 10.1016/j.annonc.2021.08.1995.

[48] Antonio Llombart-Bosch et al. "Histological Heterogeneity of Ewing's Sarcoma/PNET: An Immunohistochemical Analysis of 415 Genetically Confirmed Cases with Clinical Support". In: *Virchows Archiv* 455.5 (Nov. 1, 2009), pp. 397–411. ISSN: 1432-2307. DOI: 10.1007/s00428-009-0842-7.

[49] Michaela C. Baldauf et al. “Robust Diagnosis of Ewing Sarcoma by Immunohistochemical Detection of Super-Enhancer-Driven EWSR1-ETS Targets”. In: *Oncotarget* 9.2 (Aug. 4, 2017), pp. 1587–1601. ISSN: 1949-2553. DOI: 10.18632/oncotarget.20098.

[50] Martin F. Orth et al. “High Specificity of BCL11B and GLG1 for EWSR1-FLI1 and EWSR1-ERG Positive Ewing Sarcoma”. In: *Cancers* 12.3 (Mar. 10, 2020), p. 644. ISSN: 2072-6694. DOI: 10.3390/cancers12030644.

[51] Isidro Machado et al. “Molecular Diagnosis of Ewing Sarcoma Family of Tumors: A Comparative Analysis of 560 Cases With FISH and RT-PCR”. In: *Diagnostic Molecular Pathology* 18.4 (Dec. 2009), p. 189. ISSN: 1052-9551. DOI: 10.1097/PDM.0b013e3181a06f66.

[52] Sonja Chen et al. “Ewing Sarcoma with ERG Gene Rearrangements: A Molecular Study Focusing on the Prevalence of FUS-ERG and Common Pitfalls in Detecting EWSR1-ERG Fusions by FISH”. In: *Genes, Chromosomes and Cancer* 55.4 (2016), pp. 340–349. ISSN: 1098-2264. DOI: 10.1002/gcc.22336.

[53] J. -Y. Blay et al. “Improved Survival Using Specialized Multidisciplinary Board in Sarcoma Patients”. In: *Annals of Oncology*. Availability, out-of-Pocket Costs and Accessibility of Anti-Neoplastic Medicines Outside of Europe 28.11 (Nov. 1, 2017), pp. 2852–2859. ISSN: 0923-7534. DOI: 10.1093/annonc/mdx484.

[54] Carl W. Boyer, Theodore J. Brickner, and Ronald H. Perry. “Ewing’s Sarcoma.Case against Surgery”. In: *Cancer* 20.10 (Oct. 1967), pp. 1602–1606. ISSN: 0008-543X, 1097-0142. DOI: 10.1002/1097-0142(196710)20:10<1602::AID-CNCR2820201006>3.0.CO;2-H.

[55] Martin Stahl et al. “Risk of Recurrence and Survival after Relapse in Patients with Ewing Sarcoma”. In: *Pediatric Blood & Cancer* 57.4 (2011), pp. 549–553. ISSN: 1545-5017. DOI: 10.1002/pbc.23040.

[56] Bernadette Brennan et al. “Comparison of Two Chemotherapy Regimens in Ewing Sarcoma (ES): Overall and Subgroup Results of the Euro Ewing 2012 Randomized Trial (EE2012).” In: *Journal of Clinical Oncology* 38 (15_suppl May 20, 2020), pp. 11500–11500. ISSN: 0732-183X. DOI: 10.1200/JCO.2020.38.15_suppl.11500.

[57] Steven G. DuBois et al. “Comparative Evaluation of Local Control Strategies in Localized Ewing Sarcoma of Bone: A Report from the Children’s Oncology Group”. In: *Cancer* 121.3 (2015), pp. 467–475. ISSN: 1097-0142. DOI: 10.1002/cncr.29065.

[58] Julia Haeusler et al. "The Value of Local Treatment in Patients with Primary, Disseminated, Multifocal Ewing Sarcoma (PDMES)". In: *Cancer* 116.2 (2010), pp. 443–450. ISSN: 1097-0142. DOI: 10.1002/cncr.24740.

[59] S. E. Bosma et al. "Easy-to-Use Clinical Tool for Survival Estimation in Ewing Sarcoma at Diagnosis and after Surgery". In: *Scientific Reports* 9.1 (1 July 29, 2019), p. 11000. ISSN: 2045-2322. DOI: 10.1038/s41598-019-46721-8.

[60] Linda Granowetter et al. "Dose-Intensified Compared With Standard Chemotherapy for Nonmetastatic Ewing Sarcoma Family of Tumors: A Children's Oncology Group Study". In: *Journal of Clinical Oncology* 27.15 (May 20, 2009), pp. 2536–2541. ISSN: 0732-183X. DOI: 10.1200/JCO.2008.19.1478.

[61] Maximilian M. L. Knott et al. "Targeting the Undruggable: Exploiting Neomorphic Features of Fusion Oncoproteins in Childhood Sarcomas for Innovative Therapies". In: *Cancer and Metastasis Reviews* 38.4 (Dec. 2019), pp. 625–642. ISSN: 0167-7659, 1573-7233. DOI: 10.1007/s10555-019-09839-9.

[62] Hayriye V Erkizan et al. "A Small Molecule Blocking Oncogenic Protein EWS-FLI1 Interaction with RNA Helicase A Inhibits Growth of Ewing's Sarcoma". In: *Nature Medicine* 15.7 (July 2009), pp. 750–756. ISSN: 1078-8956, 1546-170X. DOI: 10.1038/nm.1983.

[63] Joseph Aloysius Ludwig et al. "TK216 for Relapsed/Refractory Ewing Sarcoma: Interim Phase 1/2 Results." In: *Journal of Clinical Oncology* 39 (15_suppl May 20, 2021), pp. 11500–11500. ISSN: 0732-183X. DOI: 10.1200/JCO.2021.39.15_suppl.11500.

[64] Hyuna Sung et al. "Global Cancer Statistics 2020: GLOBOCAN Estimates of Incidence and Mortality Worldwide for 36 Cancers in 185 Countries". In: *CA: A Cancer Journal for Clinicians* 71.3 (2021), pp. 209–249. ISSN: 1542-4863. DOI: 10.3322/caac.21660.

[65] Rebecca L. Siegel et al. "Cancer Statistics, 2022". In: *CA: A Cancer Journal for Clinicians* 72.1 (2022), pp. 7–33. ISSN: 1542-4863. DOI: 10.3322/caac.21708.

[66] Neil Vasan, José Baselga, and David M. Hyman. "A View on Drug Resistance in Cancer". In: *Nature* 575.7782 (7782 Nov. 2019), pp. 299–309. ISSN: 1476-4687. DOI: 10.1038/s41586-019-1730-1.

[67] N. G. Zaorsky et al. "Causes of Death among Cancer Patients". In: *Annals of Oncology* 28.2 (Feb. 1, 2017), pp. 400–407. ISSN: 0923-7534, 1569-8041. DOI: 10.1093/annonc/mdw604. pmid: 27831506.

[68] Anas El-Aneed. "Current Strategies in Cancer Gene Therapy". In: *European Journal of Pharmacology* 498.1-3 (Sept. 2004), pp. 1–8. ISSN: 00142999. DOI: 10.1016/j.ejphar.2004.06.054.

[69] Justin R. Gregg and Timothy C. Thompson. "Considering the Potential for Gene-Based Therapy in Prostate Cancer". In: *Nature Reviews Urology* 18.3 (3 Mar. 2021), pp. 170–184. ISSN: 1759-4820. DOI: 10.1038/s41585-021-00431-x.

[70] Katherine A. High and Maria G. Roncarolo. "Gene Therapy". In: *New England Journal of Medicine* 381.5 (Aug. 1, 2019), pp. 455–464. ISSN: 0028-4793, 1533-4406. DOI: 10.1056/NEJMra1706910.

[71] Craig A. Mullen. "Metabolic Suicide Genes in Gene Therapy". In: *Pharmacology & Therapeutics* 63.2 (1994), pp. 199–207. ISSN: 01637258. DOI: 10.1016/0163-7258(94)90046-9.

[72] Obeid M. Malekshah et al. "Enzyme/Prodrug Systems for Cancer Gene Therapy". In: *Current pharmacology reports* 2.6 (Dec. 2016), pp. 299–308. ISSN: 2198-641X. DOI: 10.1007/s40495-016-0073-y. pmid: 28042530.

[73] M. Siraç Dilber et al. "Suicide Gene Therapy for Plasma Cell Tumors". In: *Blood* 88.6 (Sept. 15, 1996), pp. 2192–2200. ISSN: 0006-4971. DOI: 10.1182/blood.V88.6.2192.bloodjournal8862192.

[74] C. Ryan Miller et al. "Intratumoral 5-Fluorouracil Produced by Cytosine Deaminase/5-Fluorocytosine Gene Therapy Is Effective for Experimental Human Glioblastomas1". In: *Cancer Research* 62.3 (Feb. 1, 2002), pp. 773–780. ISSN: 0008-5472.

[75] Marlon R Veldwijk et al. "Suicide Gene Therapy of Sarcoma Cell Lines Using Recombinant Adeno-Associated Virus 2 Vectors". In: *Cancer Gene Therapy* 11.8 (Aug. 2004), pp. 577–584. ISSN: 0929-1903, 1476-5500. DOI: 10.1038/sj.cgt.7700718.

[76] Ute Fischer et al. "Mechanisms of Thymidine Kinase/Ganciclovir and Cytosine Deaminase/ 5-Fluorocytosine Suicide Gene Therapy-Induced Cell Death in Glioma Cells". In: *Oncogene* 24.7 (7 Feb. 2005), pp. 1231–1243. ISSN: 1476-5594. DOI: 10.1038/sj.onc.1208290.

[77] Ye-Hyeon Ahn et al. "STAT3 Silencing Enhances the Efficacy of the HSV.Tk Suicide Gene in Gastrointestinal Cancer Therapy". In: *Clinical & Experimental Metastasis* 29.4 (Apr. 1, 2012), pp. 359–369. ISSN: 1573-7276. DOI: 10.1007/s10585-012-9458-4.

[78] Kenneth W. Culver et al. "In Vivo Gene Transfer with Retroviral Vector-Producer Cells for Treatment of Experimental Brain Tumors". In: *Science* 256.5063 (June 12, 1992), pp. 1550–1552. ISSN: 0036-8075, 1095-9203. DOI: 10.1126/science.1317968.

[79] Toshiaki Tanaka et al. "Bystander Effect from Cytosine Deaminase and Uracil Phosphoribosyl Transferase Genes in Vitro: A Partial Contribution of Gap Junctions". In: *Cancer Letters* 282.1 (Sept. 2009), pp. 43–47. ISSN: 03043835. DOI: 10.1016/j.canlet.2009.02.050.

[80] N. G. Rainov. "A Phase III Clinical Evaluation of Herpes Simplex Virus Type 1 Thymidine Kinase and Ganciclovir Gene Therapy as an Adjuvant to Surgical Resection and Radiation in Adults with Previously Untreated Glioblastoma Multiforme". In: *Human Gene Therapy* 11.17 (Nov. 20, 2000), pp. 2389–2401. ISSN: 1043-0342, 1557-7422. DOI: 10.1089/104303400750038499.

[81] Manfred Westphal et al. "Adenovirus-Mediated Gene Therapy with Sitimagene Ceradenovec Followed by Intravenous Ganciclovir for Patients with Operable High-Grade Glioma (ASPECT): A Randomised, Open-Label, Phase 3 Trial". In: *The Lancet Oncology* 14.9 (Aug. 2013), pp. 823–833. ISSN: 14702045. DOI: 10.1016/S1470-2045(13)70274-2.

[82] S. C. Anderson et al. "P53 Gene Therapy in a Rat Model of Hepatocellular Carcinoma: Intra-Arterial Delivery of a Recombinant Adenovirus". In: *Clinical Cancer Research: An Official Journal of the American Association for Cancer Research* 4.7 (July 1998), pp. 1649–1659. ISSN: 1078-0432. pmid: 9676839.

[83] J. Nemunaitis et al. "Adenovirus-Mediated P53 Gene Transfer in Sequence With Cisplatin to Tumors of Patients With Non–Small-Cell Lung Cancer". In: *Journal of Clinical Oncology* 18.3 (Feb. 2000), pp. 609–609. ISSN: 0732-183X. DOI: 10.1200/JCO.2000.18.3.609.

[84] Stephen G. Swisher et al. "Induction of P53-Regulated Genes and Tumor Regression in Lung Cancer Patients after Intratumoral Delivery of Adenoviral P53 (INGN 201) and Radiation Therapy". In: *Clinical Cancer Research: An Official Journal of the American Association for Cancer Research* 9.1 (Jan. 2003), pp. 93–101. ISSN: 1078-0432. pmid: 12538456.

[85] Frederick F. Lang et al. "Phase I Trial of Adenovirus-Mediated P53 Gene Therapy for Recurrent Glioma: Biological and Clinical Results". In: *Journal of Clinical Oncology* 21.13 (July 2003), pp. 2508–2518. ISSN: 0732-183X. DOI: 10.1200/JCO.2003.21.13.2508.

[86] Wei-Wei Zhang et al. "The First Approved Gene Therapy Product for Cancer Ad-p53 (Gendicine): 12 Years in the Clinic". In: *Human Gene Therapy* 29.2 (Feb. 2018), pp. 160–179. ISSN: 1043-0342. DOI: 10.1089/hum.2017.218.

[87] Giorgio Trinchieri. "Interleukin-12 and the Regulation of Innate Resistance and Adaptive Immunity". In: *Nature Reviews Immunology* 3.2 (2 Feb. 2003), pp. 133–146. ISSN: 1474-1741. DOI: 10.1038/nri1001.

[88] John A. Barrett et al. “Regulated Intratumoral Expression of IL-12 Using a RheoSwitch Therapeutic System® (RTS®) Gene Switch as Gene Therapy for the Treatment of Glioma”. In: *Cancer Gene Therapy* 25.5 (5 June 2018), pp. 106–116. ISSN: 1476-5500. DOI: 10.1038/s41417-018-0019-0.

[89] E. Antonio Chiocca et al. “Regulatable Interleukin-12 Gene Therapy in Patients with Recurrent High-Grade Glioma: Results of a Phase 1 Trial”. In: *Science Translational Medicine* 11.505 (Aug. 14, 2019), eaaw5680. DOI: 10.1126/scitranslmed.aaw5680.

[90] M. Lee Lucas and Richard Heller. “IL-12 Gene Therapy Using an Electrically Mediated Nonviral Approach Reduces Metastatic Growth of Melanoma”. In: *DNA and Cell Biology* 22.12 (Dec. 2003), pp. 755–763. ISSN: 1044-5498, 1557-7430. DOI: 10.1089/104454903322624966.

[91] Adil I. Daud et al. “Phase I Trial of Interleukin-12 Plasmid Electroporation in Patients With Metastatic Melanoma”. In: *Journal of Clinical Oncology* 26.36 (Dec. 20, 2008), pp. 5896–5903. ISSN: 0732-183X. DOI: 10.1200/JCO.2007.15.6794. pmid: 19029422.

[92] Alain P. Algazi et al. “Phase II Trial of IL-12 Plasmid Transfection and PD-1 Blockade in Immunologically Quiescent Melanoma”. In: *Clinical Cancer Research* 26.12 (June 15, 2020), pp. 2827–2837. ISSN: 1078-0432. DOI: 10.1158/1078-0432.CCR-19-2217.

[93] Tsunao Kishida et al. “Interleukin (IL)-21 and IL-15 Genetic Transfer Synergistically Augments Therapeutic Antitumor Immunity and Promotes Regression of Metastatic Lymphoma”. In: *Molecular Therapy* 8.4 (Oct. 1, 2003), pp. 552–558. ISSN: 1525-0016, 1525-0024. DOI: 10.1016/S1525-0016(03)00222-3.

[94] E. Eriksson et al. “Activation of Myeloid and Endothelial Cells by CD40L Gene Therapy Supports T-cell Expansion and Migration into the Tumor Microenvironment”. In: *Gene Therapy* 24.2 (2 Feb. 2017), pp. 92–103. ISSN: 1476-5462. DOI: 10.1038/gt.2016.80.

[95] C. M. Iqbal Ahmed et al. “Interferon A2b Gene Delivery Using Adenoviral Vector Causes Inhibition of Tumor Growth in Xenograft Models from a Variety of Cancers”. In: *Cancer Gene Therapy* 8.10 (10 Oct. 2001), pp. 788–795. ISSN: 1476-5500. DOI: 10.1038/sj.cgt.7700364.

[96] William F. Benedict et al. “Intravesical Ad-IFNa Causes Marked Regression of Human Bladder Cancer Growing Orthotopically in Nude Mice and Overcomes Resistance to IFN-a Protein”. In: *Molecular Therapy* 10.3 (Sept. 1, 2004), pp. 525–532. ISSN: 1525-0016, 1525-0024. DOI: 10.1016/j.ymthe.2004.05.027. pmid: 15336652.

[97] Neal D. Shore et al. "Intravesical rAd–IFNa/Syn3 for Patients With High-Grade, Bacillus Calmette-Guerin–Refractory or Relapsed Non–Muscle-Invasive Bladder Cancer: A Phase II Randomized Study". In: *Journal of Clinical Oncology* 35.30 (Oct. 20, 2017), pp. 3410–3416. ISSN: 0732-183X. DOI: 10.1200/JCO.2017.72.3064.

[98] Stephen A Boorjian et al. "Intravesical Nadofaragene Firadenovec Gene Therapy for BCG-unresponsive Non-Muscle-Invasive Bladder Cancer: A Single-Arm, Open-Label, Repeat-Dose Clinical Trial". In: *The Lancet Oncology* 22.1 (Jan. 1, 2021), pp. 107–117. ISSN: 1470-2045. DOI: 10.1016/S1470-2045(20)30540-4.

[99] Sarah L. Greig. "Talimogene Laherparepvec: First Global Approval". In: *Drugs* 76.1 (Jan. 1, 2016), pp. 147–154. ISSN: 1179-1950. DOI: 10.1007/s40265-015-0522-7.

[100] Robert H.I. Andtbacka et al. "Talimogene Laherparepvec Improves Durable Response Rate in Patients With Advanced Melanoma". In: *Journal of Clinical Oncology* 33.25 (Sept. 2015), pp. 2780–2788. ISSN: 0732-183X. DOI: 10.1200/JCO.2014.58.3377.

[101] Antoni Ribas et al. "Oncolytic Virotherapy Promotes Intratumoral T Cell Infiltration and Improves Anti-PD-1 Immunotherapy". In: *Cell* 170.6 (Sept. 7, 2017), 1109–1119.e10. ISSN: 0092-8674. DOI: 10.1016/j.cell.2017.08.027.

[102] Malcolm K Brenner et al. "Is Cancer Gene Therapy an Empty Suit?" In: *The Lancet Oncology* 14.11 (Oct. 1, 2013), e447–e456. ISSN: 1470-2045. DOI: 10.1016/S1470-2045(13)70173-6.

[103] Jote T. Bulcha et al. "Viral Vector Platforms within the Gene Therapy Landscape". In: *Signal Transduction and Targeted Therapy* 6.1 (1 Feb. 8, 2021), pp. 1–24. ISSN: 2059-3635. DOI: 10.1038/s41392-021-00487-6.

[104] Jessica Pahle and Wolfgang Walther. "Vectors and Strategies for Non-viral Cancer Gene Therapy". In: *Expert Opinion on Biological Therapy* 16.4 (Apr. 2, 2016), pp. 443–461. ISSN: 1471-2598, 1744-7682. DOI: 10.1517/14712598.2016.1134480.

[105] Charles Lu et al. "Phase I Clinical Trial of Systemically Administered TUSC2(FUS1)-Nanoparticles Mediating Functional Gene Transfer in Humans". In: *PloS One* 7.4 (2012), e34833. ISSN: 1932-6203. DOI: 10.1371/journal.pone.0034833. pmid: 22558101.

[106] Joanna Rejman, Alessandra Bragonzi, and Massimo Conese. "Role of Clathrin- and Caveolae-Mediated Endocytosis in Gene Transfer Mediated by Lipo- and Polyplexes". In: *Molecular Therapy* 12.3 (Sept. 1, 2005), pp. 468–474. ISSN: 1525-0016. DOI: 10.1016/j.ymthe.2005.03.038.

[107] Zongmin Zhao, Aaron C. Anselmo, and Samir Mitragotri. "Viral Vector-Based Gene Therapies in the Clinic". In: *Bioengineering & Translational Medicine* 7.1 (2022), e10258. ISSN: 2380-6761. DOI: 10.1002/btm2.10258.

[108] Cynthia E. Dunbar et al. "Gene Therapy Comes of Age". In: *Science* 359.6372 (Jan. 12, 2018), eaan4672. ISSN: 0036-8075, 1095-9203. DOI: 10.1126/science.aan4672.

[109] Ulrich T. Hacker et al. "Towards Clinical Implementation of Adeno-Associated Virus (AAV) Vectors for Cancer Gene Therapy: Current Status and Future Perspectives". In: *Cancers* 12.7 (7 July 2020), p. 1889. ISSN: 2072-6694. DOI: 10.3390/cancers12071889.

[110] Amit C. Nathwani et al. "Adenovirus-Associated Virus Vector–Mediated Gene Transfer in Hemophilia B". In: *New England Journal of Medicine* 365.25 (Dec. 22, 2011), pp. 2357–2365. ISSN: 0028-4793. DOI: 10.1056/NEJMoa1108046. pmid: 22149959.

[111] J. F. de Graaf et al. "Armed Oncolytic Viruses: A Kick-Start for Anti-Tumor Immunity". In: *Cytokine & Growth Factor Reviews* 41 (June 1, 2018), pp. 28–39. ISSN: 1359-6101. DOI: 10.1016/j.cytogfr.2018.03.006.

[112] Darren J Korbie and John S Mattick. "Touchdown PCR for Increased Specificity and Sensitivity in PCR Amplification". In: *Nature Protocols* 3.9 (Sept. 2008), pp. 1452–1456. ISSN: 1754-2189, 1750-2799. DOI: 10.1038/nprot.2008.133.

[113] Christopher Ede et al. "Quantitative Analyses of Core Promoters Enable Precise Engineering of Regulated Gene Expression in Mammalian Cells". In: *ACS Synthetic Biology* 5.5 (May 20, 2016), pp. 395–404. DOI: 10.1021/acssynbio.5b00266.

[114] Berkley E. Gryder et al. "PAX3–FOXO1 Establishes Myogenic Super Enhancers and Confers BET Bromodomain Vulnerability". In: *Cancer Discovery* 7.8 (Aug. 2017), pp. 884–899. ISSN: 2159-8274, 2159-8290. DOI: 10.1158/2159-8290.CD-16-1297.

[115] Jin Hee Kim et al. "High Cleavage Efficiency of a 2A Peptide Derived from Porcine Teschovirus-1 in Human Cell Lines, Zebrafish and Mice". In: *PLOS ONE* 6.4 (Apr. 29, 2011), e18556. ISSN: 1932-6203. DOI: 10.1371/journal.pone.0018556.

[116] Margaret E. Black, Mark S. Kokoris, and Peter Sabo. "Herpes Simplex Virus-1 Thymidine Kinase Mutants Created by Semi-Random Sequence Mutagenesis Improve Prodrug-mediated Tumor Cell Killing". In: *Cancer Research* 61.7 (Apr. 1, 2001), pp. 3022–3026. ISSN: 0008-5472, 1538-7445. pmid: 11306482.

[117] Takashi Uemori et al. “Amplification of the 16S-23S Spacer Region in rRNA Operons of Mycoplasmas by the Polymerase Chain Reaction”. In: *Systematic and Applied Microbiology* 15.2 (May 1, 1992), pp. 181–186. ISSN: 0723-2020. DOI: 10.1016/S0723-2020(11)80089-5.

[118] Wilhelm G. Dirks et al. “Cell Line Cross-Contamination Initiative: An Interactive Reference Database of STR Profiles Covering Common Cancer Cell Lines”. In: *International Journal of Cancer* 126.1 (2010), pp. 303–304. ISSN: 1097-0215. DOI: 10.1002/ijc.24999.

[119] Thibault Robin, Amanda Capes-Davis, and Amos Bairoch. “CLASTR: The Cellosaurus STR Similarity Search Tool - A Precious Help for Cell Line Authentication”. In: *International Journal of Cancer* 146.5 (2020), pp. 1299–1306. ISSN: 1097-0215. DOI: 10.1002/ijc.32639.

[120] R. A. Bailly et al. “DNA-binding and Transcriptional Activation Properties of the EWS-FLI-1 Fusion Protein Resulting from the t(11;22) Translocation in Ewing Sarcoma”. In: *Molecular and Cellular Biology* (May 1994). DOI: 10.1128/mcb.14.5.3230-3241.1994.

[121] Jian Ye et al. “Primer-BLAST: A Tool to Design Target-Specific Primers for Polymerase Chain Reaction”. In: *BMC Bioinformatics* 13.1 (June 18, 2012), p. 134. ISSN: 1471-2105. DOI: 10.1186/1471-2105-13-134.

[122] Kenneth J. Livak and Thomas D. Schmittgen. “Analysis of Relative Gene Expression Data Using Real-Time Quantitative PCR and the $2-\Delta\Delta CT$ Method”. In: *Methods* 25.4 (Dec. 1, 2001), pp. 402–408. ISSN: 1046-2023. DOI: 10.1006/meth.2001.1262.

[123] Hitoshi Kuroda et al. “Production of Lentiviral Vectors in Protein-free Media”. In: *Current Protocols in Cell Biology* 50.1 (Mar. 2011). ISSN: 1934-2500, 1934-2616. DOI: 10.1002/0471143030.cb2608s50.

[124] Danit Finkelshtein et al. “LDL Receptor and Its Family Members Serve as the Cellular Receptors for Vesicular Stomatitis Virus”. In: *Proceedings of the National Academy of Sciences* 110.18 (Apr. 30, 2013), pp. 7306–7311. ISSN: 0027-8424, 1091-6490. DOI: 10.1073/pnas.1214441110. pmid: 23589850.

[125] Kouki Morizono et al. “Lentiviral Vector Retargeting to P-glycoprotein on Metastatic Melanoma through Intravenous Injection”. In: *Nature Medicine* 11.3 (Mar. 2005), pp. 346–352. ISSN: 1078-8956, 1546-170X. DOI: 10.1038/nm1192.

[126] Aruna Marchetto and Laura Romero-Pérez. “Western Blot Analysis in Ewing Sarcoma”. In: *Ewing Sarcoma : Methods and Protocols*. Ed. by Florencia Cidre-Aranaz and Thomas G. P. Grünewald. Methods in Molecular Biology. New York, NY: Springer US, 2021, pp. 15–25. ISBN: 978-1-07-161020-6. DOI: 10.1007/978-1-0716-1020-6_2.

[127] Daniel F. Gilbert and Oliver Friedrich, eds. *Cell Viability Assays: Methods and Protocols*. Vol. 1601. Methods in Molecular Biology. New York, NY: Springer New York, 2017. ISBN: 978-1-4939-6959-3 978-1-4939-6960-9. DOI: 10.1007/978-1-4939-6960-9.

[128] Christian Ritz et al. "Dose-Response Analysis Using R". In: *PLOS ONE* 10.12 (Dec. 30, 2015). Ed. by Yinglin Xia, e0146021. ISSN: 1932-6203. DOI: 10.1371/journal.pone.0146021.

[129] Laurent Gautier et al. "Affy—Analysis of Affymetrix GeneChip Data at the Probe Level". In: *Bioinformatics* 20.3 (Feb. 12, 2004), pp. 307–315. ISSN: 1367-4803. DOI: 10.1093/bioinformatics/btg405.

[130] Matthew E. Ritchie et al. "Limma Powers Differential Expression Analyses for RNA-sequencing and Microarray Studies". In: *Nucleic Acids Research* 43.7 (Apr. 20, 2015), e47. ISSN: 0305-1048. DOI: 10.1093/nar/gkv007.

[131] R. A. Irizarry. "Summaries of Affymetrix GeneChip Probe Level Data". In: *Nucleic Acids Research* 31.4 (Feb. 15, 2003), 15e–15. ISSN: 13624962. DOI: 10.1093/nar/gng015.

[132] Leonard D. Shultz et al. "Human Lymphoid and Myeloid Cell Development in NOD/LtSz-scid IL2R null Mice Engrafted with Mobilized Human Hemopoietic Stem Cells 12". In: *The Journal of Immunology* 174.10 (May 15, 2005), pp. 6477–6489. ISSN: 0022-1767. DOI: 10.4049/jimmunol.174.10.6477.

[133] Mukund Patel et al. "Tumor-Specific Retargeting of an Oncogenic Transcription Factor Chimera Results in Dysregulation of Chromatin and Transcription". In: *Genome Research* 22.2 (Feb. 1, 2012), pp. 259–270. ISSN: 1088-9051, 1549-5469. DOI: 10.1101/gr.125666.111. pmid: 22086061.

[134] Tilman L. B. Hölting et al. "Neomorphic DNA-binding Enables Tumor-Specific Therapeutic Gene Expression in Fusion-Addicted Childhood Sarcoma". In: *Molecular Cancer* 21.1 (Oct. 13, 2022), p. 199. ISSN: 1476-4598. DOI: 10.1186/s12943-022-01641-6.

[135] Nonia Pariente et al. "A Novel Dual-targeted Lentiviral Vector Leads to Specific Transduction of Prostate Cancer Bone Metastases In Vivo After Systemic Administration". In: *Molecular Therapy* 15.11 (Nov. 2007), pp. 1973–1981. ISSN: 15250016. DOI: 10.1038/sj.mt.6300271.

[136] Marie Lafitte et al. "In Vivo Gene Transfer Targeting in Pancreatic Adenocarcinoma with Cell Surface Antigens". In: *Molecular Cancer* 11.1 (2012), p. 81. ISSN: 1476-4598. DOI: 10.1186/1476-4598-11-81.

[137] Francesca Del Bufalo et al. "GD2-CART01 for Relapsed or Refractory High-Risk Neuroblastoma". In: *New England Journal of Medicine* 388.14 (Apr. 6, 2023), pp. 1284–1295. ISSN: 0028-4793. DOI: 10.1056/NEJMoa2210859.

[138] Sareetha Kailayangiri et al. "EZH2 Inhibition in Ewing Sarcoma Upregulates GD2 Expression for Targeting with Gene-Modified T Cells". In: *Molecular Therapy* 27.5 (May 2019), pp. 933–946. ISSN: 15250016. DOI: 10.1016/j.ymthe.2019.02.014.

[139] Poul H.B. Sorensen et al. "PAX3-FKHR and PAX7-FKHR Gene Fusions Are Prognostic Indicators in Alveolar Rhabdomyosarcoma: A Report From the Children's Oncology Group". In: *Journal of Clinical Oncology* 20.11 (June 1, 2002), pp. 2672–2679. ISSN: 0732-183X. DOI: 10.1200/JCO.2002.03.137.

[140] Nathalie Gaspar et al. "Ewing Sarcoma: Current Management and Future Approaches Through Collaboration". In: *Journal of Clinical Oncology* 33.27 (Sept. 20, 2015), pp. 3036–3046. ISSN: 0732-183X, 1527-7755. DOI: 10.1200/JCO.2014.59.5256.

[141] Celine Chen et al. "Current and Future Treatment Strategies for Rhabdomyosarcoma". In: *Frontiers in Oncology* 9 (Dec. 20, 2019), p. 1458. ISSN: 2234-943X. DOI: 10.3389/fonc.2019.01458. pmid: 31921698.

[142] Stephen X. Skapek et al. "Rhabdomyosarcoma". In: *Nature Reviews Disease Primers* 5.1 (Dec. 2019), p. 1. ISSN: 2056-676X. DOI: 10.1038/s41572-018-0051-2.

[143] Aashi Chaturvedi et al. "Molecular Dissection of the Mechanism by Which EWS/FLI Expression Compromises Actin Cytoskeletal Integrity and Cell Adhesion in Ewing Sarcoma". In: *Molecular Biology of the Cell* 25.18 (Sept. 15, 2014), pp. 2695–2709. ISSN: 1059-1524. DOI: 10.1091/mbc.e14-01-0007.

[144] Marie-Ming Aynaud et al. "Transcriptional Programs Define Intratumoral Heterogeneity of Ewing Sarcoma at Single-Cell Resolution". In: *Cell Reports* 30.6 (Feb. 11, 2020), 1767–1779.e6. ISSN: 2211-1247. DOI: 10.1016/j.celrep.2020.01.049.

[145] Sónia Duarte et al. "Suicide Gene Therapy in Cancer: Where Do We Stand Now?" In: *Cancer Letters* 324.2 (Nov. 28, 2012), pp. 160–170. ISSN: 0304-3835. DOI: 10.1016/j.canlet.2012.05.023.

[146] David Killock. "Viral Gene Therapy Active in Ovarian Cancer". In: *Nature Reviews Clinical Oncology* 17.7 (7 July 2020), pp. 391–391. ISSN: 1759-4782. DOI: 10.1038/s41571-020-0371-5.

[147] Lindsey A. George et al. “Multiyear Factor VIII Expression after AAV Gene Transfer for Hemophilia A”. In: *New England Journal of Medicine* 385.21 (Nov. 18, 2021), pp. 1961–1973. ISSN: 0028-4793. DOI: 10.1056/NEJMoa2104205.

[148] Chao Chen et al. “Promoter-Operating Targeted Expression of Gene Therapy in Cancer: Current Stage and Prospect”. In: *Molecular Therapy - Nucleic Acids* 11 (June 1, 2018), pp. 508–514. ISSN: 2162-2531. DOI: 10.1016/j.omtn.2018.04.003.

[149] Mariela Montaño-Samaniego et al. “Strategies for Targeting Gene Therapy in Cancer Cells With Tumor-Specific Promoters”. In: *Frontiers in Oncology* 10 (2020), p. 2671. ISSN: 2234-943X. DOI: 10.3389/fonc.2020.605380.

[150] A. S. Majumdar et al. “The Telomerase Reverse Transcriptase Promoter Drives Efficacious Tumor Suicide Gene Therapy While Preventing Hepatotoxicity Encountered with Constitutive Promoters”. In: *Gene Therapy* 8.7 (7 Apr. 2001), pp. 568–578. ISSN: 1476-5462. DOI: 10.1038/sj.gt.3301421.

[151] W. Peng et al. “Tightly-Regulated Suicide Gene Expression Kills PSA-expressing Prostate Tumor Cells”. In: *Gene Therapy* 12.21 (21 Nov. 2005), pp. 1573–1580. ISSN: 1476-5462. DOI: 10.1038/sj.gt.3302580.

[152] Diana Y. Lu et al. “The ETS Transcription Factor ETV6 Constrains the Transcriptional Activity of EWS–FLI to Promote Ewing Sarcoma”. In: *Nature Cell Biology* 25.2 (2 Feb. 2023), pp. 285–297. ISSN: 1476-4679. DOI: 10.1038/s41556-022-01059-8.

[153] Yuan Gao et al. “ETV6 Dependency in Ewing Sarcoma by Antagonism of EWS-FLI1-mediated Enhancer Activation”. In: *Nature Cell Biology* 25.2 (2 Feb. 2023), pp. 298–308. ISSN: 1476-4679. DOI: 10.1038/s41556-022-01060-1.

[154] Mayanne M. T. Zhu, Elahe Shenasa, and Torsten O. Nielsen. “Sarcomas: Immune Biomarker Expression and Checkpoint Inhibitor Trials”. In: *Cancer Treatment Reviews* 91 (Dec. 1, 2020), p. 102115. ISSN: 0305-7372. DOI: 10.1016/j.ctrv.2020.102115.

[155] Michael Conroy and Jarushka Naidoo. “Immune-Related Adverse Events and the Balancing Act of Immunotherapy”. In: *Nature Communications* 13.1 (1 Jan. 19, 2022), p. 392. ISSN: 2041-1723. DOI: 10.1038/s41467-022-27960-2.

[156] Alexandra McCarron et al. “Challenges of Up-Scaling Lentivirus Production and Processing”. In: *Journal of Biotechnology* 240 (Dec. 20, 2016), pp. 23–30. ISSN: 0168-1656. DOI: 10.1016/j.jbiotec.2016.10.016.

[157] Michael C. Milone and Una O'Doherty. "Clinical Use of Lentiviral Vectors". In: *Leukemia* 32.7 (7 July 2018), pp. 1529–1541. ISSN: 1476-5551. DOI: 10.1038/s41375-018-0106-0.

[158] Franco Locatelli et al. "Betibeglogene Autotemcel Gene Therapy for Non–B0/B0 Genotype -Thalassemia". In: *New England Journal of Medicine* 386.5 (Feb. 3, 2022), pp. 415–427. ISSN: 0028-4793. DOI: 10.1056/NEJMoa2113206. pmid: 34891223.

[159] Morton J. Cowan et al. "Lentiviral Gene Therapy for Artemis-Deficient SCID". In: *New England Journal of Medicine* 387.25 (Dec. 22, 2022), pp. 2344–2355. ISSN: 0028-4793. DOI: 10.1056/NEJMoa2206575. pmid: 36546626.

[160] Julie Kanter et al. "Biologic and Clinical Efficacy of LentiGlobin for Sickle Cell Disease". In: *New England Journal of Medicine* 386.7 (Feb. 17, 2022), pp. 617–628. ISSN: 0028-4793. DOI: 10.1056/NEJMoa2117175. pmid: 34898139.

[161] Frederic D. Bushman. "Retroviral Insertional Mutagenesis in Humans: Evidence for Four Genetic Mechanisms Promoting Expansion of Cell Clones". In: *Molecular Therapy* 28.2 (Feb. 5, 2020), pp. 352–356. ISSN: 1525-0016. DOI: 10.1016/j.ymthe.2019.12.009.

[162] Chae-Ok Yun, JinWoo Hong, and A-Rum Yoon. "Current Clinical Landscape of Oncolytic Viruses as Novel Cancer Immunotherapeutic and Recent Preclinical Advancements". In: *Frontiers in Immunology* 13 (2022). ISSN: 1664-3224.